STRENGTH CHARACTERISTICS OF A MODELLING SILTY CLAY

LING LIN

STRENGTH CHARACTERISTICS OF A MODELLING SILTY CLAY

by

©LING LIN, B. Sc.

A thesis submitted to the School of Graduate Studies
in partial fulfillment of the requirements for
the degree of Master of Engineering

Faculty of Engineering and Applied Science
Memorial University of Newfoundland

March 1995

St. John's Newfoundland Canada

ISBN 0-612-01883-0

DEDICATED TO

MY MOTHER

AND

MY SISTERS

Abstract

Shear strength is an important soil parameter. Many geotechnical failures have been caused by inadequate shear strength. In order to obtain a high strength modelling silty clay for use in centrifuge model tests of soil-pipeline interaction, direct shear tests, shear vane tests and cone penetration tests were conducted to investigate its shear strength behaviour.

This thesis first presents some background on the shear strength of soils and measurement techniques. The details of the direct shear tests, the shear vane tests, the cone penetration tests and centrifuge modelling are also discussed. The silty clays used in this study were kaolin and a kaolin-silt mixture; the plasticity indices were 30.6% and 19.5% respectively. The kaolin-silt mixture (K-S) was obtained by mixing equal amounts of kaolin and silt by weight.

Direct shear and shear vane tests were conducted on both clays at different vertical stresses under various overconsolidation ratios (OCR's). This thesis presents these test procedures and the test results. Cone penetration tests were also conducted in a centrifuge at 50 gravities to verify the results from the direct shear and shear vane tests and to correlate the cone penetration resistance to the undrained shear strength from shear vane and direct shear tests. Centrifuge modelling principles and the current methods to convert cone tip resistance to shear strength are also presented. Test results show that the shear strength of K-S is higher than that of pure kaolin. Shear strengths of heavily overconsolidated clays obtained from the shear vane tests are higher than those obtained from the direct shear tests. A

correlation between cone tip resistance and undrained shear strength is presented. The shear strength of K-S interpreted from CPT results was found to lie between the direct shear and shear vane test results and shows a good correlation in the measurement of shear strength.

Acknowledgments

I would like to acknowledge the assistance of many people in my study for the degree of Master of Engineering. Particular thanks are due my supervisor, Dr. J. I. Clark, for his guidance and financial support throughout this program, and Dr. R. Phillips and Mr. M. Paulin for their guidance and help during the tests. Appreciation and gratitude are also extended to:

(a) Mr. D. Cameron and all the other members of geotechnical group at C-CORE for their help.

(b) Mr. H. Dye and other staff in the Machine Shop of the Faculty of Engineering for their help and suggestions in manufacturing the test device.

(c) Dr. P. Morin and Mr. C. Ward of the Faculty of Engineering for their help in preparing the direct shear test device.

(d) NOVA Corporation for supplying the test materials and sponsoring the test program.

Contents

List of Figures

List of Tables

List of Symbols

a	centrifuge acceleration
a_m	centrifuge model acceleration
a_p	prototype acceleration
a_v	coefficient of compressibility
A_m	centrifuge model area
A_p	prototype area
CPT	cone penetration test
c'	cohesion of soil
C_c	compression index
C_s	swelling index
c_u	undrained shear strength
c_u/σ'_v	normalized shear strength
c_v	coefficient of consolidation
d	diameter of vane shaft
D	vane diameter
DSS	direct shearbox test
D_{50}	mean grain size

e_o, e, e_1, e_2	void ratios
F_m	external force in model
F_p	external force in prototype
F_{wm}	self-weight force in model
F_{wp}	self-weight force in prototype
f_s	side friction of cone penetration test
g	gravitational acceleration
G_s	specific gravity
h_m	centrifuge model depth
H	vane height sample height in oedometer test
H_o	initial sample height in oedometer test
H_s	solids height in oedometer test
$\bar{h}$	length of drainage path
$\bar{H}$	average sample height in oedometer test
I_P	plasticity index
I_L	liquidity index
k, k_v	coefficient of permeability
K_o	coefficient of earth pressure at rest
$K-S$	kaolin-silt mixture

L_m	model length dimension
L_p	prototype length dimension
LDT	linear deformation transducer
m_v	coefficient of volume compressibility
M_s	resisting moment along the surface of cylinder
M_e	resisting moment at two ends of cylinder
N	dimension scale
N_c	cone factor
OCR	overconsolidation ratio
PPT	pore pressure transducer
p'	mean effective stress
p_c'	preconsolidation stress
q_c	cone tip resistance
r	centrifuge rotational radius
R_a	vane area ratio
R_f	friction ratio of cone penetration test
t	vane blade thickness
t_{90}	time required to reach 90% consolidation
T	torque applied to vane

T_v	time factor
TXE	triaxial extension test
u	pore pressure
v	specific volume
w_f	final water content after direct shear test
w_L	liquid limit
w_o	initial water content
w_P	plastic limit
$\alpha,\ \beta$	strength constants
γ_p	unit weight of prototype
δ_p	vertical load increment
Δe	change in void ratio
ΔH	vertical deformation
ΔH_f	final vertical deformation
Δp	change in vertical load
ε_m	strain in model
ε_p	strain prototype
κ	slope of loading-reloading line in v:lnp' plane
λ	slope of normal compression line in v:lnp' plane
ρ	material density

$\sigma_1, \sigma_2, \sigma_3$	principal stresses
$\sigma, \sigma_v, \sigma_{vo}$	total vertical stress
$\sigma', \sigma'_{v1}, \sigma'_{v2}, \sigma'_v, \sigma'_{vc}$	effective vertical stress
σ'_h	effective lateral stress
σ_m	stress in model
σ_p	stress in prototype
τ	shear stress
τ_f	shear stress at failure
ϕ'	effective angle of internal friction
ω	angular velocity

Chapter 1

Introduction

The determination of soil strength is an important aspect of geotechnical engineering. The undrained shear strength of clays is affected by the soils physical properties and stress conditions (Ladd *et al.*, 1977). The undrained strength can be estimated from field tests as well as laboratory tests. As field tests are usually expensive and time-consuming, laboratory shear tests are widely used to provide insight into the strength behaviour of clays.

In 1991, the Centre for Cold Ocean Resources Engineering (C-CORE) at Memorial University of Newfoundland undertook a contract project entitled "Centrifuge Modelling of Laterally Loaded Pipelines". The aim of this study was to investigate the load transfer behaviour of buried pipelines using centrifuge model tests and to determine the soil-pipeline interaction factors and the effects of trench geometry. Kaolin clay was used as the model clay. The undrained shear strength of kaolin was estimated using the following empirical equation (Poorooshasb, 1991):

$$c_u = 0.19\sigma_v'(OCR)^{0.59} \tag{1.1}$$

where c_u is the undrained shear strength, σ_v' is the effective vertical stress and OCR

is the overconsolidation ratio. However, the undrained strength of the soil estimated using the above equation was found to not correlate well with the centrifuge cone penetration test results.

Further centrifuge modelling of laterally loaded pipelines is being conducted at the C-CORE centrifuge centre. The effective vertical stress, σ_v' can be estimated using

$$\sigma_v' = \rho N g h_m \tag{1.2}$$

where ρ is the density of the soil (submerged density for the soil below water table), Ng is the acceleration level during the centrifuge test and h_m is the soil depth.

The one-dimensionally consolidated undrained direct simple shear test results of clays presented by Ladd and Edgers (1972) indicated that strength of some overconsolidated clays can be expressed using

$$\frac{(c_u/\sigma_{vc}')_{(OC)}}{(c_u/\sigma_{vc}')_{(NC)}} = OCR^m \tag{1.3}$$

where the value of m is a soil parameter, σ_{vc}' is the effective vertical stress at the beginning of shear, OC represents overconsolidated soils and NC represents normally consolidated soils.

In order to predict the undrained shear strength profile, it is necessary to develop a reliable relationship between the undrained shear strength c_u and the effective vertical stress σ_v'. Such relationships are typically assumed to be of the form

$$\frac{c_u}{\sigma_v'} = \alpha(OCR)^\beta \tag{1.4}$$

where the parameters α and β should be properly estimated.

Equation (1.3) and Equation (1.4) are essentially identical. For normally consolidated clays, Equation (1.4) becomes

$$\frac{c_u}{\sigma'_v} = \alpha. \tag{1.5}$$

The purposes of this thesis are to investigate the undrained shear strength of the kaolin clay and to develop a higher strength model clay for use in the centrifuge model study of soil-pipeline interaction. Kaolin clay and a kaolin-silt mixture were tested as the modelling silty clays. The following chapters of this thesis introduce the test techniques and the results of direct shear tests, shear vane tests and cone penetration tests for the estimation of the undrained shear strength of the kaolin and the kaolin-silt mixture.

Chapter 2

Literature Review

One of the purpose of this thesis is to investigate the strength behaviour of kaolin and a kaolin-silt mixture using direct shear tests, shear vane tests and cone penetration tests. In order to provide some background related to the study, this chapter presents a review of direct shear tests, shear vane tests and cone penetration tests, and introduces the applications of centrifuge modelling in geotechnical engineering. A review of the behaviour of kaolin-based clays is also presented.

2.1 Shear Strength of Clays

Shear strength of a soil is the internal resistance per unit area that the soil mass can offer to resist failure and sliding along any plane inside it (Das, 1985). In geotechnical engineering, many failures of soil structures and foundations result from inadequate shear strength. Shear strength is an important mechanical characteristic of soil, is influenced by many factors and may be estimated from field and laboratory test results.

The shear strength of a soil is directly related to its normal stress; the relationship

between the normal stress and shear stress on a failure plane can be expressed as

$$\tau_f = c' + \sigma' tan\phi'. \tag{2.1}$$

where, τ_f is the shear stress at failure, σ' is the effective normal stress, ϕ' is the effective angle of internal friction and c' is cohesion. This equation is well known as Mohr-Coulomb failure criterion. For cohesionless materials, such as sand, the value of c' is usually zero.

However, the strength behaviour of soils is very complicated. The shear strength of soils is affected by soil physical properties (such as mineralogy and consistency), confining pressure, stress history and other factors. Some main factors influencing soil shear strength are as follows:

Void ratio: Void ratio is perhaps the most important parameter affecting the shear strength of sands. Generally speaking, the lower the void ratio, the higher the shear strength (Holtz and Kovacs, 1981). The parameter ϕ' in Equation (2.1) changes not only with soil type, but also with soil void ratio.

Time effect: Creep of soil is the time-dependent strain which develops at a rate controlled by the soil viscous resistance (Mitchell, 1976). Secondary consolidation of soils which continues after primary consolidation is a kind of creep. Creep of a soil causes not only strain but also stress redistribution within the soil (Kavazanjian and Mitchell, 1984).

Anisotropy: The anisotropy of soil includes three aspects: the anisotropy of the soil structure, the stresses applied to the soil and the boundary conditions

(Duncan and Seed, 1966). During one-dimensional deposition and loading, particles of soils tend to become horizontally oriented (Ladd *et al.*, 1977). This orientation of particles causes inherent anisotropy of the soils and results in changes of strength and other properties of the soils. Duncan and Seed (1966) have shown that the anisotropy of particle orientation of a kaolinite causes as much as a 10% change in undrained strength.

Stress history: One of the most important characteristics of soils is that soil strength is significantly influenced by stress history. In many cases, stress history of a soil is represented by the overconsolidation ratio (OCR). In one dimensional testing, an overconsolidated soil has not only a lower void ratio but also a higher lateral stress than a normally consolidated soil; the undrained strength of overconsolidated soil is higher than that of normally consolidated soil. The one-dimensionally consolidated undrained direct simple shear test results of clays presented by Ladd and Edgers (1972) indicated that the undrained strength of overconsolidated clays increases with overconsolidation ratio and effective vertical stress (σ'_v) at the beginning of shear.

The shear strength of clays is also affected by the degree of saturation, sample disturbance, soil type, grain size distribution, rate of shearing, temperature and other environmental conditions.

2.2 Measurement of Shear Strength

Shear strength of soil can be estimated from the empirical correlation and also can be determined directly by some of the laboratory tests. As discussed above, there are many factors which may affect the strength of soils. The shear strength determined by different laboratory tests may also change, depending not only on the type of test but also on the drainage and consolidation conditions. Among the many test methods, the direct shear test and triaxial test are the two main types of shear tests. The laboratory vane test is also a commonly used test, especially for soft clays.

2.2.1 Direct Shear Test

The direct shear test is one of the oldest strength tests because it has been used for more than 200 years since Coulomb. This test relates shear strength at failure directly to normal stress and thus can be used to define the Mohr-Coulomb failure envelop.

In this test, a specimen container, called 'shearbox', is separated horizontally into two halves. One-half is fixed, while the other is either pulled or pushed horizontally. A normal load may be applied to the soil specimen. A stress- or strain-controlled shear force can be applied to the specimen. As the applied shear force is horizontal, the failure plane is restrained to be horizontal (Holtz and Kovacs, 1981).

There are some limitations and disadvantages associated with direct shear test. In the test, the soil specimen is forced to fail along the horizontal split plane and not along the weakest plane (Das, 1985). In addition, the shear stress distribution over

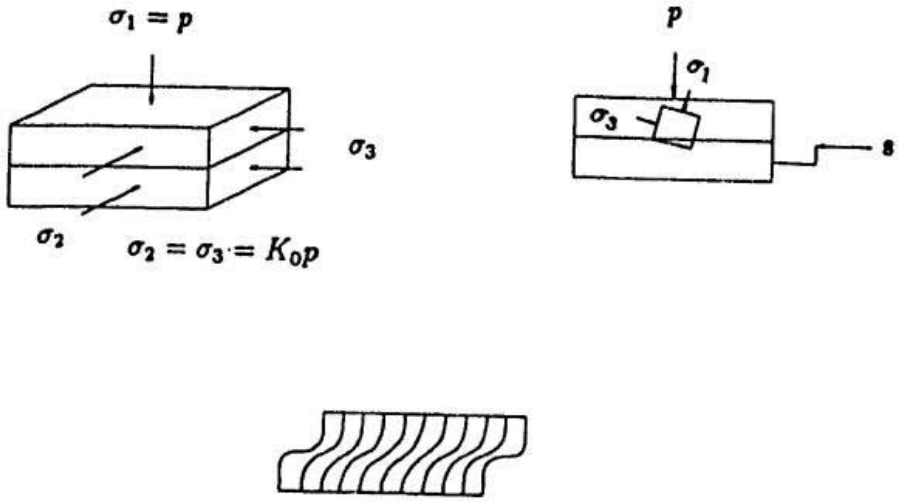

Figure 2.1: Stress States and Shear Strain Distribution in Direct Shear Test

the shear surface is not uniform (Wood, 1990). The stress states and shear strain distribution of soil of direct shear test is shown in Figure 2.1. During shearing, the principal stress plane changes. Another disadvantage of the direct shear test is that the pore pressure generated during the test cannot be measured (Vickers, 1983) and therefore the drainage condition is hard to control; the only way to judge the test being drained or undrained is to control the rate of shearing (Head, 1982).

2.2.2 Triaxial Test

The triaxial test is the most widely used method for the determination of shear strength parameters. In this test, a cylindrical soil sample is encased by a thin rubber membrane and placed inside a pressurised chamber which is usually filled with water. The sample is subjected to an isotropic stress by pressurising the fluid

in the chamber. To shear the specimen, an axial stress is normally applied through a vertical loading ram to cause shear failure (Das, 1985). Compared with the direct shear test, the triaxial test has the following advantages:

(1) Drainage condition can be controlled according to the test purposes;

(2) Pore pressure in undrained tests can be monitored and volume change observations in drained tests can be conducted;

(3) The soil failure can occur on any plane depending on the stress conditions;

(4) Back pressure may be applied to increase the degree of saturation of soil samples.

2.2.3 Shear Vane Test

The laboratory shear vane test is another simple way to determine the undrained shear strength of soils. During testing, the vane is pushed into a soil, and a torque is applied to the rod of the vane at a constant rate. The shear strength of the soil can be obtained by measuring the maximum torque required to cause a cylindrical failure surface prescribed by the vane blade edges. The maximum torque is usually measured from the spring rotation angle. As described by Flaate (1966), there are several factors affecting the results of vane test:

(1) Vane Shape and Size

The most popular type of vane is the 4-blade rectangular vane with a H/D (Height/Diameter) ratio of 2, although Silvestri *et al.* (1993) used different shapes in their studies. Flaate (1966) and Arman *et al.* (1975) indicated that the effect of the vane size on the measured shear strength is insignificant for field vane tests. Cadling

and Odenstad (1950) also showed that when an H/D ratio of 2 is maintained, the vane blade diameter has no effect on the results. For laboratory vane tests, Vey (1955) found that a vane with higher H/D ratio may have a large degree of sample disturbance. Almeidaphysical and Parry (1983) recommend a vane size of 18mm in diameter and 14mm in height. Area ratio, defined as the ratio of the cross section area of the vane to the cross section area of the sheared soil cylinder, is directly proportional to the vane size. Vickers (1983) suggests that the area ratio should be less than 12%.

(2) Disturbance due to Insertion

During penetration of the vane, some disturbance to the soil sample would occur due to the vane rod and the vane itself. The soil can stick to the vane as it is pushed into the soil thus the area ratio of the vane increases. Davies *et al.* (1989) found that the disturbance of the soil around the vane shaft was symmetrical and extended to about 2 times the radius of the shaft from its center line.

(3) Shear Velocity

Although in ASTM D4648-87, it is mentioned that the vane device should rotate the torque spring at a constant rate of 60° per minute, there is no standard vane rotation rate for the laboratory vane test. Extremely fast rotation rates may cause the undrained shear strength to increase because of viscous effects. At very low speed, significant consolidation occurs which may also cause higher values of shear strength (Springman, 1993). Perlow and Richards (1977) studied the effect of shear velocity on vane shear strength and pointed out that since the shear velocity at the edge of the vane increases considerably with increasing vane diameter, significant

differences in the shearing rate at the failure surface exist between large and small vanes at similar rotation rates. The wide range of vane sizes and rotation rates can result in significant differences in shear velocity. Monney (1969) found that laboratory strengths obtained at a rotation rate of 90° per minute were nearly 30% higher than strengths measured at 1° per minute on relatively undisturbed marine clayey silts.

(4) Other Factors

Other factors such as nonuniformity of stress distribution in the soil, shaft friction (water between the shaft and soil may decrease the friction) and the standing time between vane insertion and rotation may also affect the vane test results.

2.3 Properties of Kaolin and Kaolin-Based Mixtures

Kaolin clay is widely used as a modelling clay in fundamental studies. It has been used in centrifuge modelling tests to investigate many practical problems (Springman, 1993). The behaviour of kaolin clay has been investigated by many people such as Atkinson *et al.* (1987), Rossato *et al.* (1992), Lawrence (1980), Springman (1993) and Parry and Nadarajah (1973). Table 2.1 and 2.2 summarized the properties and compressibility of Speswhite kaolin obtained by some of these researchers.

As discussed previously, the undrained shear strength can be expressed as:

$$c_u/\sigma_v' = \alpha(OCR)^{\beta}. \tag{2.2}$$

The constants α and β in above equation for kaolin were obtained by some re-

Table 2.1: Physical Properties of Speswhite Kaolin

		Atkinson *et al.* (1987)	Rossato *et al.* (1992)	Lawrence (1980)
Liquid Limit	%	65	63	69
Plastic Limit	%	35	33	38
Plastic Index	%	30	30	31
Specific Gravity			2.61	2.61
Clay Fraction ($< 2\mu m$)	%		80	82

Table 2.2: Consolidation Parameters of Speswhite Kaolin
(after Springman, 1993)

σ'_v kPa	e	c_v mm^2/s	k_v $10^{-6}mm/s$	Source
400-700	1.10	0.35	0.68	Al-Tabbaa (1987)
120-450	1.21	0.57	0.34	Bransby (1993)
100-200	1.30	0.18	0.95	Ellis (1993)
54-91	1.54	0.25	2.87	Sharma (1993)
43-86	1.54	0.27	2.06	Springman (1993)

searchers through shear vane tests conducted in-flight in the centrifuge and are listed in table 2.3.

From Table 2.1, it can be seen that the plasticity index of kaolin is about 30%. The clay fraction of kaolin is about 80% which is much higher than natural clays and results in a lower stiffness and weaker shear strength. This disadvantage may be improved by mixing kaolin with some granular material to obtain kaolin mixtures

Table 2.3: Strength Constants of Speswhite Kaolin

Reference	α	β
Nunez (1989)	0.22	0.62
Bolton *et al.* (1993)	0.19	0.67
Springman (1989)	0.22	0.706

Note: α, β are mean values.

Table 2.4: Properties of Some Kaolin-Based Mixtures
(after Rossato *et al.* (1992) and Springman (1993))

		Pure Kaolin	KSS	KRF	Natural Clay ($I_P = 30\%$)
w_L	%	63	38	35.5	
w_P	%	33	21	17	
I_P	%	30	17	18.5	30
G_s		2.61		2.63	
Clay Fraction($< 2\mu m$)	%	82	55-65	43	
c_u/σ'_{vmax}	TXC	0.197	0.244	0.233	0.308
c_u/σ'_{vmax}	TXE	0.180		0.166	0.199
c_u/σ'_{vmax}	DSS	0.152		0.180	0.222

with higher strength. The kaolin-based modelling clays have been shown to have some advantages compared to pure kaolin (Rossato *et al.*, 1992). Springman (1993) obtained a kaolin-based mixture by mixing 70% Speswhite kaolin with 30% 180 grade silica rock flour (KRF). Rossato *et al.* (1992) obtained another mixture by combining 50% Speswhite kaolin, 25% fine quartz sand and 25% industrial quartz silt (KSS). The physical properties of these two materials are listed in Table 2.4, where TXC is the short form for triaxial compression test, TXE is triaxial extension test and DSS is direct simple shear test. From table 2.4, it can be seen that the shear strength of the kaolin mixtures are higher than pure kaolin.

2.4 Cone Penetration Test

The cone penetration test (CPT) is a technique for the measurement of soil properties by pushing an instrumented cone into soils at a constant rate. The main applications of CPT are to determine the soil profile and identify soils and to evaluate soil engineering parameters. In some cases, CPTs may be accompanied by borings to achieve more reliable test results. The CPT can provide continuous measurement of ground conditions; it also causes less disturbance of soil layers associated with boring and sampling. The CPT technique has been widely used in research and engineering practice. Because of the complex changes of stress, strain and pore pressure during the cone penetration test, it is difficult to make a comprehensive theoretical analysis. In engineering practice, the analysis of CPT is highly empirical (Meigh, 1987).

For a standard cone penetrometer, the cone is 60° and the cross-sectional area is

usually 10, 15 or 20 cm^2. In centrifuge modelling, much smaller cone penetrometers have been used (Ferguson and Ko, 1981; Davies *et al.*, 1989). The standard rate of in-situ cone penetration is 20±5 mm/s (Meigh, 1987). Some penetrometers can measure both tip resistance (q_c) and side friction (f_s); others can only provide q_c. Other piezocone penetrometers have also been developed for additional measurement of pore water pressure in soils during cone penetration (Konrad and Law, 1987; Mayne and Holtz, 1988; Sully and Campanella, 1991).

Another important parameter of CPT is the friction ratio, R_f, which is defined as the ratio of side friction to tip resistance and expressed as

$$R_f = \frac{f_s}{q_c} \tag{2.3}$$

and which is very useful for soil classification.

CPT data can be used for estimation of the relative density of normally consolidated sand (Jamiolkowski, 1985) and overconsolidated sand (Schmertmann, 1975), sand strength (Durgunoglu and Mitchell, 1975) and other parameters (Meigh, 1987). Also, extensive investigations have been carried out for determining the properties of clays using CPT, including undrained shear strength of normally consolidated clays (Lunne and Kleven, 1981) and overconsolidated clays (Marsland and Quarterman, 1982), and deformability of clays (Meigh, 1987). In addition, CPT has also been used for the estimation of pile bearing capacity (Meigh, 1987), for the control of ground improvement (Juilie and Sherwood, 1983) and for the determination of liquefaction potential of sand layers (Zhou, 1980).

Cone tip resistance q_c, changes directly with undrained shear strength of clay,

c_u, which is usually determined by in situ vane test; the expression equating the two parameters is (Schmertmann, 1975; De Ruiter, 1982)

$$c_u = \frac{q_c - \sigma_{vo}}{N_c} \tag{2.4}$$

where σ_{vo} is total overburden pressure and N_c is a cone factor.

A range of the N_c values has been found (Amar *et al.*, 1975; Lunne *et al.*, 1976); there is no universal N_c for all clays. The value of N_c changes with soil physical properties and overconsolidation ratio.

2.5 Geotechnical Centrifuge Modelling

Although many geotechnical engineering problems, such as stability of slopes, earth pressure, bearing capacity and settlement, can be solved using theories based on a set of simplified assumptions, it is sometimes more desirable to conduct a large scale field test in order to obtain reliable data. However, the cost and the time required and the difficulty in controlling the test condition reduce the application value of field tests. Laboratory tests, on the contrary, are easy to operate and the test condition is easier to control (Mikasa and Takada, 1973). As soil is a high non-linear material and its mechanical properties depend on the state of effective stress, model similarity requires that any stress in the model be equal to that in the prototype. It is hard to find a modelling technique which may satisfy self-weight stresses between model and prototype using the same material. For example, a model of an earth slope 50 cm high experiences very different self-weight stresses than an actual earth slope with a height of 50 m. The stress intensity due to self-

weight of the small scale model is much less than that in the prototype and hence the stress-strain behaviour and the patterns of deformations can be quite different in the two situations. In order to solve this problem, the centrifuge technique has been introduced for geotechnical applications. In centrifuge modelling tests, the gravitational effect can be modelled. By applying a centrifugal acceleration, the self-weight stress distribution can be corrected to simulate the stress conditions in the prototype.

The idea of centrifuge modelling and its possible use came to birth as early as 1868 (Craig, 1989). In the 1930's, investigators in the USA and the former USSR introduced this technique to geotechnical engineering (Rowe, 1975). Many important developments of the centrifuge technique for geotechnical problems were made at the University of Manchester and the University of Cambrige in the United Kingdom in the 1960's and 70's (Rowe, 1975; Schofield, 1980). Currently, there are geotechnical centrifuge facilities in the USA, United Kingdom, France, Japan, Canada, China and other countries.

Geotechnical centrifuge modelling has been a well-recognized research technique to fulfill similarity in model tests for investigating many kinds of problems in geotechnical engineering. The centrifuge technique has been used for studies of soil consolidation (Kimura *et al.*, 1984), retaining structures (Schcherbina, 1988), dams and embankments (Lee and Schofield, 1988; Feng and Hu, 1988), shallow and deep foundations (Kutter *et al.*, 1988), cone penetration tests (Ferguson and Ko, 1981; Springman, 1993) and soil liquefaction potential (Hushmand *et al.*, 1988).

Chapter 3

Materials Testing

Two types of remoulded soils were used in this study: kaolin clay and a kaolin-silt mixture (K-S). The former was obtained by mixing Speswhite kaolin powder with water while the latter was obtained by mixing equal amounts of Speswhite kaolin and Sil-Co-Sil silt with water. This chapter introduces the physical characteristics of these two clays and the oedometer consolidation test results.

3.1 Physical Characteristics

In order to classify the kaolin and the kaolin-silt mixture, the plastic limit, liquid limit, specific gravity and grain size distribution were determined for both soils. Plastic limit tests were done following the procedures described in ASTM D4318-84. Liquid limits were determined using the fall cone method. The specific gravity tests were conducted following the procedures described by Bowles (1986). The test results are given in Table 3.1. In the grain size analysis tests, the hydrometer method was used and all soil particles passed through a 0.075 mm sieve. The grain size distributions of the kaolin, silt and kaolin-silt mixture are shown in Figure 3.1.

Table 3.1: Properties of Kaolin and K-S

Soil Type		Kaolin	Kaolin-Silt Mixture
Liquid Limit, w_L:	%	59.3	35.2
Plastic Limit, w_P:	%	28.7	15.7
Plasticity Index, I_P:	%	30.6	19.5
Specific Gravity, G_s:	1	2.63	2.62
Mean Grain Size, D_{50}:	mm	0.0005	0.0035
Clay Fraction (<2μm):	%	73	42

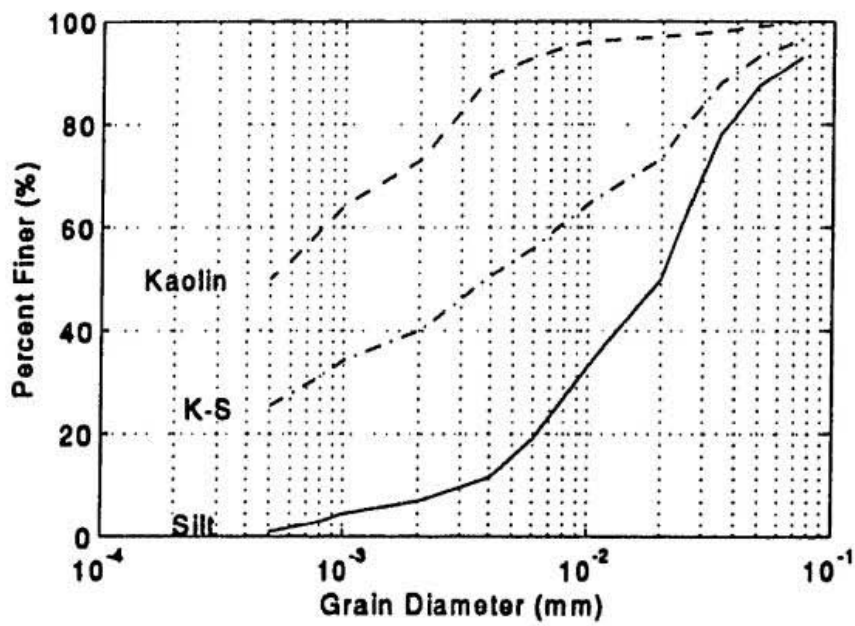

Figure 3.1: Grain Size Distribution Curves

From Table 3.1 and Table 2.1, it can be seen that the specific gravity of the kaolin of this study is close to those obtained by Rossato *et al.* (1992) and Lawrence (1980). Both the liquid limit and the plastic limit of the kaolin of this study are lower than those listed on Table 2.1, which may be due to the fact that the clay fraction of the kaolin of this study is 73% while the clay fractions listed on Table 2.1 are 80% and 82% respectively. The plastic indices on Table 3.1 and Table 2.1 are very close.

The kaolin and the kaolin-silt mixture are inorganic clays. According to ASTM D2487 (1993), the kaolin is a fat clay of high plasticity, classified as CH; the kaolin-silt mixture is a lean clay, classified as CL. The kaolin will have low strength and low permeability.

3.2 Oedometer Consolidation Test

3.2.1 Test Program

To determine the consolidation characteristics of the two soils, oedometer consolidation testing was carried out by applying vertical loads to a laterally confined specimen and observing the vertical deformation of the specimen with time.

The inner diameter of the oedometer used in this test was 61.8 mm. The specimen was tested under two-way drainage conditions. Vertical loads were applied to the specimen by dead weights through a loading frame. The load increment ratio ($\delta\sigma_v/\sigma_v$) was kept to 1 (except the first load increment step) according to ASTM D2435-90. Each load increment was applied for approximately 24 hours. Vertical deformation of the specimen was monitored using a dial gauge.

The kaolin and K-S slurries were prepared at initial water contents of approximately 100% and 70% respectively and were stored for 24 hours for the purpose of better saturation. After the specimen was spooned into the oedometer ring, the initial height and water content of the specimen were measured. The loading frame which gave a 14 kPa vertical stress was applied on the specimen through a loading plate and a ball-bearing. The dial gauge was set up and water was added all around the specimen. The timer was started and the readings of the dial gauge were taken at approximate times of 0.1, 0.25, 0.5, 1, 2, 4, 8, 15, 30 min, and 1, 2, 4, 8, 24 h after it was loaded. The next stress increment was then applied with the same procedure. The total vertical pressure was increased to 25, 50, 100, 200, 400, 800 and 1200 kPa in steps. After the specimen was consolidated under 1200 kPa, the specimen was unloaded and swelling was monitored. The unloading was made in steps with the unloading increment equal or less than 200 kPa. The duration of each unloading increment was from 4 to 6 hours for the completion of soil swelling. The final water content was measured when the unloading process had been completed.

3.2.2 Test Results

For the two clays, the initial water content, w_o, and specimen height, H_o, were measured before the tests were conducted. The observed accumulated deformation of the two specimens are shown in Figure 3.2 and Figure 3.3. The initial void ratio, e_o, and the height of solids, H_s, can be calculated using (assuming 100% saturation)

$$e_o = w_o \, G_s \tag{3.1}$$

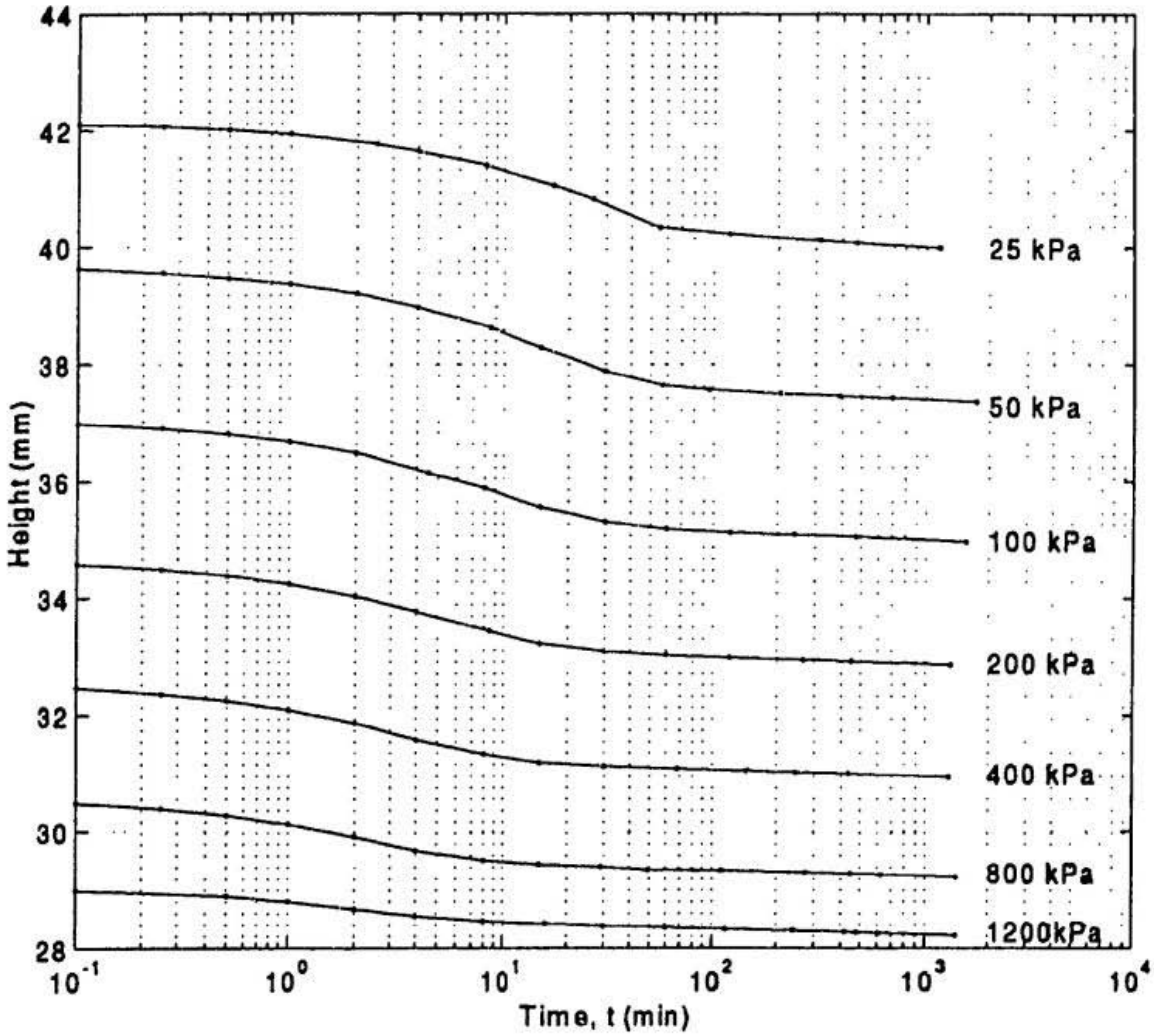

Figure 3.2: Accumulated Deformation with Time of Kaolin

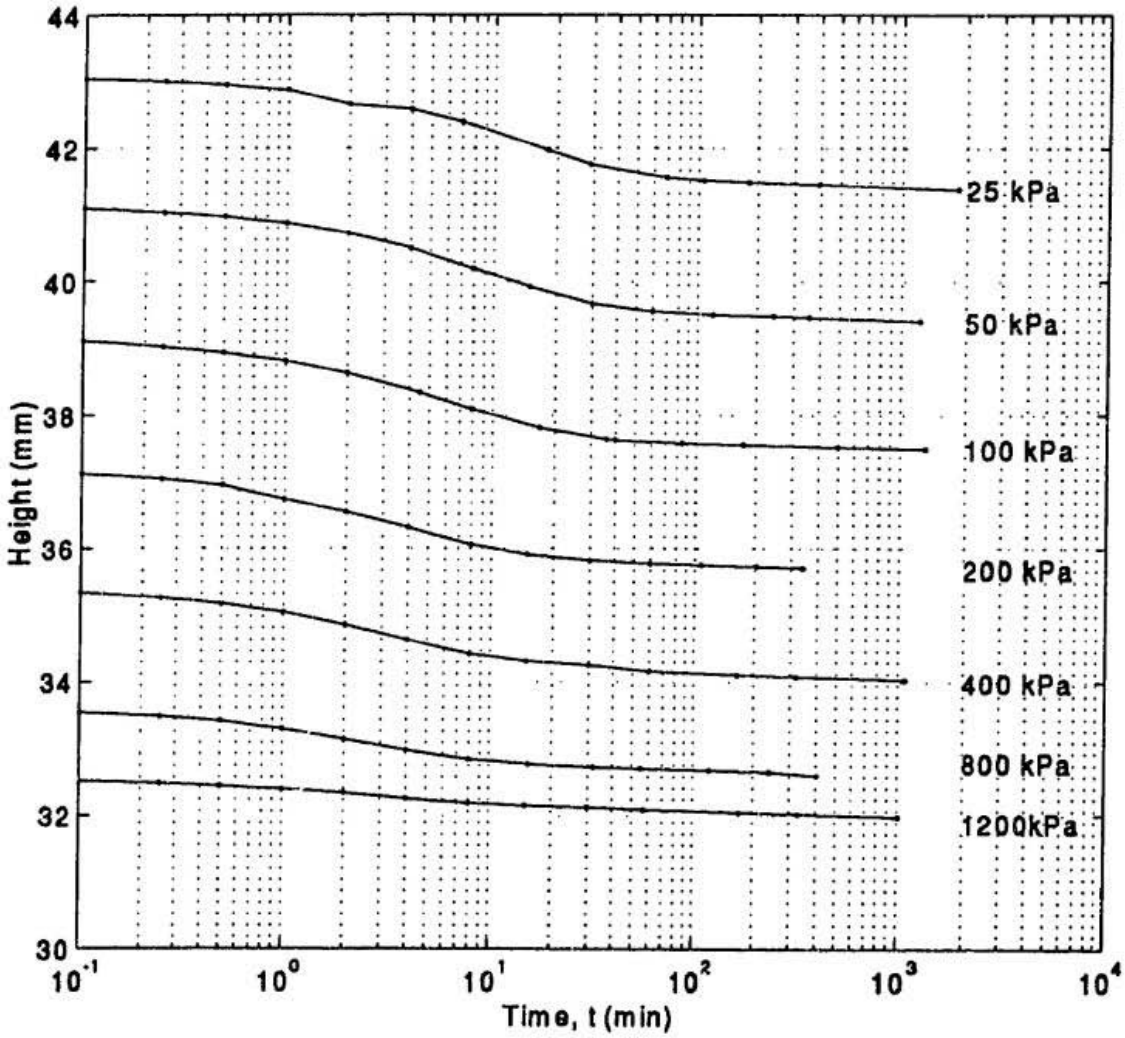

Figure 3.3: Accumulated Deformation with Time of K-S

Table 3.2: Parameters for the Calculation of Void Ratio

Soil Type	w_o (%)	G_s	H_o (mm)	e_o	H_s (mm)
Pure Kaolin	91.3	2.63	54	2.401	15.9
K-S Mixture	67.6	2.62	55	1.771	19.8

and

$$H_s = \frac{H_o}{(1+e_o)} \tag{3.2}$$

where G_s is the specific gravity of soil. The results are shown in Table 3.2. According to ASTM D2435-90, the void ratio of the specimen of any height can be calculated using the following equation:

$$e = \frac{H - H_s}{H_s} \tag{3.3}$$

where H is the sample final height at each load increment.

The coefficient of compressibility, a_v, the coefficient of volume compressibility, m_v, and compression index, C_c, are important parameters used to estimate soil compression. The definitions of these parameters are

$$a_v = \frac{\Delta e}{\Delta \sigma'_v} = \frac{e_1 - e_2}{\sigma'_{v2} - \sigma'_{v1}}, \tag{3.4}$$

$$m_v = \frac{a_v}{1+e_1}, \text{ and} \tag{3.5}$$

$$C_c = \frac{\Delta e}{log(\sigma'_{v2}/\sigma'_{v1})} \tag{3.6}$$

where e_1 and e_2 are the void ratios at the beginning and the end of the consolidation, Δe is the change of the void ratio, σ'_{v1} and σ'_{v2} are the corresponding effective

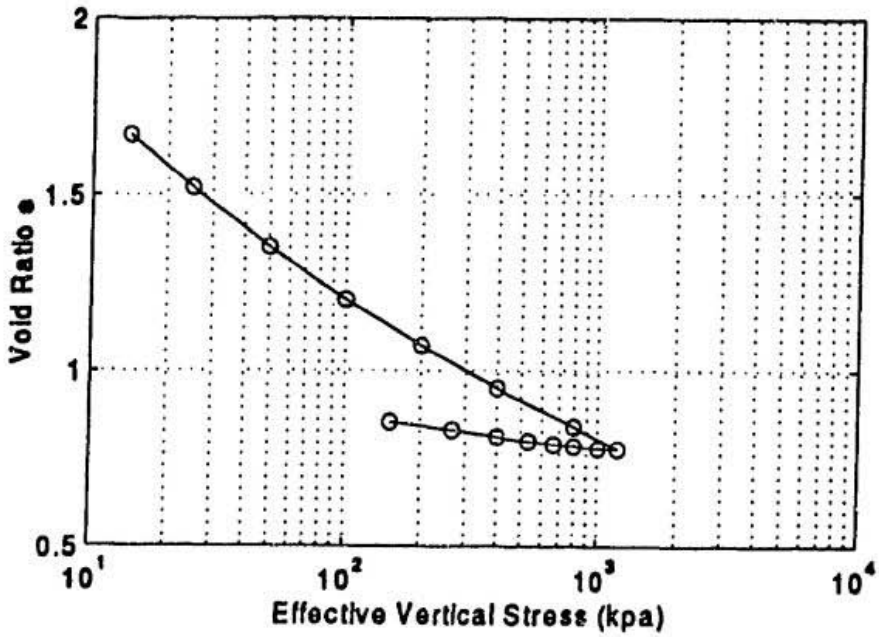

Figure 3.4: e-σ_v' Curve for Kaolin

vertical pressures at e_1 and e_2, and $\Delta\sigma_v'$ is the change of vertical effective stress. The coefficient of consolidation c_v can be determined using

$$c_v = \frac{0.848 T_v \bar{h}^2}{t_{90}} \tag{3.7}$$

where t_{90} obtained using the square root of time method (Bowles, 1986) is the time required to reach 90% consolidation. T_v is the time factor (at consolidation degree of 90%, T_v is 0.848), and $\bar{h}$ is the length of the drainage path which is equal to half of the average sample height. The results of c_v, a_v, C_c and m_v are given in Table 3.3 and 3.4, in which, $\bar{H}$ is the average sample height at any loading step. From the consolidation test results, e-p curves of both soils are shown in Figure 3.4 and Figure 3.5.

Table 3.3: Compression Parameters of Kaolin

σ'_v (kPa)	$\overline{H}$ (mm)	t_{90} (s)	c_v (mm^2/s)	Δe	Average e	a_v (1/MPa)	C_c	m_v (1/MPa)
0~14	48.183	9000	0.0547	0.7328	2.035	55.100		
14~25	41.183	3480	0.1033	0.1490	1.593	12.732	0.5435	4.77
25~50	38.678	1980	0.1602	0.1665	1.436	6.661	0.5532	2.64
50~100	36.161	1110	0.2497	0.1506	1.278	3.012	0.5003	1.28
100~200	33.915	778	0.3134	0.1323	1.136	1.323	0.4394	0.60
200~400	31.903	540	0.3996	0.1212	1.009	0.606	0.4028	0.29
400~800	30.080	290	0.6614	0.1083	0.895	0.271	0.3599	0.14
800~1200	28.722	280	0.7030	0.0628	0.809	0.157	0.3566	0.09

Table 3.4: Compression Parameters of K-S Mixture

σ'_v (kPa)	$\overline{H}$ (mm)	t_{90} (s)	c_v (mm^2/s)	Δe (10^{-2})	Average e	a_v (1/MPa)	C_c	m_v (1/MPa)
0~14	49.163	7260	0.0706	58.818	1.477	44.2243		
14~25	42.353	2340	0.1625	9.805	1.134	8.3801	0.3577	3.84
25~50	40.395	1215	0.2847	9.926	1.036	3.9703	0.3297	1.90
50~100	38.452	735	0.4265	9.654	0.938	1.9307	0.3207	0.97
100~200	36.603	540	0.5260	8.983	0.834	0.8983	0.2984	0.48
200~400	34.875	420	0.6139	8.429	0.747	0.4215	0.2800	0.24
400~800	33.318	290	0.8115	7.255	0.679	0.1814	0.2410	0.11
800~1200	32.292	276	0.9009	3.089	0.627	0.0772	0.1754	0.05

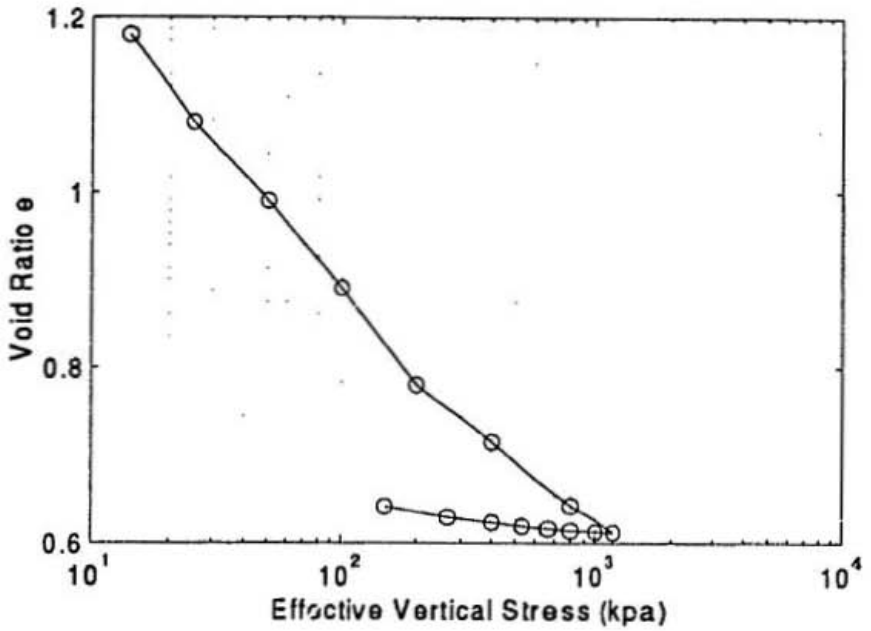

Figure 3.5: e-σ_v' Curve for K-S

3.2.3 Result Analyses

In critical state theory, the compression and swelling lines are assumed to be straight in $ln(p')$-v space with slopes -λ and -κ respectively. Here p' is the mean effective principal stress and v is the specific volume (v=1+e). The value of p' can be calculated using

$$p' = \frac{1}{3}(1 + 2K_o)\sigma_v' \tag{3.8}$$

where σ_v' is effective vertical stress and K_o is the coefficient of earth pressure at rest which can be expressed as (Mayne and Kulhawy, 1982)

$$K_o = (1 - sin\phi')(OCR)^{sin\phi} \tag{3.9}$$

where ϕ' is the effective angle of internal friction and OCR is overconsolidation ratio.

For kaolin, ϕ'=23° (Al-Tabbaa, 1987) and using Equation (3.8) the data in

Table 3.3 results in λ=0.187 and κ=0.051. The average values of kaolin obtained by Al-Tabbaa (1987) are λ=0.187 and κ=0.028.

Wood (1990) introduces the estimations of λ and κ using

$$\lambda \approx 2.3 C_c \tag{3.10}$$

$$\kappa \approx 2.3 C_s \tag{3.11}$$

where C_c is the compression index and C_s is the swelling index in one-dimentionally consolidation tests. According to the data shown in Figure 3.4 and Figure 3.5, the average values of C_c=0.453 and C_s=0.0926 of the kaolin yield λ=0.197 and κ=0.0402 while the values of C_c=0.294 and C_s=0.0361 of the K-S mixture yield λ=0.128 and κ=0.0157.

Using the data in Table 3.3 and Table 3.4, the relationship between c_v and void ratio, e, of the kaolin can be expressed as

$$c_v = 4.39 \times 10^{-7} e^{-2.89} \tag{3.12}$$

and for K-S mixture,

$$c_v = 2.68 \times 10^{-7} e^{-2.99} \tag{3.13}$$

where c_v is in m^2/s. The results of this study and the result of kaolin tested by King (1993) are shown in Figure 3.6. It can be seen that for kaolin, the c_v values of the two studies are close at high void ratio levels. From Table 3.3, Table 3.4 and Figure 3.6, it can be seen that for both the kaolin and K-S mixture, the c_v values of this study increase much slower with vertical stress when the vertical stress is greater than 400 kPa. The results are in accordance with the fact that c_v reaches

a plateau of $0.35 \times 10^{-6}\ m^2/s$ when vertical stress is between 400 kPa and 700 kPa (Al-Tabbaa, 1987).

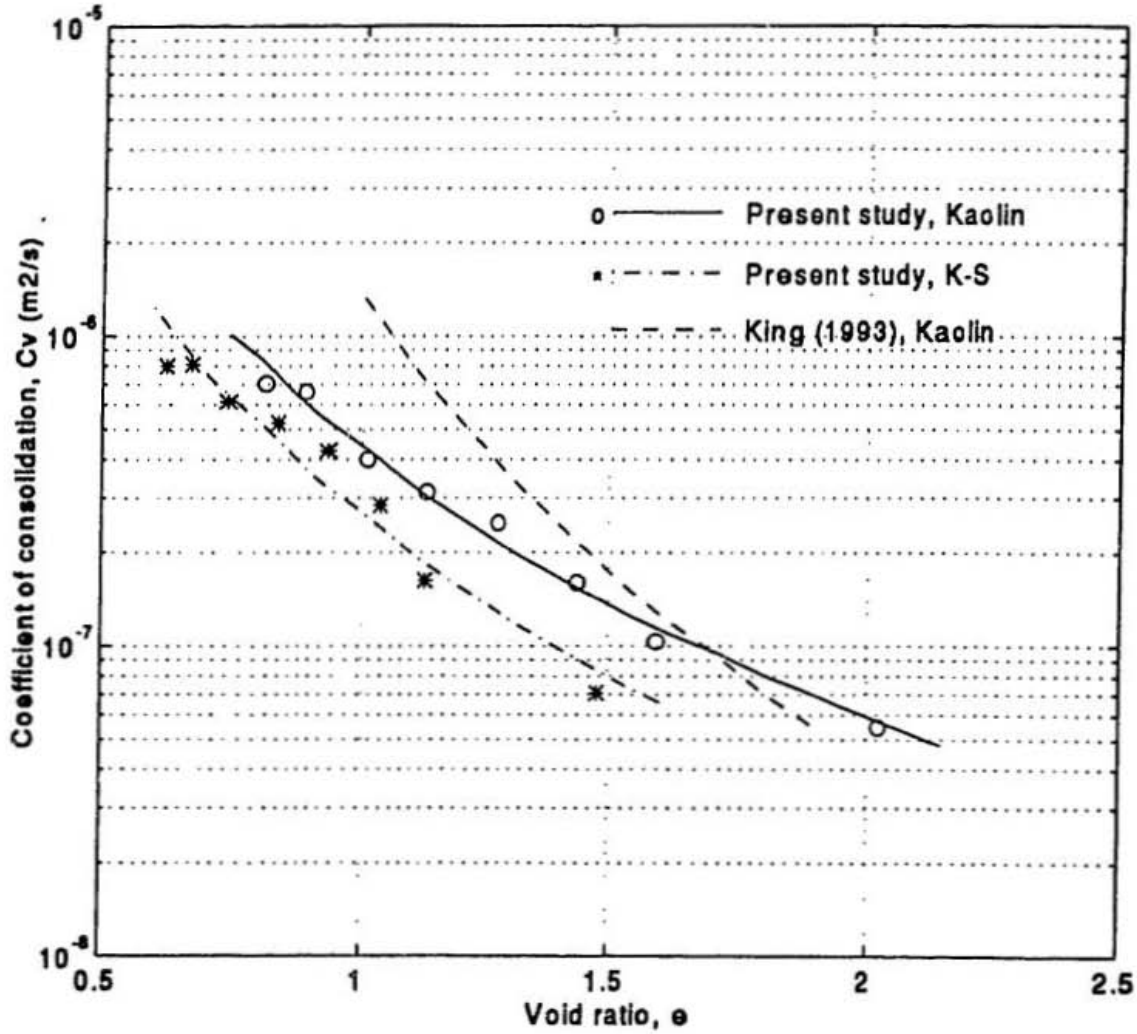

Figure 3.6: Comparison of c_v Results

Chapter 4

Shear Strength Tests

As described previously, there are many test methods for measuring the shear strength of soils. The shear strength is influenced by many factors, such as soil type, confining stress, soil density and stress history. In order to determine the shear strength parameters α and β of Equation (1.4), a series of consolidated undrained direct shear and shear vane tests were conducted on both the kaolin and the kaolin-silt mixture at different effective normal stress and OCR levels. This chapter will present the test techniques and results of the direct shear tests and shear vane tests on the two soils.

In the direct shear and shear vane tests, the soil specimens were normally one-dimensionally consolidated under total stress increments similar to that described in Chapter 3. During consolidation, vertical deformation was monitored. When 90% of primary consolidation was complete, the next loading increment was applied. The overconsolidation ratio (OCR) of a specimen is the ratio of the maximum preconsolidation stress σ'_{v1} to the current effective vertical stress σ'_{v2}, that is, OCR=$\sigma'_{v1}/\sigma'_{v2}$. In both direct shear and shear vane tests, specimens with OCR values of 1, 2, 4, 6,

8 were used to investigate the strength behaviour of the soils.

4.1 Direct Shear Test

The direct shear tests were carried out for the determination of shear strength of both kaolin and K-S. The specimens were consolidated and sheared in shearbox under OCR values of 1, 2, 4, 6 and 8. This section introduces the direct shear test apparatus, test procedures and the test results.

4.1.1 Test Apparatus

The direct shear test apparatus used in this study is that of the Soils Laboratory of the Faculty of Engineering and Applied Science at Memorial University of Newfoundland. The diagram of this apparatus is shown in Figure 4.1. The components of this shear device are described below.

Driving unit: A motor is used to apply a horizontal strain-controlled shear displacement to the specimen. In the direct shear test, the driven speed of the horizontal displacement is usually from 0.5 to 2 mm/min (Bowles, 1986). In this study, a shearing rate of 1.26 mm/min was used which is the maximum shearing rate of this device.

Shearbox carriage: The carriage is used to mount the shearbox and is filled with water during the test. This carriage moves horizontally when the driving motor is working to supply the shear force to the specimen.

Shearbox: This box is the specimen container consisting of two halves which can be fixed together by means of two clamping screws. Two lifting screws enable

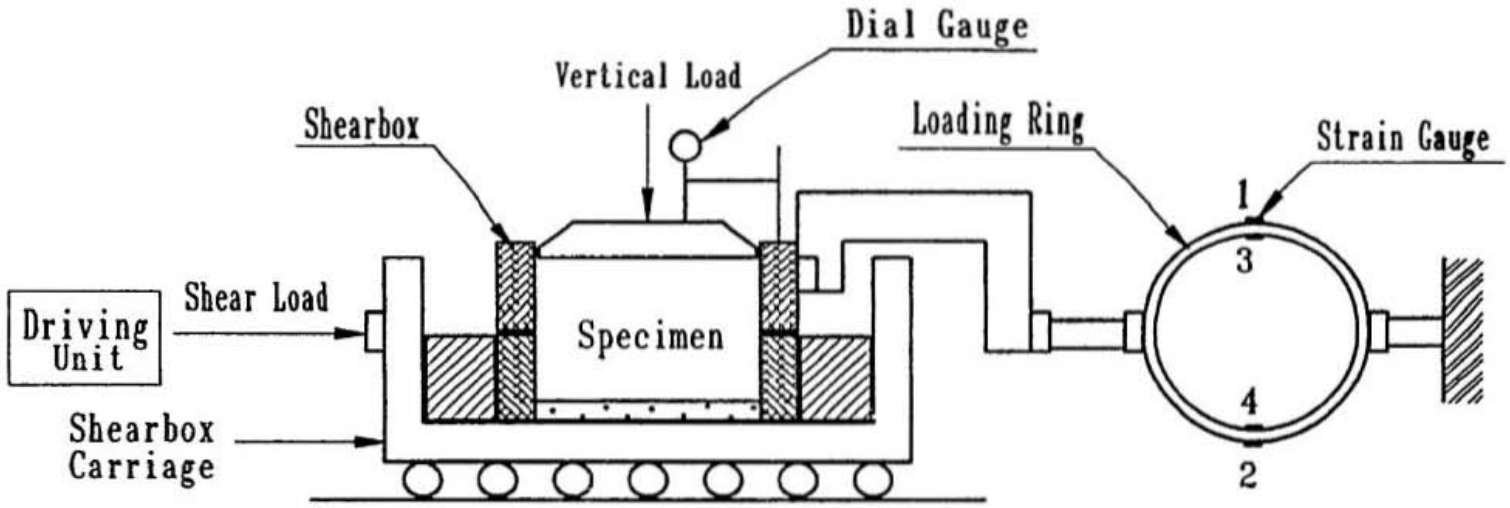

Figure 4.1: Direct Shear Test Diagram

the upper half to be lifted slightly to reduce the friction force at the surface of the two halves. The inside diameter of the shearbox is 61.8 mm.

Load hanger: It is made with a spherical seating and ball bearing for applying the normal pressure through a loading plate to the specimen.

Loading ring: Strain gauges are used for measuring the horizontal shear force; the details are to be introduced later in this section.

Dial gauge: When necessary, a dial gauge is used for the measurement of vertical deformation during consolidating and shearing.

X-Y plotter: It is used to record the shear load applied to the specimen.

There are two ways of using a loading ring to measure the shear stress applied to the specimen. A dial gauge can be used to measure the loading ring deformation caused by the shear force and this deformation can be converted to load using the calibration curve of the load ring. The other method is to use strain gauges to measure load applied to the loading ring, as shown in Figure 4.1.

In this study, four electrical resistance strain gauges were glued to the loading ring. The strain gauges were of foil type; the gauge resistance was 120 ohms. When a load is applied to the loading ring as shown in Figure 4.1, the two strain gauges on the outside surface of the ring are extended and the other two gauges on the inside surface are compressed. These four gauges were connected together to form a full Wheatstone-bridge circuit, as shown in Figure 4.2.

This arrangement of strain gauges has two advantages. The strain sensed by each of the four gauges is added together hence the accuracy of load measurement is

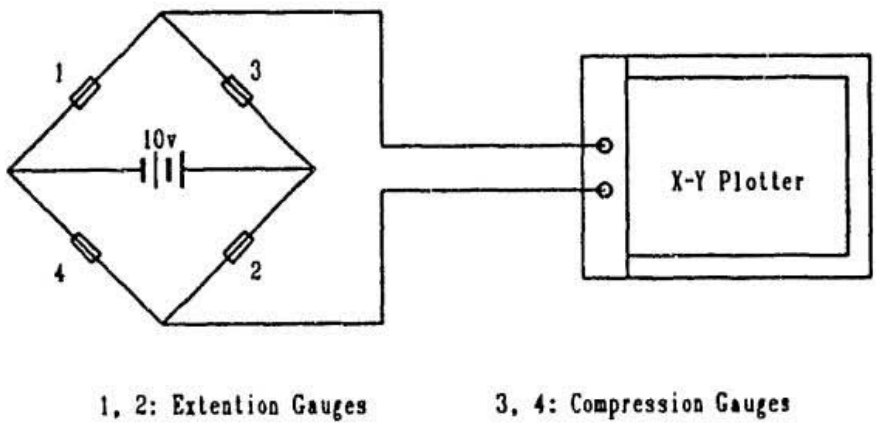

Figure 4.2: Wheatstone-Bridge Circuit for Shear Stress Measurement

increased. The other advantage is that this circuit can provide temperature compensation. With a full Wheatstone-bridge circuit, the measurement results will not be influenced by the changes of environmental temperature or by the exciting electrical current through the gauges. This circuit was excited by a 10 volt direct current power supply and the measurement was taken by an X-Y plotter. The loading ring was calibrated using dead weights.

4.1.2 Testing Procedures

The overall height of the original shearbox was 50 mm; the upper part was 25 mm and the lower half was also 25 mm. According to the compression test results of the kaolin presented in Chapter 3, more than 40% compression would occur under

a 1000 kPa vertical load. In order to obtain a thicker specimen, an upper half extension giving a total 60 mm in height was manufactured and used in the tests.

The two halves of the shearbox were fixed together by the clamping screws, and placed in the carriage. The soil slurry was placed into the shearbox using a tea spoon. Two porous stones were used at the top and bottom end of the specimen. The initial height of the specimen was measured immediately after the slurry had been poured.

The load plate was then placed on the specimen. The load hanger was gently put onto the load plate through a ball-bearing and the vertical dial gauge was set. Water was added all around the specimen. After putting on the load hanger, the timer was started and vertical dial gauge readings were taken at time intervals according to ASTM D2435-90. When 90% consolidation at a load step was achieved, the next load increment was applied with the same procedure. The self-weight of the hanger was the first load step of 14 kPa. The load increment was applied according to ASTM D2435-90. The degree of consolidation required was 90% but 100% was required for the last load increment. To obtain an overconsolidated specimen, the specimen was unloaded to the required stress level, σ'_{v2}, after consolidation at the maximum load increment, σ'_{v1}. When the specimen was loaded or unloaded to the required stress level the clamping screws were removed and two lifting screws were driven. After the screws contacted the lower half, a further half-turn rotation separated the two halves. These two lifting screws were removed before shear load was applied.

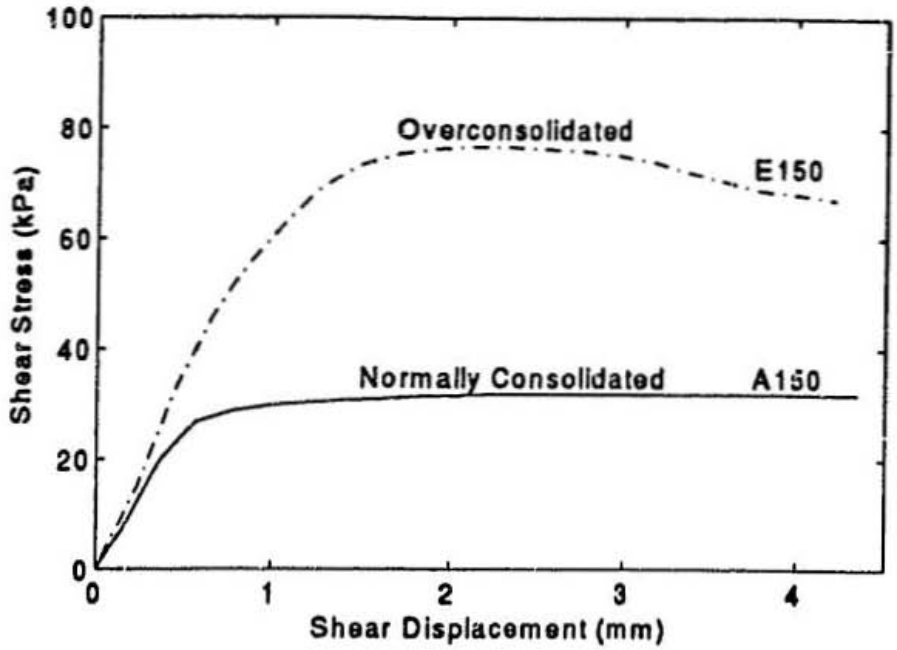

Figure 4.3: Typical Shear Stress vs Shear Displacement from Direct Shear Test

Specimens were sheared at a rate of 1.26mm per minute. The speed of the plotter recording paper was 1 mm per second. The shearing of the specimen was stopped if a peak value of shear load occurred, otherwise the specimen was sheared for more than 200 seconds in order that the horizontal shear displacement was 1/15 of the specimen diameter. After the driving machine of the shearbox was stopped, the sheared specimen was immediately removed and the water content of the specimen was measured.

The shear rate was constant in all the tests. When an overconsolidated sample was sheared, there was a peak shear force (Figure 4.3), which was used in the calculation of shear strength. It was noted that for normally consolidated specimens, there was no apparent peak shear force value as shown in Figure 4.3 . In this figure, A150 was a normally consolidated specimen sheared under an effective

vertical stress of 150 kPa. E150 was an overconsolidated specimen with OCR value of 8 and sheared under an effective vertical stress of 150 kPa. In the case when there is no peak shear force, the shear force at failure was considered to be at a horizontal deformation of 1/15 of the original sample diameter, which was 4.12 mm. As the shear rate was set at 1.26 mm/min, this shear force was taken 200 seconds after starting. Because when the sample was sheared, the horizontal cross-sectional area of the specimen was reduced, an area correction for the calculation of specimen shear strength must be made. The details of area correction are presented in Appendix A.

4.1.3 Test Results of Kaolin

In order to evaluate the strength behaviour of kaolin, 21 direct shear tests with various stress and OCR levels were conducted. The test results are shown in Table 4.1, where c_u is the undrained shear strength after the area correction was applied, w_f is the final water content of the specimen. The initial water content of the kaolin was 100%.

Using the data of Table 4.1, the relationship between normal stress and shear strength of the specimens with different OCR value is shown in Figure 4.4 where linear regression lines have been fitted to the data of each OCR. It can be seen that at each OCR level, the shear strength is proportional to the normal stress at shearing. Under the same normal stress, shear strength increases with increasing OCR. The test results indicate that the undrained strength of the kaolin is related to stress level and stress history. For a normally consolidated specimen, the slope of the OCR=1 line in Figure 4.4 gives the value of α. Figure 4.5 shows that the

Table 4.1: Direct Shear Test Results of Kaolin

OCR	Test	σ'_{v1} (kPa)	σ'_{v2} (kPa)	c_u (kPa)	c_u/σ'_{v2}	w_f (%)
1	A50	50.0	50.0	12.0	0.240	51.7
	A100	100.0	100.0	22.5	0.225	48.0
	A150	150.0	150.0	35.0	0.233	47.3
	A200	200.0	200.0	46.3	0.232	43.6
	A250	250.0	250.0	54.9	0.220	41.9
2	B50	100.0	50.0	15.6*	0.312	48.3
	B100	200.0	100.0	33.6*	0.336	46.0
	B150	300.0	150.0	50.1*	0.334	42.0
	B200	400.0	200.0	64.8*	0.324	40.7
	B250	500.0	250.0	79.5*	0.318	38.8
4	C50	200.0	50.0	20.6*	0.412	45.9
	C100	400.0	100.0	40.2*	0.402	41.0
	C150	600.0	150.0	67.7*	0.451	40.0
	C200	800.0	200.0	89.0*	0.445	38.4
	C250	1000.0	250.0	105.5*	0.422	37.4
6	D50	300.0	50.0	27.7*	0.554	44.1
	D100	600.0	100.0	53.4*	0.534	40.4
	D150	900.0	150.0	74.5*	0.497	39.1
8	E50	400.0	50.0	29.1*	0.582	41.1
	E100	800.0	100.0	58.0*	0.580	38.8
	E150	1200.0	150.0	81.8*	0.545	36.6

Note: Data with * are obtained using the peak values of the shear forces.

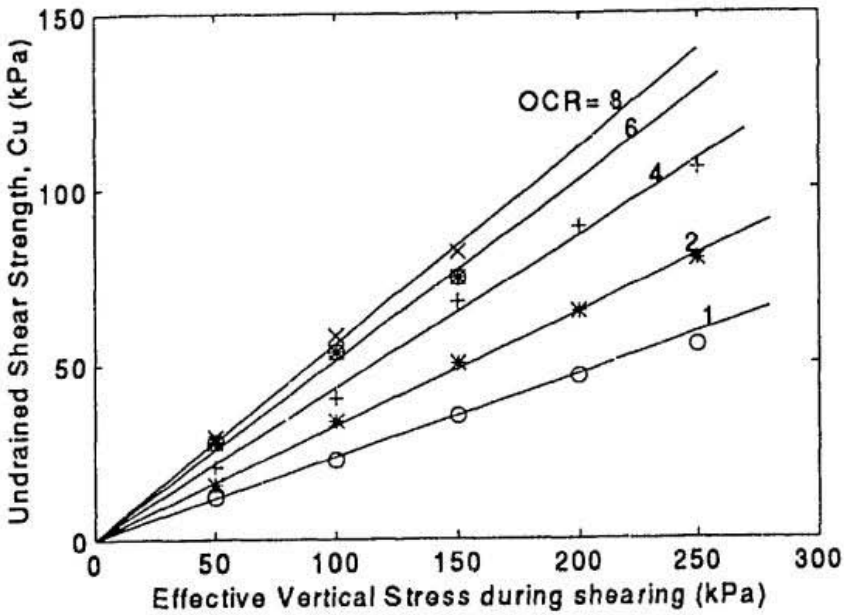

Figure 4.4: Shear Strength of Kaolin from Direct Shear Tests

normalized strength c_u/σ'_{v2} is dependent on OCR and independent of normal stress state.

The last column of Table 4.1 shows the water content of specimens after shearing. It can be seen that the water content decreases with both normal stress and overconsolidation ratio. These results are shown in Figure 4.6.

The undrained shear strength parameters α and β in Equation (1.4) can be determined by linear regression analysis. Mathematically, Equation (1.4) can be rewritten as

$$log(\frac{c_u}{\sigma'_v}) = log(\alpha) + \beta(OCR). \tag{4.1}$$

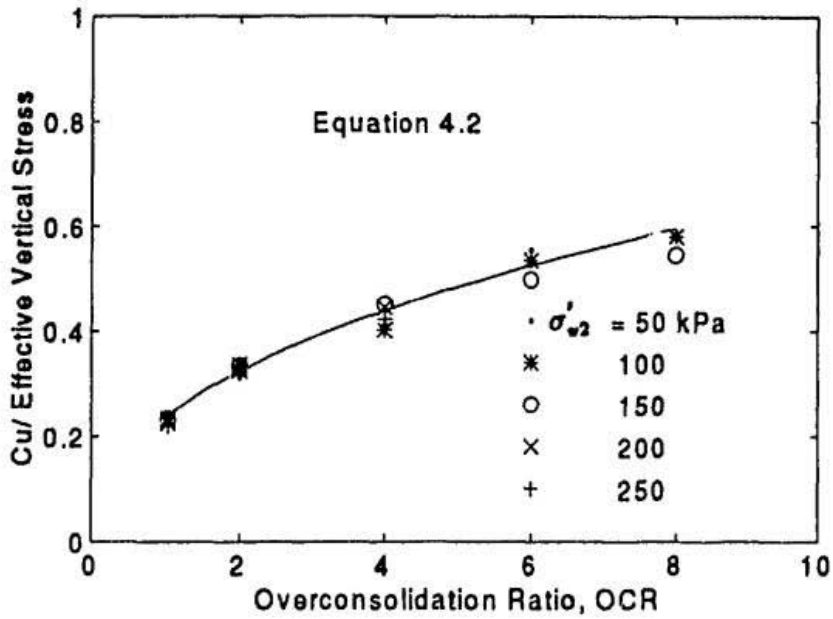

Figure 4.5: Normalized Shear Strength of Kaolin from Direct Shear Tests

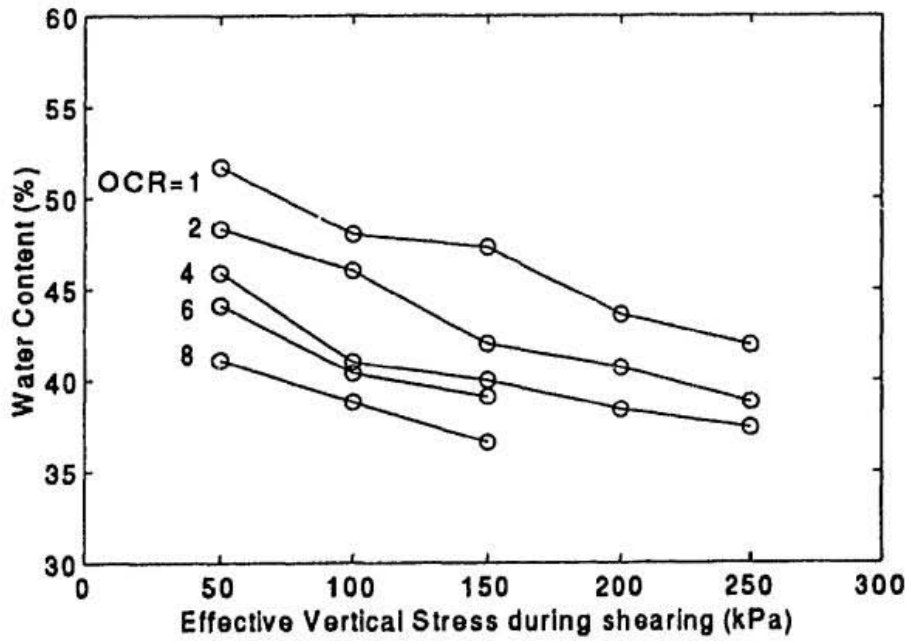

Figure 4.6: Water Content of Kaolin after Direct Shear Tests

Using the data in Table 4.1, the following values can be obtained:

$$log(\alpha) = -0.6234; \qquad \alpha = 0.238;$$

and

$$\beta = 0.441.$$

Therefore, the undrained shear strength of the kaolin has the following expression:

$$\frac{c_u}{\sigma_v'} = 0.238(OCR)^{0.441} \tag{4.2}$$

where c_u is the undrained shear strength, σ_v' is the effective vertical stress at the beginning of shearing, and OCR is the overconsolidation ratio. This curve has been plotted to the data of Figure 4.5.

4.1.4 Test Results of Kaolin-Silt Mixture

To investigate the strength of the kaolin-silt mixture, 20 direct shear tests were carried out under various vertical stress and OCR levels. The initial water content for the K-S specimen was 70%. The test results are given in Table 4.2, in which, area correction has been applied.

The relationship between undrained shear strength and effective vertical stress is shown in Figure 4.7 where linear regression lines have been fitted to the data of each OCR. The relationship between normalized shear strength and overconsolidation ratio is shown in Figure 4.8. Figure 4.9 shows the final water contents after direct shear testing.

These test results indicate that the undrained shear strength of K-S is also a function of effective normal stress and OCR. The undrained shear strength parame-

Table 4.2: Direct Shear Test Results of K-S

OCR	Test	σ'_{v1} (kPa)	σ'_{v2} (kPa)	c_u (kPa)	c_u/σ'_{v2}	w_f (%)
1	A50	50.0	50.0	16.1	0.322	33.2
	A100	100.0	100.0	32.1	0.321	31.9
	A150	150.0	150.0	48.7	0.325	30.5
	A200	200.0	200.0	64.5	0.323	29.1
	A250	250.0	250.0	82.3	0.329	28.7
2	B100	200.0	100.0	45.8	0.458	29.2
	B150	300.0	150.0	68.7	0.458	28.2
	B200	400.0	200.0	90.1	0.451	27.7
	B250	500.0	250.0	112.6	0.450	27.0
4	C50	200.0	50.0	26.2	0.524	29.9
	C100	400.0	100.0	53.8	0.538	27.9
	C150	600.0	150.0	79.2	0.528	26.4
	C200	800.0	200.0	104.6	0.523	25.8
6	D50	300.0	50.0	30.9*	0.618	28.3
	D100	600.0	100.0	62.3*	0.623	26.5
	D150	900.0	150.0	95.7*	0.638	25.0
	D200	1200.0	200.0	127.0*	0.635	24.3
8	E50	400.0	50.0	38.5*	0.770	27.5
	E100	800.0	100.0	70.6*	0.706	25.8
	E150	1200.0	150.0	103.3*	0.689	24.5

Note: Data with * are obtained using the peak values of the shear forces. The values of c_u of A100, A150 and A200 are the mean values of three tests.

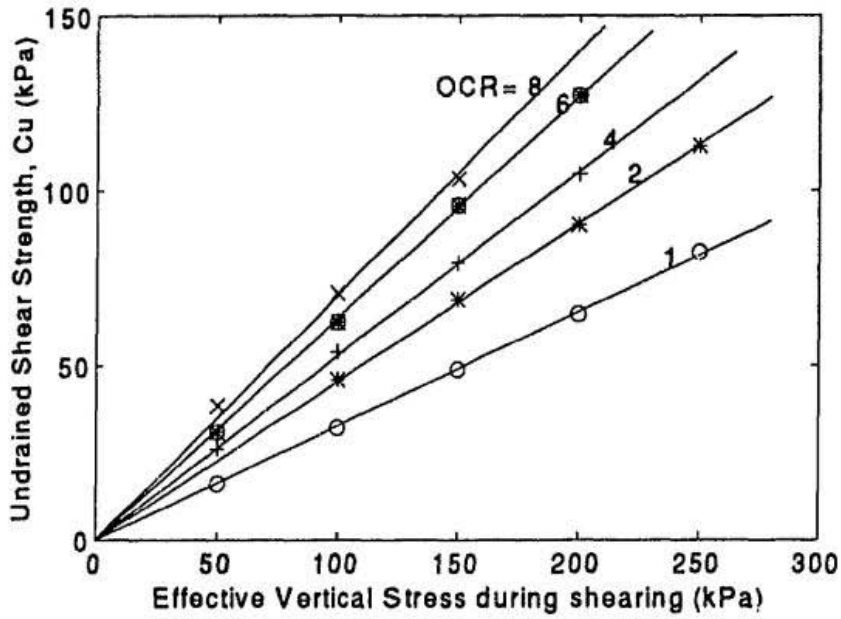

Figure 4.7: Shear Strength of K-S from Direct Shear Tests

ters α and β can be determined using the same method as for kaolin. The following relationship between normalized shear strength and OCR can be obtained for the mixture:

$$\frac{c_u}{\sigma_v'} = 0.330(OCR)^{0.370}. \tag{4.3}$$

This curve has been plotted to the data of Figure 4.8.

4.2 Shear Vane Tests

Laboratory shear vane testing has been proven to be an effective method of determining the shear strength of clays. In this study, vane tests were carried out on specimens in a specially designed circular sample tub using a rectangular vane with 4 blades. The vane test device was manufactured by the Wykeham-

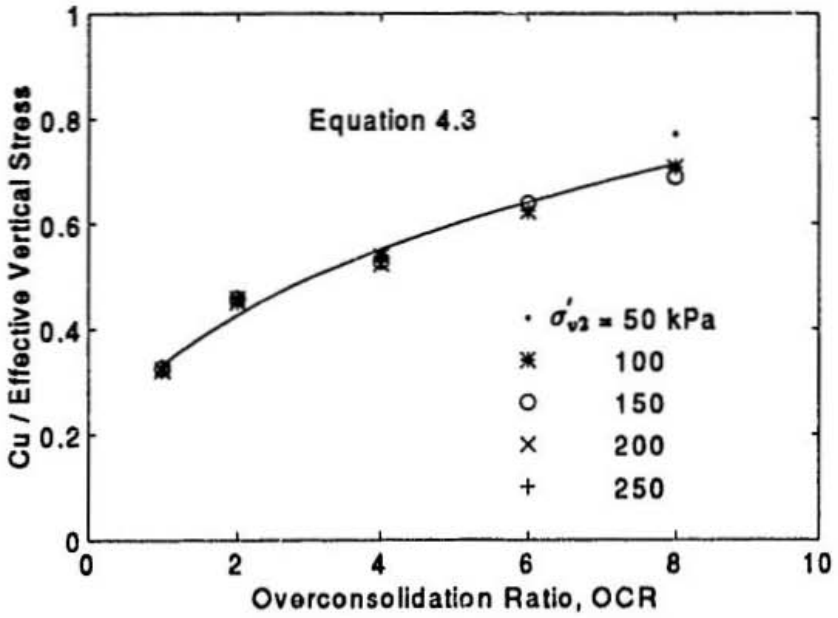

Figure 4.8: Normalized Shear Strength of K-S from Direct Shear Tests

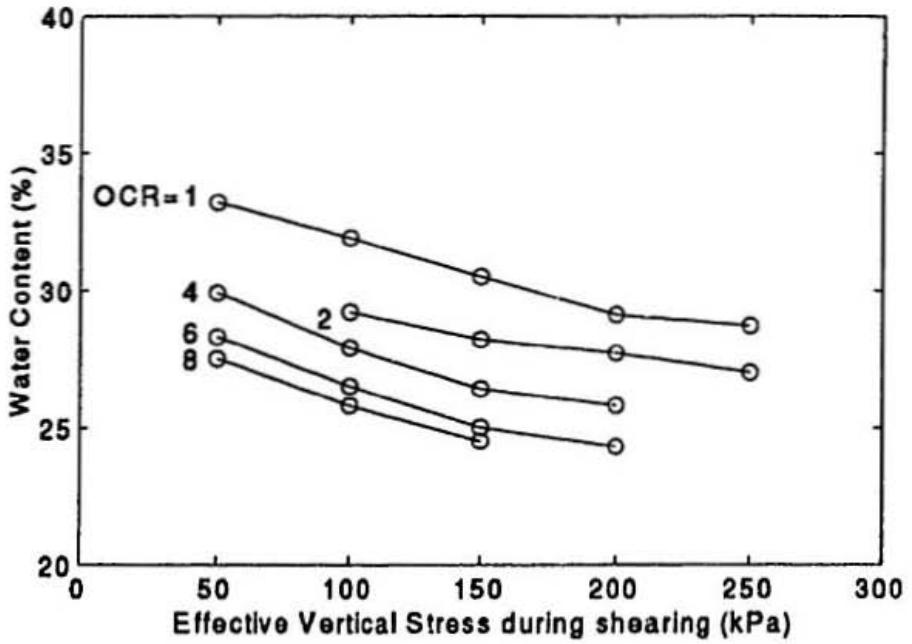

Figure 4.9: Water Content of K-S after Direct Shear Tests

Farrance Company in England. The soil specimens were consolidated to a 400 kPa preconsolidation stress and then unloaded to obtain OCR value of 1, 2, 4, 6 or 8. The shear vane tests were conducted at effective normal stress of 50, 66.7, 100, 200, and 400 kPa on samples of both the kaolin and K-S mixtures.

4.2.1 Principles

During vane testing, a vane is pushed into the specimen and rotated at a uniform speed by applying a torque at the top of the vane shaft. If the vane has a diameter of D and a height of H (as shown in Figure 4.10), then a soil cylinder of height, H, and diameter, D, resists the torque until failure occurs. The applied torque at failure can be measured by means of a torsional spring and converted to an equivalent shear strength according to the size of the vane. The resistance of soil to the vane can be reflected by the rotation of the spring. Neglecting the friction between the vane shaft and soil during rotation, the applied torque (T) should be equal to the sum of the resisting moment of the shear force along the side surface of the soil cylinder (M_s) and the resisting moment of the shear force at two ends of the cylinder (M_e). That is

$$T = M_s + 2M_e. \tag{4.4}$$

As discussed in Chapter 2, there are many factors which may influence the vane test results. The following assumptions in the calculation of the undrained shear strength of soils using vane test data are made based on the analyses by Flaate (1966):

(1) The soil is completely undrained;

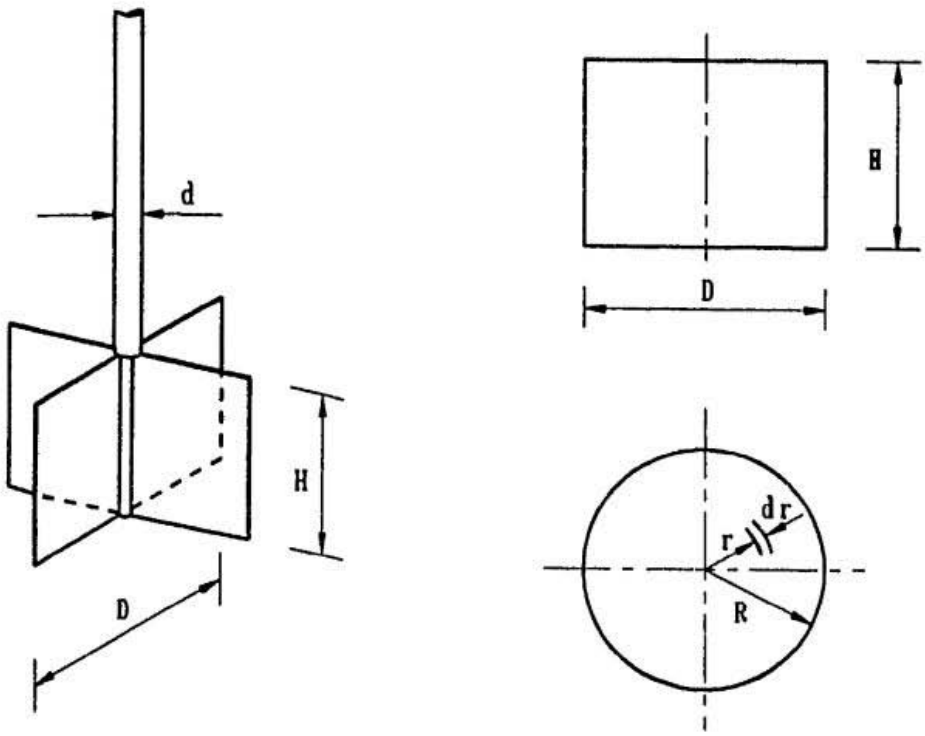

Figure 4.10: Shear Vane Diagram

(2) No disturbance is caused by the insertion of the vane;

(3) The remoulded zone around the vane is very small;

(4) There is no progressive failure. The maximum applied torque overcomes the fully-mobilized shear strength along a cylindrical surface; and

(5) Isotropic strength condition exists within the soil mass.

For a rectangular 4-blade vane, assuming the undrained strength of soil is c_u, equation (4.4) can be written as (Vickers, 1983):

$$T = c_u \pi D H \times \frac{D}{2} + c_u \times 2 \times \int_0^{\frac{D}{2}} 2\pi r \times dr \times r. \tag{4.5}$$

That is

$$c_u = \frac{T}{\pi D^2 (\frac{H}{2} + \frac{D}{6})} \tag{4.6}$$

where c_u is the undrained shear strength of the specimen, T is the torque applied to the vane, D is the diameter of the vane blade, and H is the height of the vane.

4.2.2 Tub and Vane Design

The sample container used for the vane tests is a circular steel tub which is 300 mm in diameter and 400 mm in height. The vertical load can be applied to the soil sample by a loading frame through a loading bar and a loading plate on the top surface of the sample. Dead weights were used for the loading. Four threaded holes which were plugged with bolts during soil consolidation were drilled on the loading plate for the insertion of the vane as shown in Figure 4.11. These holes have a diameter of 25 mm.

The vane used in this study has four equal-size rectangular blades; this is the most commonly used type of vane in geotechnical engineering. Almeida and Parry (1983) conducted vane tests using different sizes of vane and recommended a vane with a diameter of 18 mm and a height of 14 mm which was adopted in this study. The thickness of the vane blade was determined in consideration of the strength of the vane. The diameter of the vane shaft was determined in consideration of the vane area ratio which should be less than 12% as discussed in Chapter 2. The summary of the vane dimensions is given in Table 4.3. The area ratio of the vane is defined as the ratio of the cross sectional area of the vane to the crossed-sectional area of the sheared cylinder. For this type of vane, the area ratio can be calculated using the following equation:

$$R_A = \frac{8t(D-d) + \pi d^2}{\pi D^2} \times 100\% \tag{4.7}$$

Table 4.3: Geometry of the Vane Used in the Test

Vane Type	Blade Diameter $D(mm)$	Blade Height $H(mm)$	Shaft Diameter $d(mm)$	Blade Thickness $t(mm)$	Area Ratio (%)
4-Blades Rectangle	18	14	3.5	0.6	10.6

where R_A is the area ratio in percentage and d is the diameter of the vane shaft. The value of R_A in this study is 10.6%, as shown in Table 4.3.

4.2.3 Spring Calibration

As presented above, the torque is applied to the vane shaft through a torsional spring. The rotation angle of the spring reflects the shear resistance of the specimen. It is important to choose a suitable spring and properly calibrate it. In calibrating the torsional spring, a pulley was used to apply loads step by step to the spring and the readings of the rotation angle of the spring were taken from the graduated scale. A linear relationship between the torque applied and the rotation angle of the spring was observed. The spring has a constant of 4.63×10^{-3} N-m/degree.

4.2.4 Testing Procedures

As the shear vane tests were conducted in the tub which is 400 mm in depth and 300 mm in diameter, a large amount of clay slurry with a prescribed water

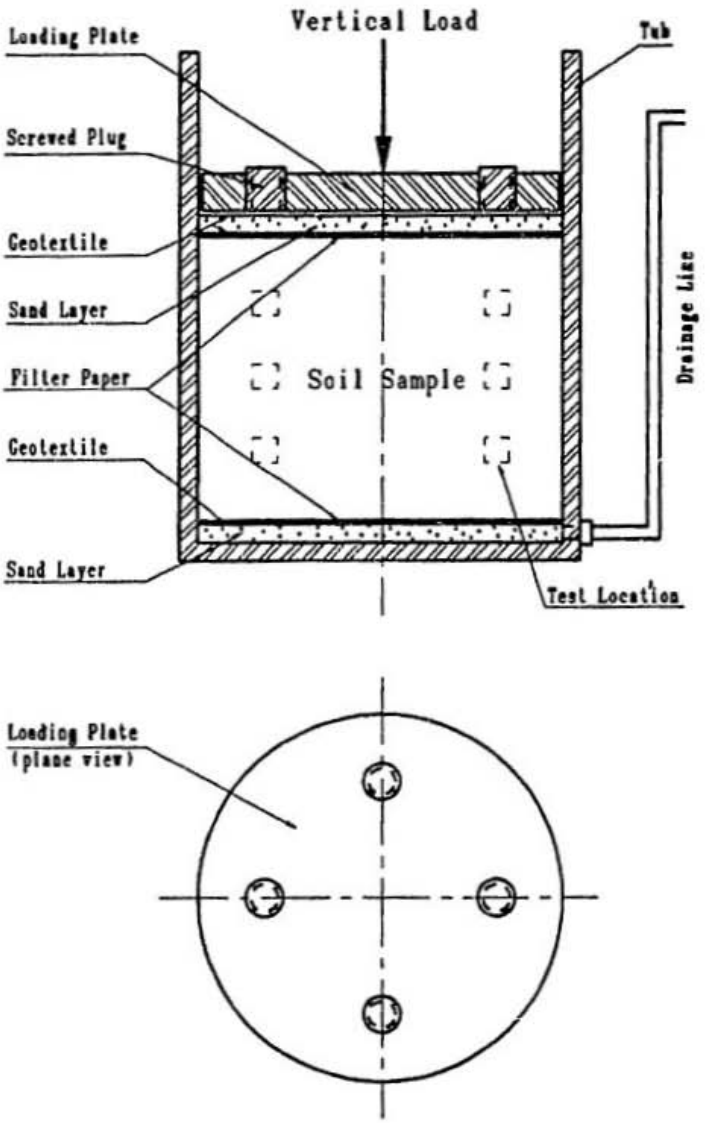

Figure 4.11: The Tub Used in the Vane Tests

content was mixed under vacuum. The initial water content of the kaolin and K-S was 100% and 70% respectively. In order to reduce friction between the soil and the wall of the container, the inside wall of the tub was coated with Vaseline before the slurry was poured in. Two pieces of geotextile and a 10mm layer of sand were placed at the bottom of the tub to permit bottom drainage. At the top surface of the slurry, geotextile with 4 holes cut according to the location of the holes on the loading plate was used. At the hole positions, filter papers were used instead of the geotextile. A layer of sand was placed on the geotextile; the sand was covered with a piece of geotextile which also had four hole positions covered by filter paper. The loading plate was placed gently on the specimen according to the hole positions of the geotextile as shown in Figure 4.11.

The loading bar was then placed on the plate and the vertical load was applied. The final vertical preconsolidation pressure (σ'_{v1}) was 400 kPa which was achieved through incremental loads of 4, 12, 25, 50, 100, 200 and 400kPa. During consolidation, vertical deformation was monitored. Each of the first 4 loading increments was maintained for 24 hours; the degree of consolidation at vertical loads of 100 and 200 kPa was 90% and 100% at 400 kPa before unloading or testing. The unloading increment was less than 150 kPa and swelling was permitted for at least 5 hours. The OCR values of the soil specimens during the vane tests ranged from 1 to 8 while the effective vertical stresses (σ'_{v2}) were 400, 200, 100, 66.7 and 50 kPa respectively.

In the ASTM D4648 (1993), it is recommended that the miniature vane test be conducted in soils with undrained shear strength less that 100 kPa. For the normally

consolidated K-S specimen under effective vertical stress of 400 kPa, the measured undrained strength of the soil was greater than 100 kPa; and so this measured result may not be reliable . Therefore, a vane test on a normally consolidated specimen under effective vertical stress of 200 kPa was conducted; the result of this test was used to obtain the undrained shear strength of the K-S mixture when OCR=1.

When the required effective vertical stress was achieved, free water at the top of the soil surface was removed using a vacuum cleaner. The screw plugs on the loading plate were removed and the water, drainage sand and filter paper in the holes were cleaned out before the vane tests were conducted.

The vane apparatus was attached to the tub by a mounting plate. The surface of the vane blades and the shaft was coated with Vaseline. The vane was carefully pushed through the hole until the top surface of the vane was just at the surface of the specimen. At this point the depth of the vane insertion was considered to be zero. The vane was then inserted at a penetration rate of 10 mm/min into the specimen to a depth 5 cm below the surface as shown in Figure 4.11. There was a 60 seconds delay for the kaolin before the vane shear was conducted and 30 seconds for K-S mixture. The difference of the time delay for the two soils was due to consideration for the difference in the coefficients of consolidation of the two materials.

The initial readings of the pointer on both inner and outer angular scales were taken. The vertical handle was rotated clockwise at such a steady rate that the rotation rate of the spring was 60° per minute. After the peak torque, the reading

on the inner scale did not increase and remained in position indicating the maximum rotation angle of the spring, from which the soil strength could be calculated. The time to cause failure in the soil was also recorded.

The spring was then released and refixed. The vane was inserted at the same rate as mentioned above to a depth 10 cm below the specimen surface. At this depth, another shear vane test was conducted in the same way as that at the 5 cm depth. Similarly, another vane test was also conducted at a depth of 15 cm. After completion of the vane tests, the vane was steadily raised out of the soil.

It should be mentioned that as the vane was inserted into the soil, shaft friction induced some resistance to the spring during the shear testing. This extra resistance should be deducted from the test data. As described above, the shear vane tests were conducted at depths of 5, 10, and 15 cm from the surface of the soil. Assuming that the resistance caused by the shaft friction is proportional to the length of the insertion, the real shear strength c_u can be obtained through linear regression using the test data at 5, 10 and 15 cm.

4.2.5 Test Results of Kaolin

The vane test results of the kaolin are shown in Table 4.4. In this table, $\bar{c_u}^*$ is the average value of 4 tests calculated from Equation (4.6) which includes the shaft friction part. c_u is the undrained shear strength with the shaft friction deducted from the average data. It can be seen that the undrained shear strength of the kaolin increases with increasing normal effective stress at shearing. The normalized shear strength c_u/σ'_{v2} increases with OCR. The data are shown in Figure 4.12.

Table 4.4: Shear Vane Test Results of Kaolin

OCR	σ'_{v1} (kPa)	σ'_{v2} (kPa)	Depth (cm)	$\bar{c}_u$ (kPa)	c_u (kPa)	c_u/σ'_{v2}
1	400	400	5.0 10.0 15.0	86.45 95.30 113.50	71.37	0.178
2	400	200	5.0 10.0 15.0	61.00 78.95 86.45	50.02	0.250
4	400	100	5.0 10.0 15.0	50.40 61.00 65.75	43.70	0.437
6	400	66.7	5.0 10.0 15.0	46.65 56.65 60.95	40.45	0.606
8	400	50	5.0 10.0 15.0	42.10 44.85 50.70	37.28	0.746

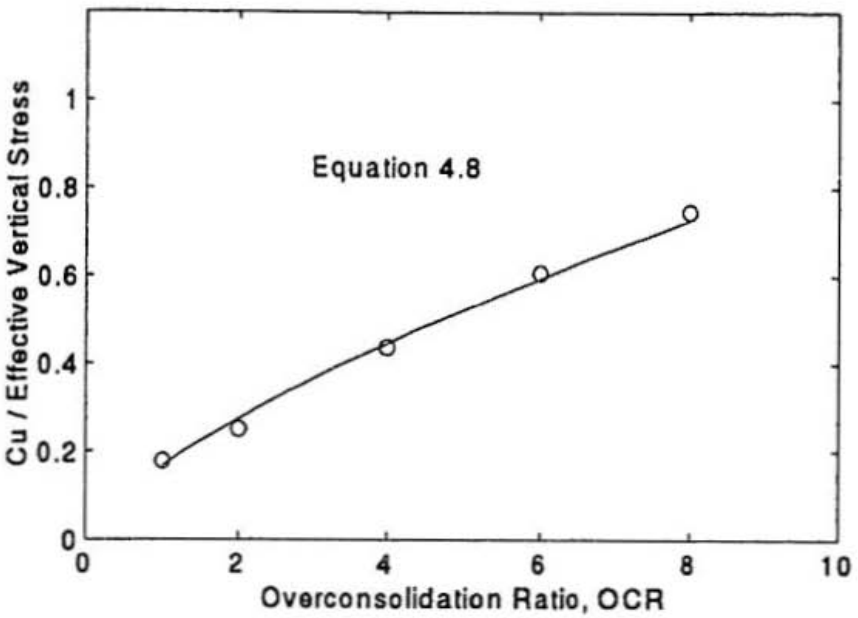

Figure 4.12: Normalized Shear Strength of Kaolin with OCR by Vane

These test results can also be used to determine the soil parameters α and β of Equation (1.4). The undrained shear strength determined from vane testing can be expressed as

$$\frac{c_u}{\sigma_v'} = 0.167(OCR)^{0.707}. \tag{4.8}$$

4.2.6 Test Results of Kaolin-Silt Mixture

The shear vane results of the K-S mixture are shown in Table 4.5. In the table, $\bar{c}_u^*$ is the average value of 2 to 5 tests of undrained shear strength calculated from Equation (4.6) which includes the shaft friction part. c_u is the undrained shear strength with the shaft friction deducted from the average data. The results are shown in Figure 4.13.

Table 4.5: Shear Vane Test Results of K-S

OCR	σ'_{v1} (kPa)	σ'_{v2} (kPa)	Depth (cm)	$\bar{c}^{*}_{u}$ (kPa)	c_u (kPa)	c_u/σ'_{v2}
1	200	200	5.0 10.0 15.0	62.15 72.20 81.65	52.50	0.263
2	400	200	5.0 10.0 15.0	89.54 111.17 121.97	75.13	0.376
4	400	100	5.0 10.0 15.0	69.31 78.16 86.11	61.06	0.611
6	400	66.7	5.0 10.0 15.0	66.88 75.48 82.45	59.36	0.890
8	400	50	5.0 10.0 15.0	52.70 57.35 61.90	48.12	0.962

From the test data in Table 4.5, the undrained shear stress of kaolin-silt mixture can be expressed as

$$\frac{c_u}{\sigma'_v} = 0.253(OCR)^{0.657}. \tag{4.9}$$

4.2.7 Effect of Repeated Loading

The test data shown in Table 4.4 is for kaolin under the first loading cycle. The soil was consolidated under a vertical stress of 400 kPa and then the vane test was carried out or the soil was unloaded to a prescribed OCR for the vane test. In addition, vane tests of kaolin under repeated loading and unloading were also carried

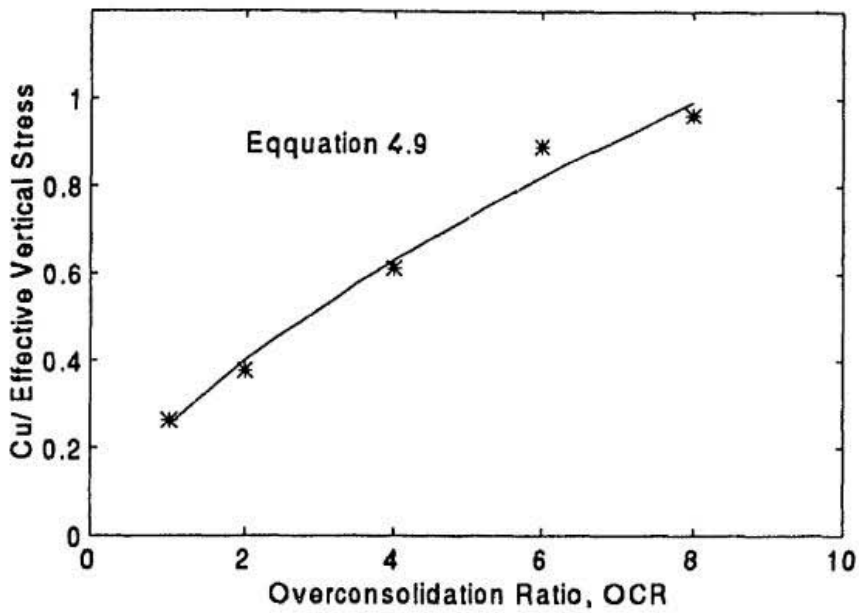

Figure 4.13: Normalized Shear Strength of K-S with OCR by Vane

out to investigate the effect of repeated loading. For the repeated loading test, the soil sample was consolidated under a vertical stress of 400 kPa and then was fully unloaded in steps; when the swelling was complete, the sample was reloaded from zero to 400 kPa. After the soil consolidation under this vertical stress of 400 kPa was complete, the vane test was carried out or the soil was unloaded to a prescribed vertical stress for testing under overconsolidation conditions. The vane tests were conducted at OCR levels of 1 to 8 while the vertical stresses were 400 to 50 kPa respectively. The test results of the kaolin which experienced repeated loading are shown in Table 4.6, in which, $\bar{c}_u^*$ is the average value of two tests. The undrained shear strength can be expressed as

$$\frac{c_u}{\sigma_v'} = 0.243(OCR)^{0.545}. \tag{4.10}$$

Table 4.6: Shear Vane Results of Kaolin under Repeated Loading

OCR	σ'_{v1} kPa	σ'_{v2} kPa	Depth (cm)	$\bar{c}_u^*$ kPa	c_u kPa	c_u/σ'_{v2}
1	400	400	5.0 10.0 15.0	104.40 111.00 118.45	97.23	0.243
2	400	200	5.0 10.0 15.0	80.10 84.40 90.55	74.57	0.373
4	400	100	5.0 10.0 15.0	53.25 60.10 67.80	45.83	0.458
6	400	66.7	5.0 10.0 15.0	50.75 57.35 58.70	44.92	0.673
8	400	50	5.0 10.0 15.0	43.00 48.00 51.85	38.77	0.775

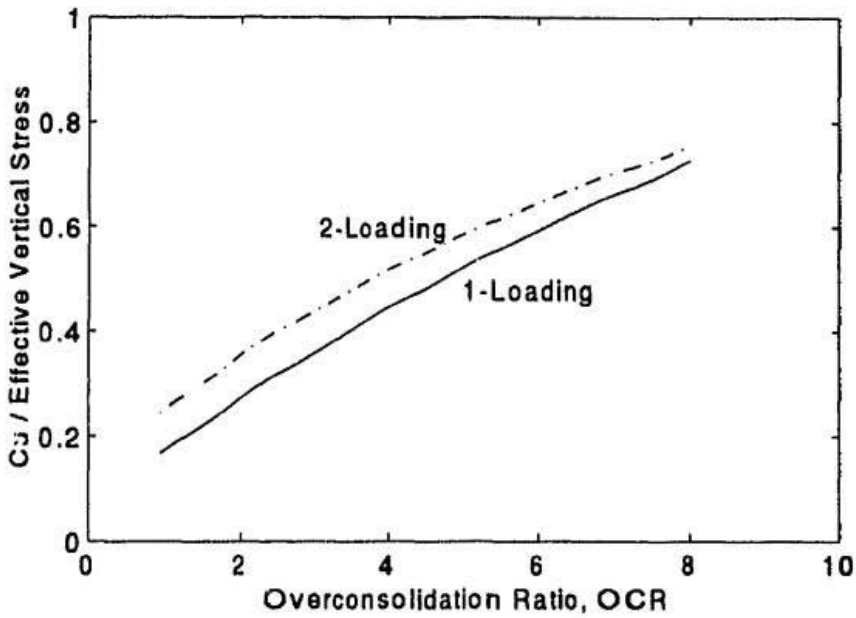

Figure 4.14: Effect of Repeated Loading on Kaolin

Comparison of Equation (4.8) and Equation (4.10) indicates the the repeated loading increases the strength parameter α value and decreased the β value, as shown in Figure 4.14. It can be seen that within the OCR levels of the tests, the strength of kaolin under repeated loading is greater than that under first loading. The ratio of the shear strength under repeated loading to that of first loading decreases with OCR. This ratio is 1.46 when OCR=1 and only 1.04 when OCR=8.

Chapter 5

Cone Penetration Testing

The shear strength of the kaolin and K-S has been investigated by the direct shear tests and shear vane tests and the results have been presented in Chapter 4. In addition, cone penetration tests on the K-S clay were conducted during flight at 50 *g* in a centrifuge. These tests were conducted in both small and large tubs. In the large tub tests, trenches were carved on the overconsolidated K-S clay and backfilled with K-S slurries of different water contents before the centrifuge was started. The cone tests were then conducted in both the native and backfilled K-S clays.

To provide some background about centrifuge modelling, this chapter introduces some basic principles of centrifuge modelling and the scaling laws, the centrifuge facility and the cone penetrometer used in this study. Procedures in specimen preparation will also be presented. The method of interpreting shear strength from cone tip resistance is discussed and the interpreted shear strength is shown.

5.1 Principles of Centrifuge Modelling

In model tests, similarity of both stresses and strains are required between the prototype and the model. In geotechnical modelling, as soil is a highly non-linear material, it is very difficult to find a model scale to provide similarity of self-weight stresses between model and prototype. However, by increasing the self-weight of the model in a centrifuge, the response of soil to self-weight loads can be properly represented in the model tests. In centrifuge tests, reduced scale soil models are normally constructed using the same materials as the prototype. They are placed in a strongbox which is rotated at a prescribed angular velocity ω. If the centrifuge radius is r, then the centripetal acceleration experienced by the model in the flight is given by

$$a = r\omega^2$$

and this acceleration a induces self-weight forces in the soil mass (Mitchell, 1991).

If a $1{:}N$ time scale model is subjected to a centripetal acceleration a, which is N times of the gravitational acceleration, that is,

$$a = Ng$$

the stress distributions of the prototype and model will be similar, as shown in Figure 5.1. The strain profile will also be similar because the constitutive laws governing the soils are the same. Furthermore, if any external loading is added to the self-weight loading, these must be scaled so that the corresponding stress profile is maintained. Under these conditions, the reaction of the model to the external loading will be similar to that of the prototype (Poorooshasb, 1990).

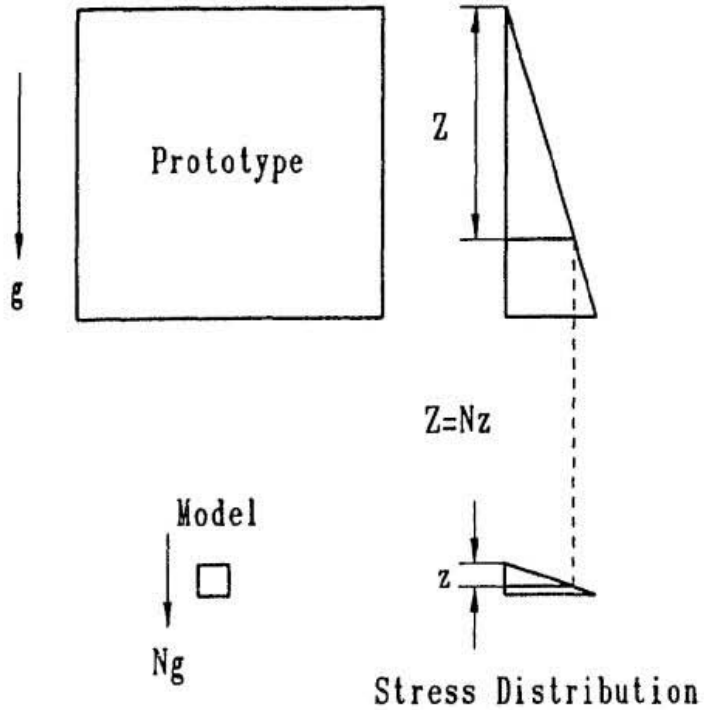

Figure 5.1: Correspondence of Stress Between Prototype and Model

If the centrifuge modelling test is conducted at Ng, the acceleration scale is given by

$$\frac{a_m}{a_p} = N$$

Where, subscript m — model

p — prototype.

Assuming the material mass density of the prototype is equal to the mass density of the model, for stress scale

$$\frac{\sigma_m}{\sigma_p} = 1,$$

and the geometric scale is given by

$$\frac{L_p}{L_m} = N.$$

Subsequently, other scale factors can be obtained as following:

Area:

$$\frac{A_p}{A_m} = N^2$$

Unit Weight:

$$\frac{\gamma_m}{\gamma_p} = \frac{\rho a_m}{\rho a_p} = N$$

Strain:

$$\frac{\varepsilon_m}{\varepsilon_p} = 1$$

External Force:

$$\frac{F_m}{F_p} = \frac{\sigma_m A_m}{\sigma_p A_p} = \frac{1}{N^2}$$

Self-weight Force:

$$\frac{F_{wm}}{F_{wp}} = \frac{\gamma_m L_m^3}{\gamma_p L_p^3} = \frac{1}{N^2}$$

The aim of centrifuge modelling is to obtain the same mechanical behaviour of the soil body at the corresponding points of the model such as at depth z in the model and at depth Nz in the prototype, as indicated in Figure 5.1.

5.2 C-CORE Centrifuge Centre

The cone penetration tests on K-S model clay were conducted at the C-CORE Centrifuge Centre which was opened on June 30, 1993. This centrifuge centre is located on the north campus of Memorial University of Newfoundland. It is a two-storey building, consisting of laboratories, workshops, offices, a control room and a circular chamber in which an Acutronic 680-2 centrifuge is housed. This centrifuge

is capable of carrying loads up to 2.2 tons to 100 gravities or 650 kg to 200 gravities. The maximum rotational speed is 189 rpm while the maximum acceleration of the package at an effective radius of 5.0 m is 200 gravities. The model is contained in a large strongbox with a usable internal area of 110cm×140cm in plan and 40cm in height. During centrifuge tests, the strongbox is placed on the swinging platform at one end of the rotor. The other end of the rotor holds counter-balancing weights. Visual monitoring of the centrifuge is achieved through television cameras mounted around the inside wall of the chamber. The models can also be monitored through a camera mounted on the strongbox. Electrical signals from transducers are acquired by a data acquisition system using a PC-compatible 486 computer. Water may be supplied to the model during testing.

5.3 Test Design

5.3.1 Cone Penetrometer

To conduct cone penetration tests during centrifuge flight, a cone penetrometer apparatus was developed (Cunard, 1993). This apparatus is capable of moving at a constant speed to different positions along a fixed direction through a horizontal driving system. It is fixed on the top of the strongbox at the required position before the centrifuge testing is started. The penetrometer used in this study has a cross-sectional area of 1 cm^2 with an apex angle of 60^0 as shown in Figure 5.2. This penetrometer measures tip resistance, q_c, through strain gauges mounted behind the cone tip. During centrifuge flight, the cone penetrometer was pushed vertically into the model clay at a rate of 3mm per second and the response of the strain gauges was recorded by the data acquisition system. Movement of the cone during the

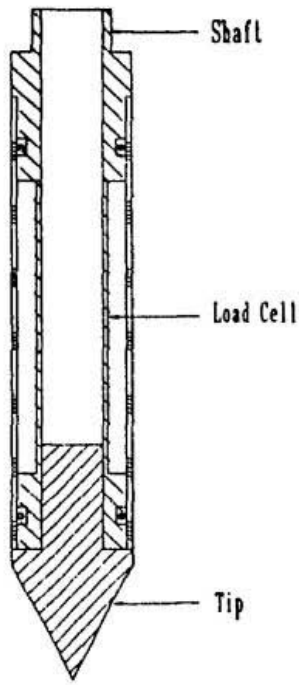

Figure 5.2: Cone Used in the Tests

test can be observed through the camera mounted inside the swinging basket. The calibration factors of the tip resistances are 808.65 kPa/mV (for small tub tests), 814.51 kPa/mV (for large tub I tests) and 843.0 kPa/mV (for large tub II tests).

5.3.2 Small Tub Cone Penetration Tests

Three cone penetration tests in small tubs were carried out to complement the direct shear and vane tests. The K-S slurry was consolidated one-dimensionally in a circular tub following the same procedures as described for the vane tests. When 100% consolidation was reached under a vertical pressure of 400 kPa, the specimen was unloaded. The unloading order was 400 - 250 - 140 - 0 kPa. When the specimen was totally unloaded, the tub was removed from the loading frame and the specimen was trimmed to the required height. Pore pressure transducer PPTs

were inserted into the specimen to monitor the dissipation of pore pressure during the consolidation of soil in centrifuge flight. A linear displacement transducer (LDT) was mounted on the surface of the specimen to monitor the vertical movement of the surface. The unit weight of the specimen was 19.1 kN/m^3. The three small tub tests are briefly introduced below:

Small Tub 1 (S1): The total height of the overconsolidated specimen was 205mm. The water table was kept approximately at 20mm above the soil surface. A PPT was inserted at a depth 102.5 mm below the surface of the specimen.

Small Tub 2 (S2): The total height of the specimen was 150 mm. The water table was approximate 90 mm below the specimen surface. A PPT was at a depth 120 mm below the specimen surface.

Small Tub 3 (S3): The total height of the specimen was 150 mm. The water table was approximate 90mm below the specimen surface. To prevent desiccation during centrifuge flight, the soil surface was covered with Vaseline. PPT#1 was at a depth of 123 mm and PPT#2 was 127 mm below the surface of the specimen.

After preparation of the specimen, the tub was transferred into the centrifuge strongbox (also known as the large tub) and connected to the water supply. Electronic cables were connected for cone control and data acquisition. Initial readings were taken just before the centrifuge was started. The centrifuge was started from rest and accelerated in increments of 10g until 50g was reached. The g-level was maintained for several minutes at each increment. Monitoring of LDT's and PPT's started while the centrifuge was still at rest. When 90% consolidation of

the soil sample was reached, the cone penetration test was conducted at the rate of 3mm/second. All data were recorded by the data acquisition system. When the test was completed, the penetrometer was removed from the soil and the centrifuge was stopped. Soil cores were taken immediately after the testing for the measurement of water content.

5.3.3 Large Tub Cone Penetration Tests

The large tub tests were designed to verify the results of the $50g$ small tub tests and direct shear and shear vane test results. Moreover, trenches were carved in the specimen and backfilled with kaolin-silt slurry. Cone penetration tests were conducted in both the native and backfilled materials.

The centrifuge cone penetration tests were carried out in the specimen consolidated in the large rectangular strongbox, noted as the large tub. The K-S mixture was consolidated under a 400 kPa vertical load and then unloaded to zero. After the specimen was unloaded, the tub was removed from the loading frame. The specimen was shaved to a 15 cm height and 4 trenches of 80mm in depth were carved and backfilled. PPTs and LDTs were mounted for monitoring the deformation and pore pressure. The details of the large tub tests are described in the next section.

Large Tub 1 (L1): Four trenches were carved in the overconsolidated soil specimen. The trenches had a depth of 80mm, a width of 60mm and a length of 150mm and were lined in two transects as shown in Figure 5.3. K-S slurry with a water content of 40% was backfilled into these trenches. Along the A-A transect, the native soil was permitted to desiccate. In the trenches $a1$ and $a2$,

no attempt was made to prevent the migration of water from the backfill material into the native material during consolidation in centrifuge flight. Along transect B-B, the soil surface was coated with Vaseline to prevent desiccation due to the air flow across the sample during rotation of the centrifuge. In trench *b*1, the wall and base were lined up with Vaseline, while in trench *b*2, the wall and base were lined up with strips of plastic film with the purpose of preventing water migration from the backfill slurry to native soil. After equilibrium was reached in the centrifuge at $50g$, the cone penetration tests were conducted in both native and backfill materials along transects A-A and B-B as shown in Figure 5.3.

Large Tub 2 (L2): The surface area of the native specimen was all coated with Vaseline. Six trenches, 190mm long, 55mm wide and 80mm deep, were carved in the specimen and lined in three transects, as shown in Figure 5.4. Along transect A-A, the two trenches were backfilled with K-S slurry with a water content of 65%. The wall and base of the trenches were coated with Vaseline. Trenches along transect B-B were backfilled with a slurry of 75% water content. Trench *b*1 was covered with Vaseline on the wall and the bottom. In trench *b*2, the backfill slurry was allowed to drain into the native material. Along transect C-C, slurry having water content of 55% was used for backfill. Trench *c*1 was coated with Vaseline on the wall and the bottom. In trench *c*2, no attempt was made to prevent backfill slurry draining into the native material. The surface of the backfill slurry was all covered with plastic film to prevent desiccation. After equilibrium was reached in the centrifuge at $50g$, a series of cone tests were conducted in both native and backfill materials along transects A-A, B-B and C-C as shown in the figure.

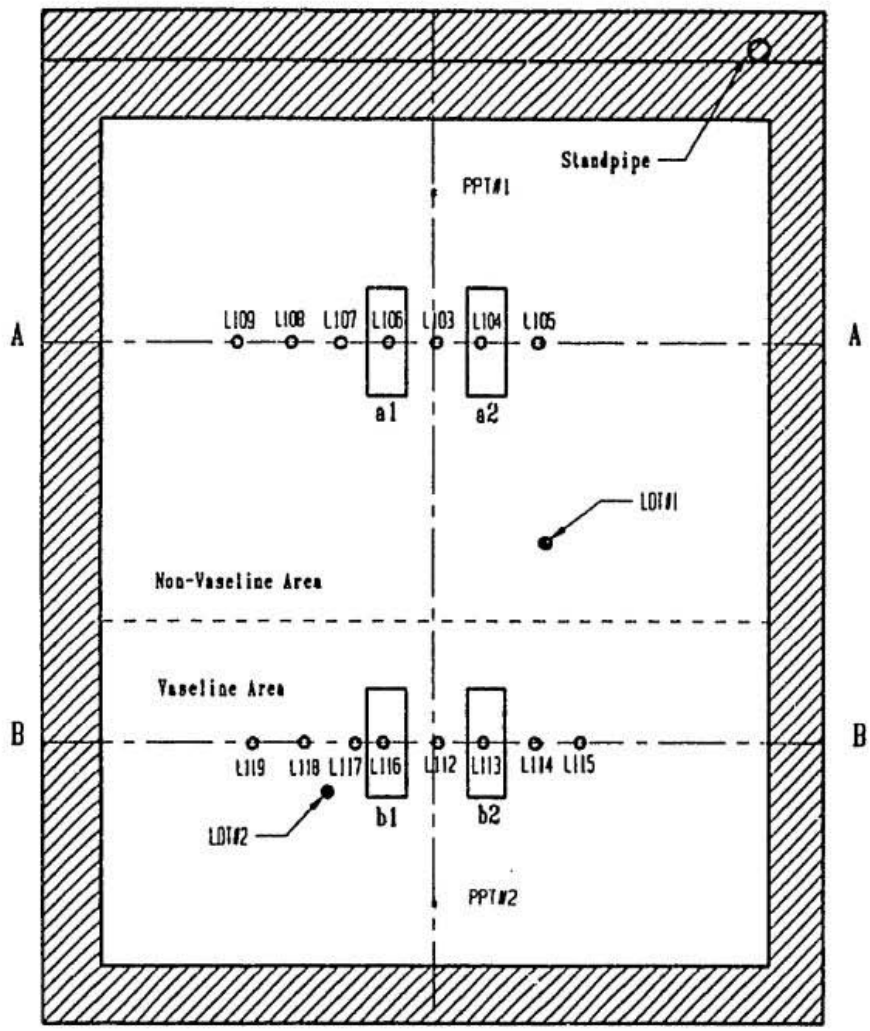

Figure 5.3: Test Design of Large Tub I

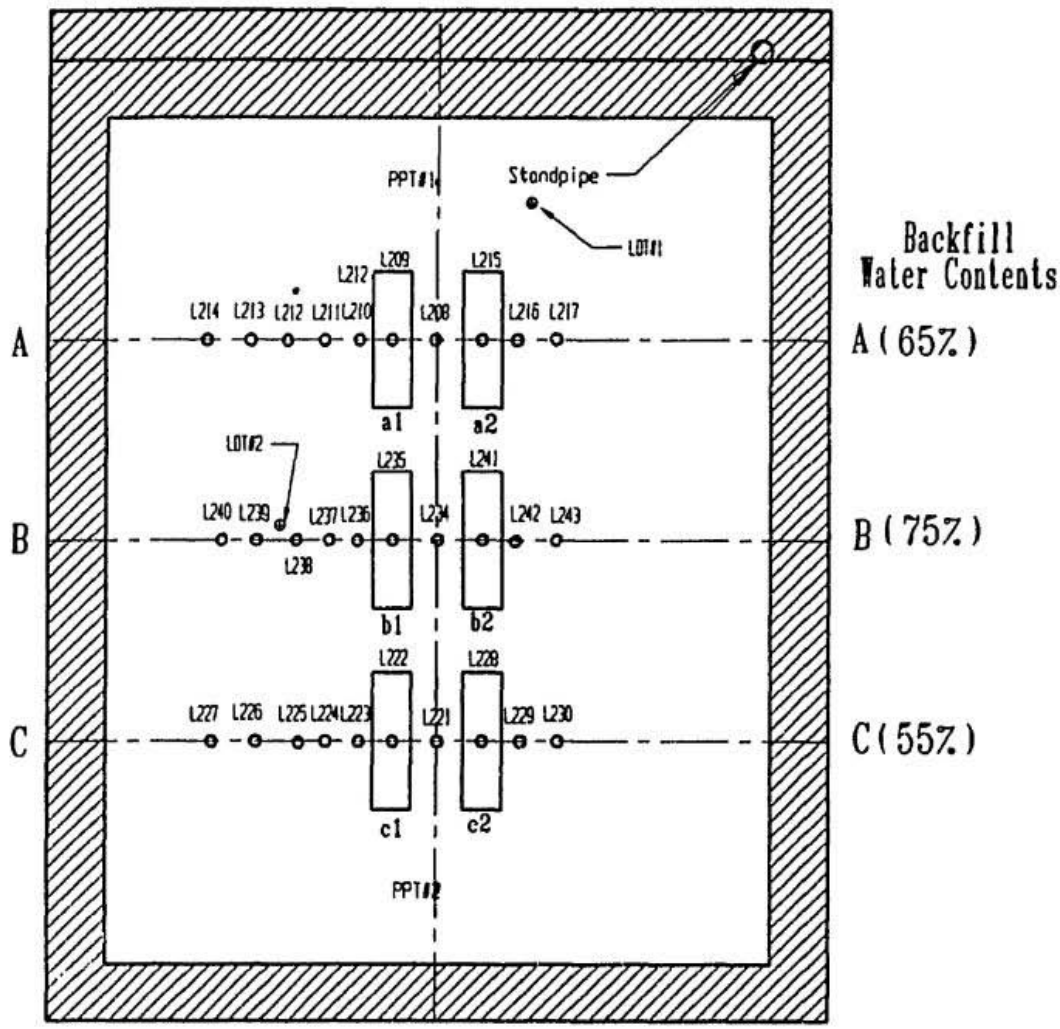

Figure 5.4: Test Design of Large Tub II

5.4 Cone Tip Resistances

The numbers and the positions of the cone tests conducted during centrifuge flight are shown in Figure 5.3 and Figure 5.4. Some results of cone tests are given in Appendix B. In cone test S103, the water table was kept above the soil surface, while in test S205, the water table was kept approximate 90 mm below the specimen surface. It can be seen from Figure 5.5 that the recorded tip resistance of the submerged specimen (S103) is lower than that of test S205.

During centrifuge flight, the surface of the model clay may exhibit desiccation which can be observed from the surface of the clay and also can be reflected in the measured tip resistance as shown in Figure 5.6. In this figure, test S205 and S303 were performed on the same material with the water table below the soil surface. However, the surface of the model clay in test S205 was exposed to air while the surface of the clay in test S303 was covered with a thin layer of Vaseline. From Figure 5.6, it can be seen that the desiccation during centrifuge flight is significant. The near surface soil shear strength of test S303 is much lower than that of test S205.

In the cone tests conducted in large tub I, the backfilled K-S slurry had an initial water content of 40%. Although the backfilled slurry may consolidate due to self-weight during centrifuge flight, it can be seen from Figure 5.7 that the tip resistance of the backfill K-S in test L106 and the native soil (L108) was different.

In large tub II cone tests, L228 and L241 were conducted in the backfill with water contents of 55% and 75% respectively. In these two tests, the backfilled

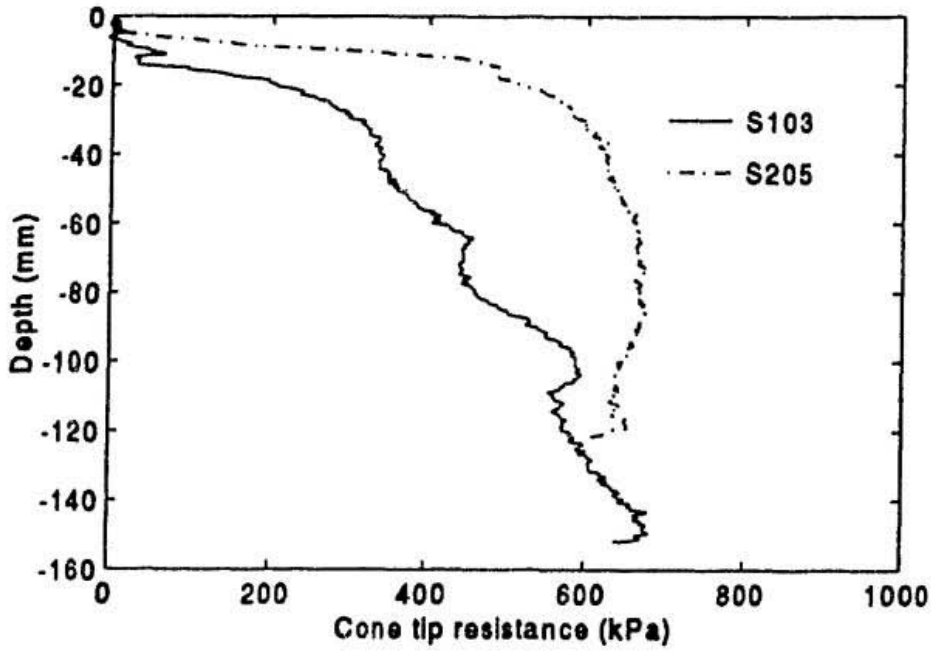

Figure 5.5: Effect of Water Table in Centrifuge Test

K-S slurry was consolidated by its self-weight under $50g$ with the water allowed to migrate into the adjacent native K-S soil. In Tests L215, L222 and L235, no water was allowed to migrate into the native soil because the trenches were covered with Vaseline. Differences in tip resistance can be seen in Figure 5.8 and Figure 5.9 It was observed that the drained water accumulated on the top of the slurry surface. In Figure 5.10, test L235 and L241 were conducted in the backfill K-S soil which has a water content of 75%, but test L235 was conducted in the trench which was surrounded with Vaseline.

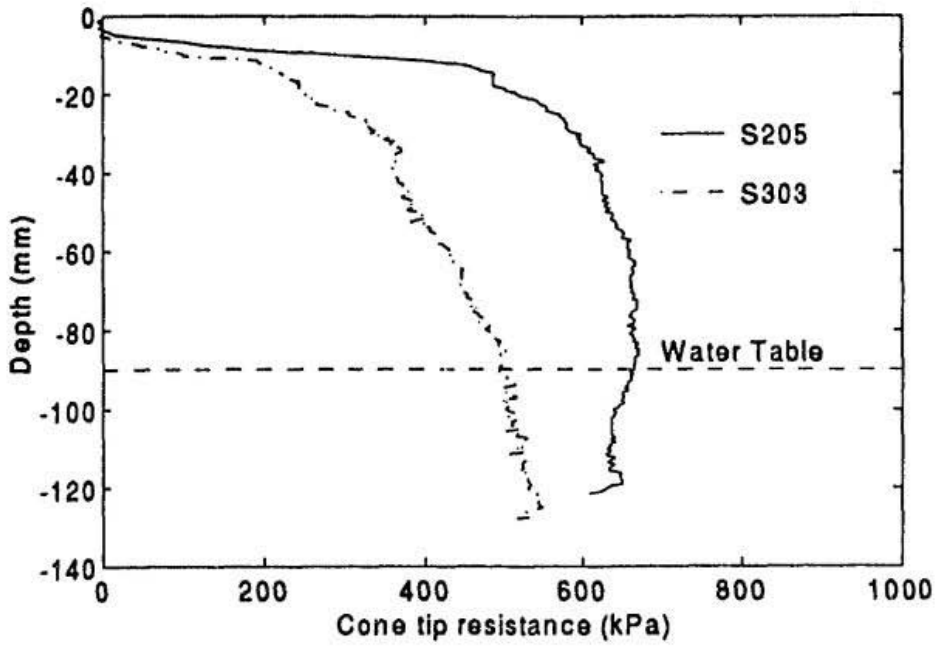

Figure 5.6: Effect of Surface Desiccation During Centrifuge Flight

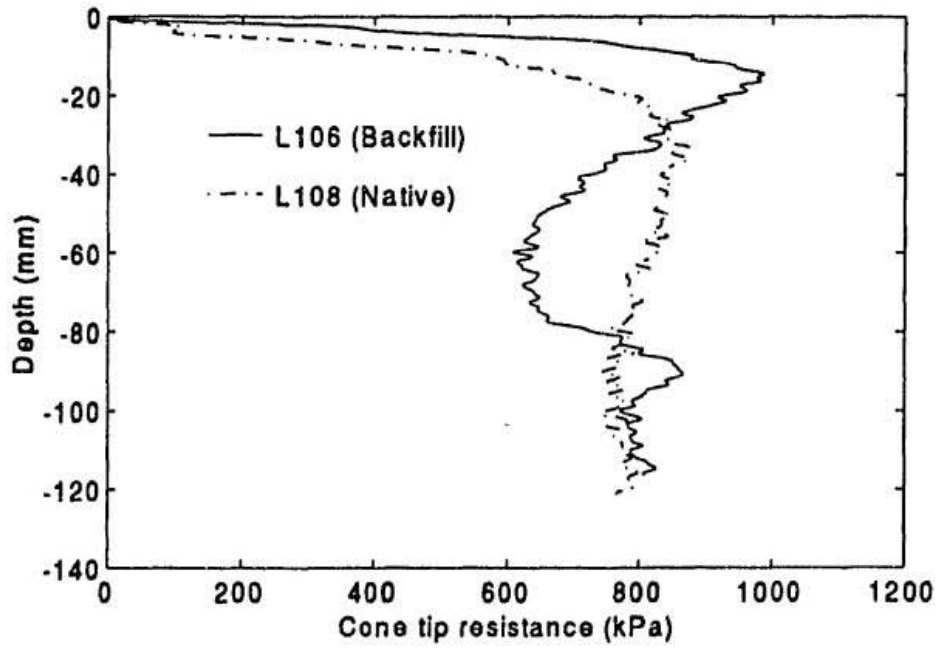

Figure 5.7: Tip Resistance of Native and Backfill Clay

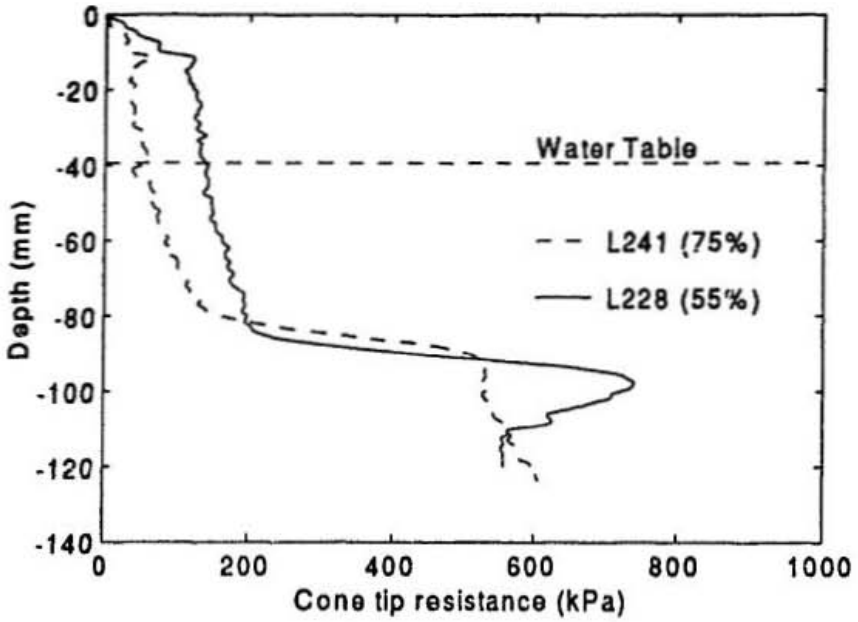

Figure 5.8: Tip Resistance of Backfill with Different Water Contents (with Water Migration to the Native Clay)

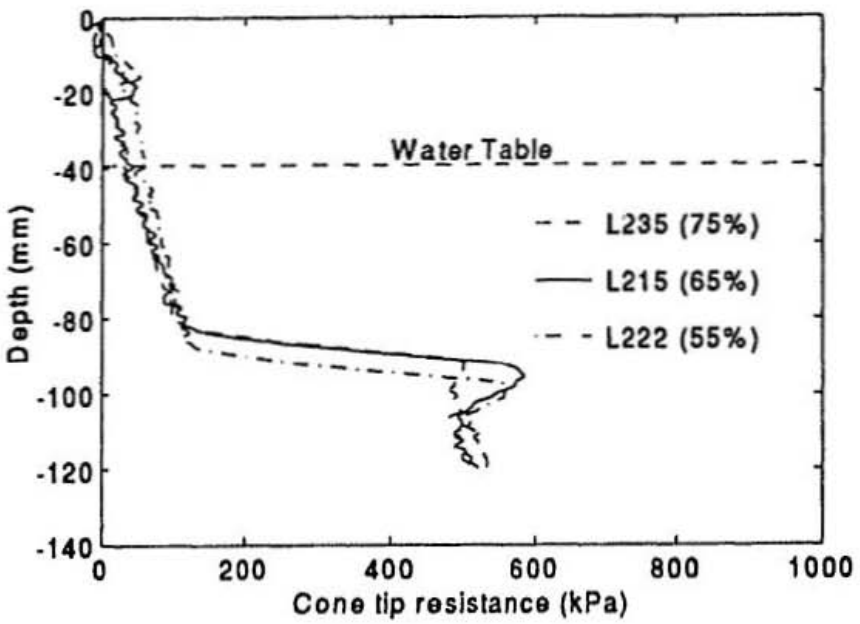

Figure 5.9: Tip Resistance of Backfill with Different Water Contents (without Water Migration to the Native Clay)

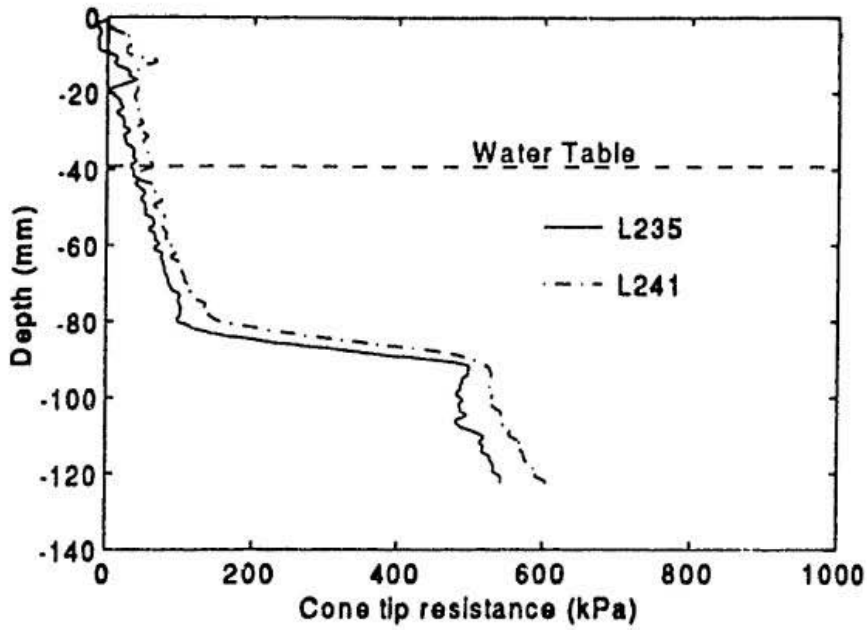

Figure 5.10: Effect of Water Migration

5.5 Undrained Shear Strength (c_u)

5.5.1 Selection of Cone Factor N_c

Schmertmann (1975) links the tip resistance with undrained shear strength using

$$c_u = \frac{q_c - \sigma_{vo}}{N_c} \tag{5.1}$$

where σ_{vo} is the total vertical stress and N_c is the cone factor.

Lunne and Kleven (1981) show that N_c is not a constant. It is related to the type of cone, the rate of penetration, the type of soil and the overburden pressure. Also, the value of N_c for normally consolidated clay is lower than that for overconsolidated clay (Meigh, 1987). Eide (1974) conducted cone tests and correlated tip resistance with field vane shear strength. The cone factor N_c ranged roughly from 8 to 12

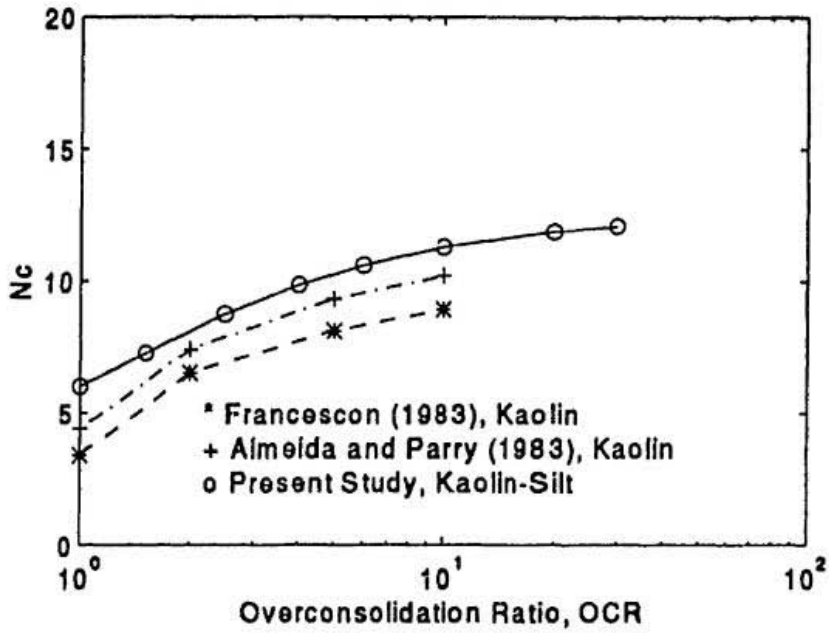

Figure 5.11: Relationship between Cone Factor N_c and OCR

for clays having shear strength values in the range of 49 to 294 kPa. Also, Bowles (1977) pointed out that for natural clays, this N_c is typically 8-12. The values of N_c of normally consolidated kaolin clay is approximately 4 to 5 (Francescon, 1983; Almeida and Parry, 1983). For the kaolin-silt mixture, as its properties are between those of kaolin clay and natural clays, a N_c value of 6 was selected in this study.

In overconsolidated clays, N_c increases with OCR (Almeida and Parry, 1983). The value of N_c for overconsolidated kaolin clay increases with OCR as shown in Figure 5.5. In the present study, an N_c value of 6 was chosen for normally consolidated K-S clay. Assuming the N_c - OCR curve is approximately parallel to the curves obtained by Almeida and Parry (1983) and Francescon (1983), as shown

in Figure 5.11, the N_c value of this study can be expressed as

$$N_c = 12.5\frac{OCR}{1.08 + OCR}. \tag{5.2}$$

This expression for N_c is used in this study for the interpretation of the shear strength of soil from cone tip resistance q_c and its reliability will be discussed in the next chapter.

5.5.2 Determination of c_u from CTP Data

As introduced before, Equation 5.1 can be used to determine shear strength c_u from the cone tip resistance. The cone factor N_c in Equation 5.1 for K-S clay is given in Equation 5.2. The cone tip resistance used to determine the typical shear strength is the average values of 4 cone tests (L214, L230, L240 and L243) from large tub II, as shown in Figure 5.12, Figure 5.13 and Figure 5.14. These four cone tests were chosen because the K-S specimen in large tub II tests was covered with Vaseline and the effects of desiccation were minimized. These tests were conducted in the positions far away from the trenches.

As the K-S clay in this study was tested under 50 gravities, the scale factor is 50 according to the centrifuge principles. The model clay may represent a 50 times thicker prototype in 1-g situation. The effective vertical stress in the soil can be expressed as

$$\sigma_v^{'} = \sigma_{vo} - u \tag{5.3}$$

where $\sigma_v^{'}$ is effective vertical stress (kPa), σ_{vo} is total stress and u is pore water pressure. The overconsolidation ratio is given by

$$OCR = \frac{\sigma_{v1}^{'}}{\sigma_{v2}^{'}} \tag{5.4}$$

where σ'_{v1} is the preconsolidation pressure, which is 400 kPa here.

The unit weight of K-S of the L2 tests was 19.1 kN/m^3 (average value of the unit weight measured directly and the unit weight calculated from water content of the soil before centrifuge testing). Part of the K-S specimen was submerged in the water. The water table can be determined from the pore pressures measured from the PPT results. Figure 5.15, Figure 5.16 and Figure 5.17 are the measured pore pressures of K-S during the consolidations in L2 tests. The cone tests were conducted at about 250 minutes after the specimen was consolidated. The surface settlements of the specimen measured from the LDTs during the consolidation are shown in Figure 5.18 for transect A-A. (The surface settlements of the transect B-B and C-C tests are shown in Appendix C).

It is assumed that the excess pore pressure generated during the swing up of the centrifuge was thoroughly dessipated when the cone tests were conducted. The pore pressure at the end of the consolidation is considered to be the hydro-static pressure. The point of zero pore pressure is located at the water table position. The average position of the water table of the large tub II tests was calculated to be 39.4 mm below the soil surface. For the specimen above the water table, as the surface of the specimen was covered with Vaseline, there was pore suction which had the same slope as the hydro-static pressure as shown in Figure 5.19. From the effective stress shown in this Figure, the OCR profile of the specimen can be obtained using Equation 5.4, as shown in Figure 5.20. The average shear strength of the K-S from the cone tests using Equation 5.2 is shown in Figure 5.21.

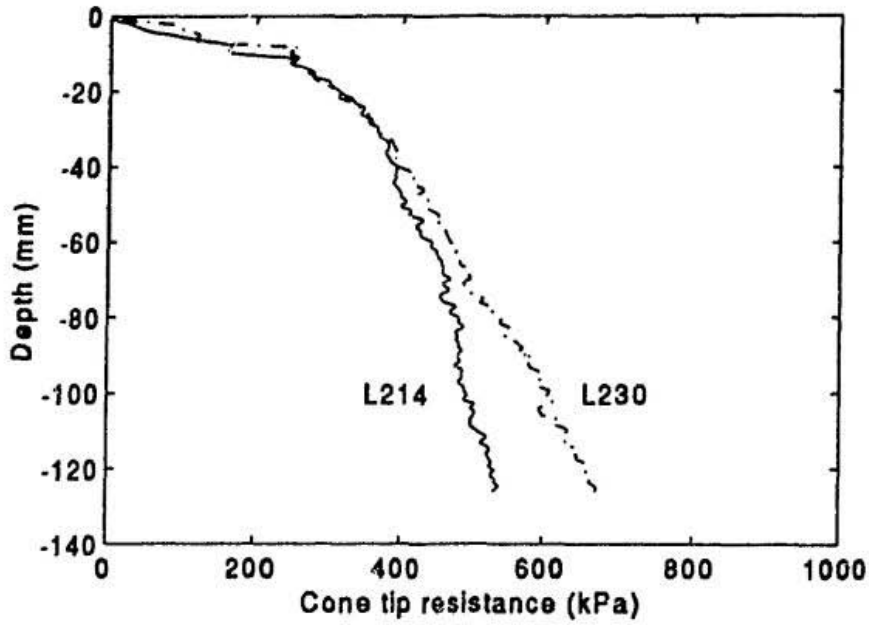

Figure 5.12: Tip Resistance of Test L214 and L230

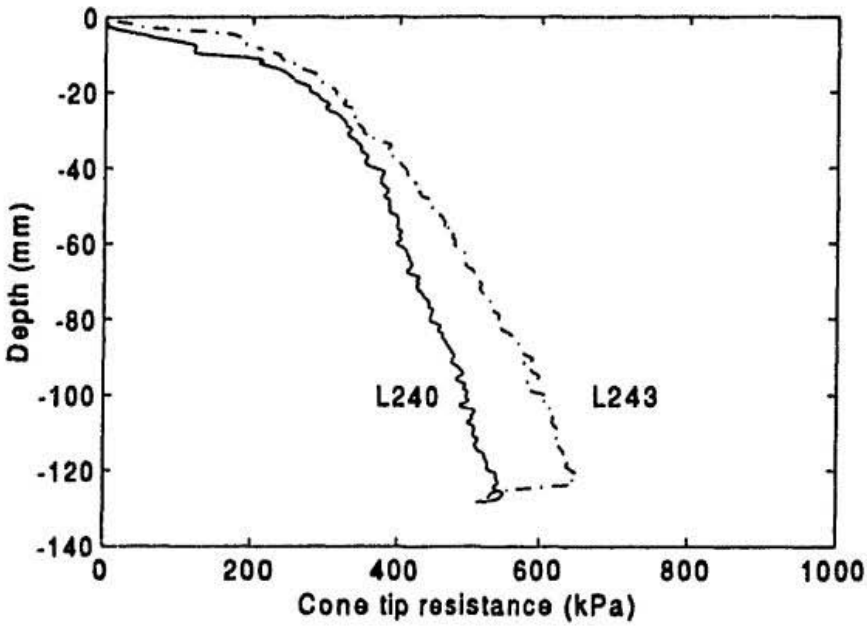

Figure 5.13: Tip Resistance of Test L240 and L243

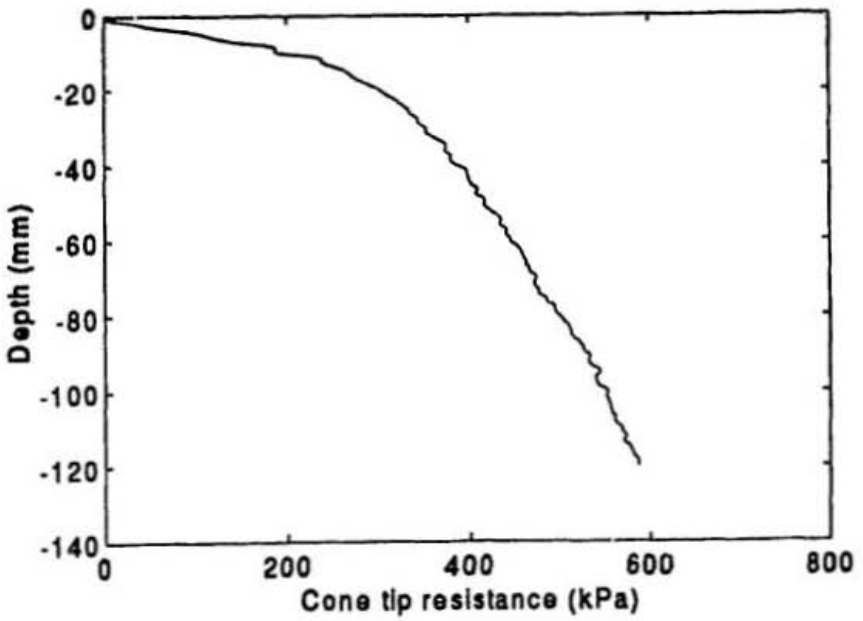

Figure 5.14: Average Tip Resistance of tests L214, L230, L240 and L243

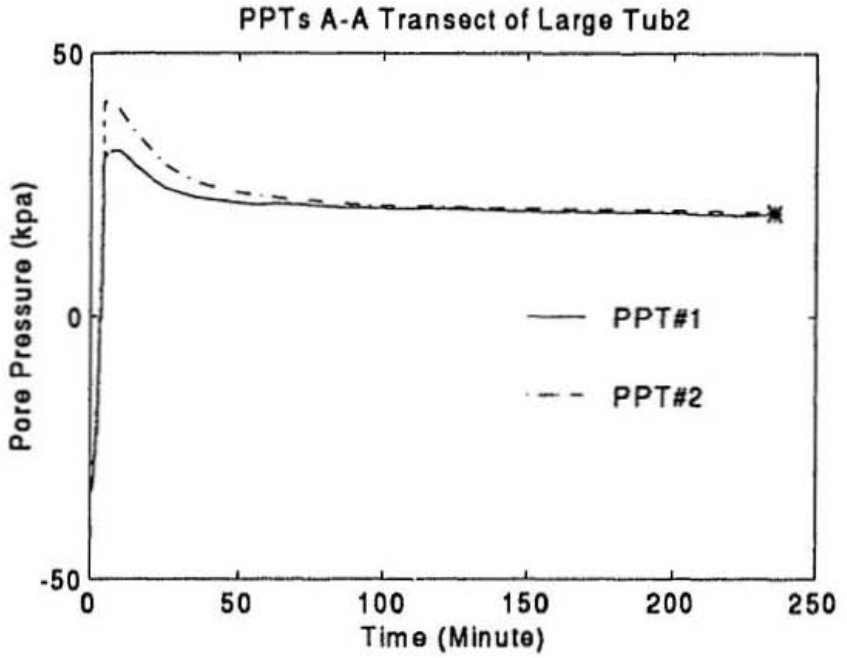

Figure 5.15: Pore Pressure during the consolidation of Transect A-A Tests

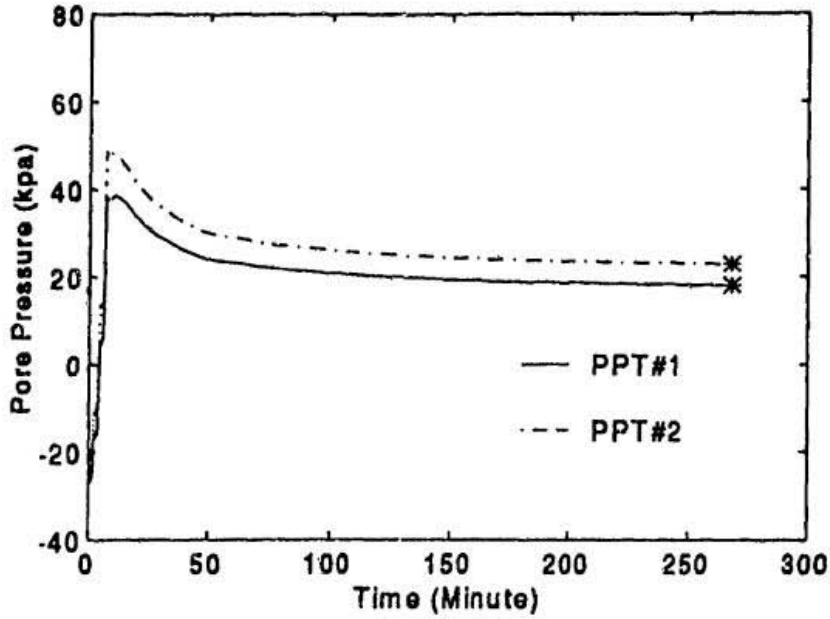

Figure 5.16: Pore Pressure during the consolidation of Transect B-B Tests

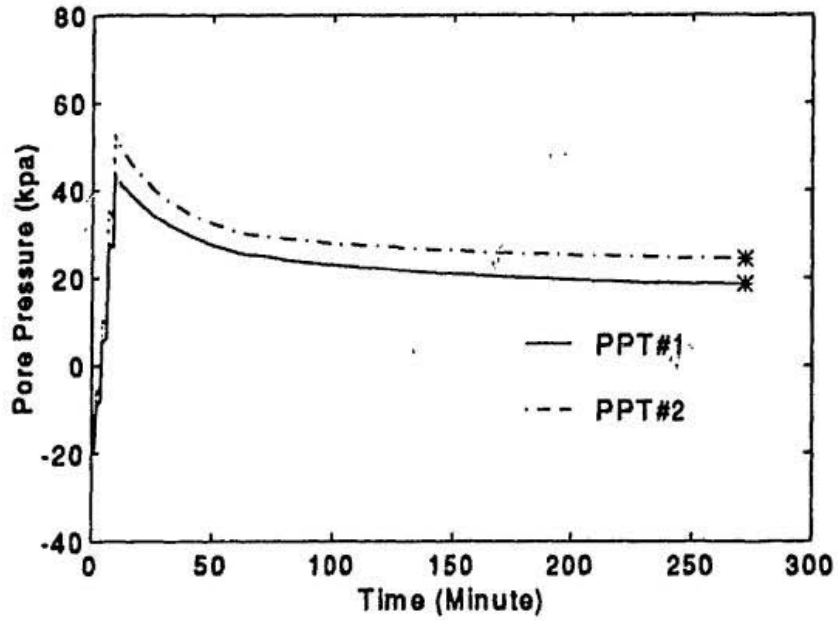

Figure 5.17: Pore Pressure during the Consolidation of Transect C-C Tests

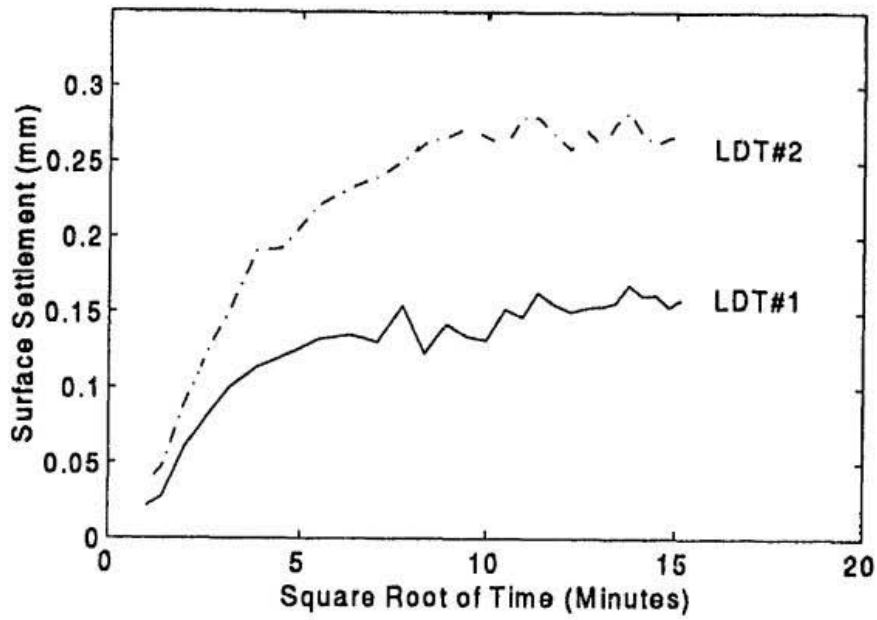

Figure 5.18: Surface Settlement during the Consolidation of Transect A-A Tests

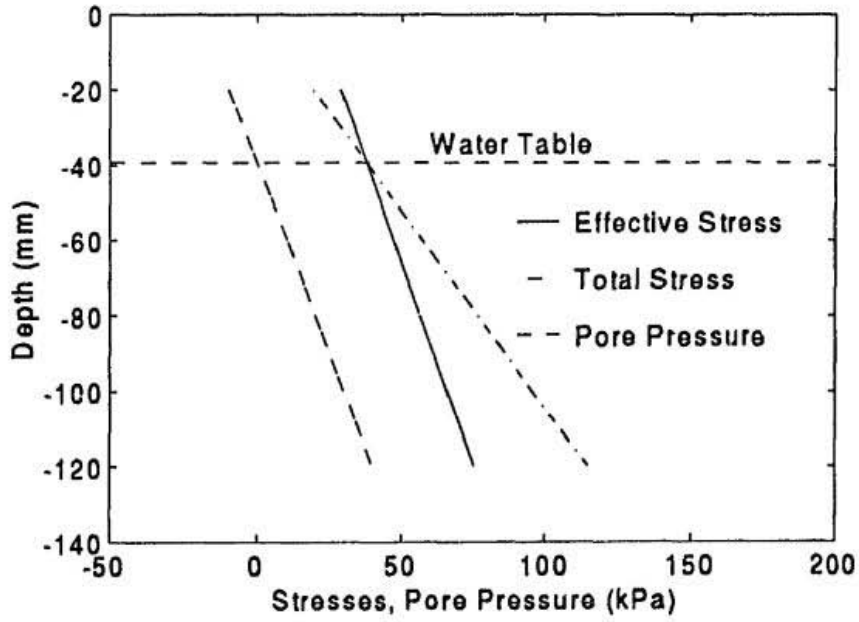

Figure 5.19: Distribution of Total Stress, Effective Stress and Pore Pressure

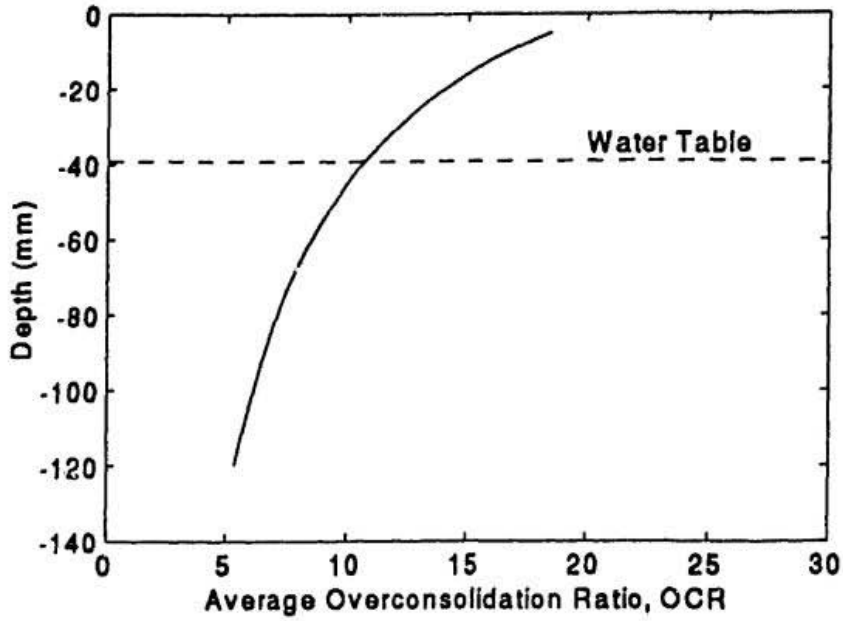

Figure 5.20: Average Overconsolidation Ratio

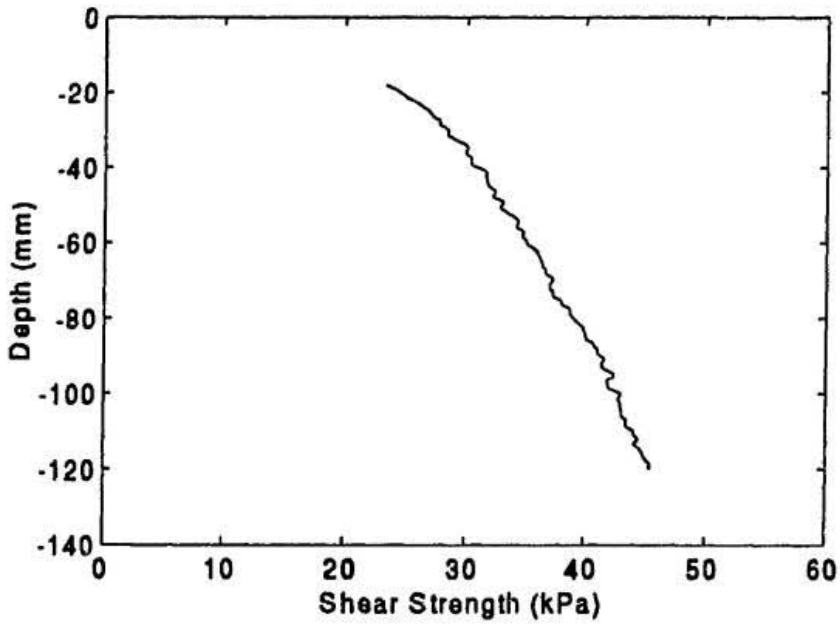

Figure 5.21: Average Undrained Shear Strength from Cone Tests

Chapter 6

Comparison and Discussion

As described in previous chapters, direct shear tests, shear vane tests and centrifuge cone penetration tests have been carried out for the investigation of the strength behaviour of kaolin and kaolin-silt mixture under various stress conditions. The test results indicate that the measured undrained shear strength of soils is affected by stress level and history, soil type and test method. Some comparison and discussion of the test results are presented below.

6.1 Strength of Kaolin and Kaolin-Silt Mixture

From direct shear tests, the strength parameter α of the kaolin-silt mixture is greater than that of the kaolin; the value of the strength parameter β of the kaolin is greater than that of the mixture, as shown in Table 6.1. Using Equation (4.2) and Equation (4.3), the comparison of shear strength of the kaolin and the kaolin-silt mixture is shown in Figure 6.1. It can be seen that the undrained shear strength of the K-S mixture is greater than that of pure kaolin at all OCR levels.

From the vane tests, it can be seen again that for the kaolin, the α value is

Table 6.1: Strength Parameters of Kaolin and K-S

Soil Type	α	β	Test Method
Kaolin	0.238	0.441	Direct Shear Test
	0.167	0.707	Vane Test
Kaolin-Silt	0.330	0.370	Direct Shear Test
	0.253	0.657	Vane Test

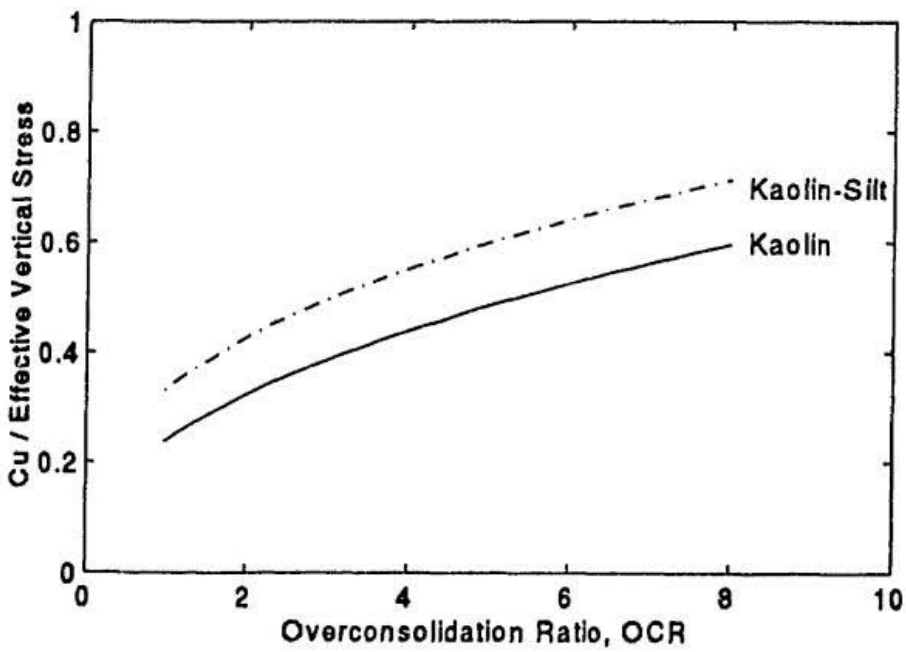

Figure 6.1: Comparison of Strength of Kaolin and K-S from Direct Shear Tests

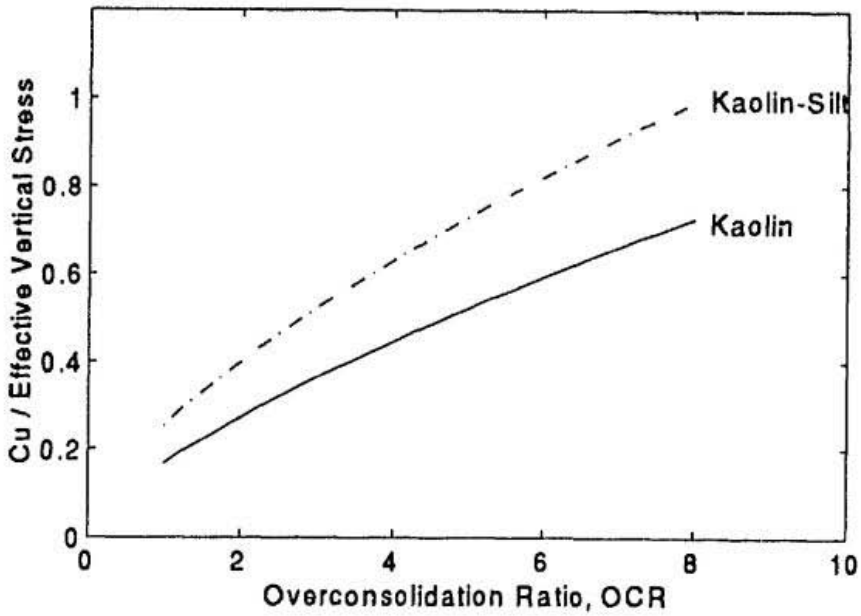

Figure 6.2: Comparison of Strength of Kaolin and K-S from Vane Tests

smaller and the β value is greater than that of the K-S mixture as shown in Table 6.1. Using Equation (4.8) and Equation (4.9), comparison of the strength of the two soils from the vane tests, as shown in Figure 6.2, indicates that the strength of the K-S mixture is greater than that of the kaolin.

The shear strength of kaolin from vane tests, as expressed by Equation (4.8), is compared with the results of Nunez (1989), Bolton *et al.* (1993) and Springman (1989) as shown in Figure 6.3. It can be seen that the strength determined from the vane tests of this study is the lowest at all overconsolidation levels. The difference between the strength of this study and the strength obtained by Bolton *et al.* (1993) is small. However, the shear strength obtained by Springman (1989) is much higher, especially at higher OCR levels.

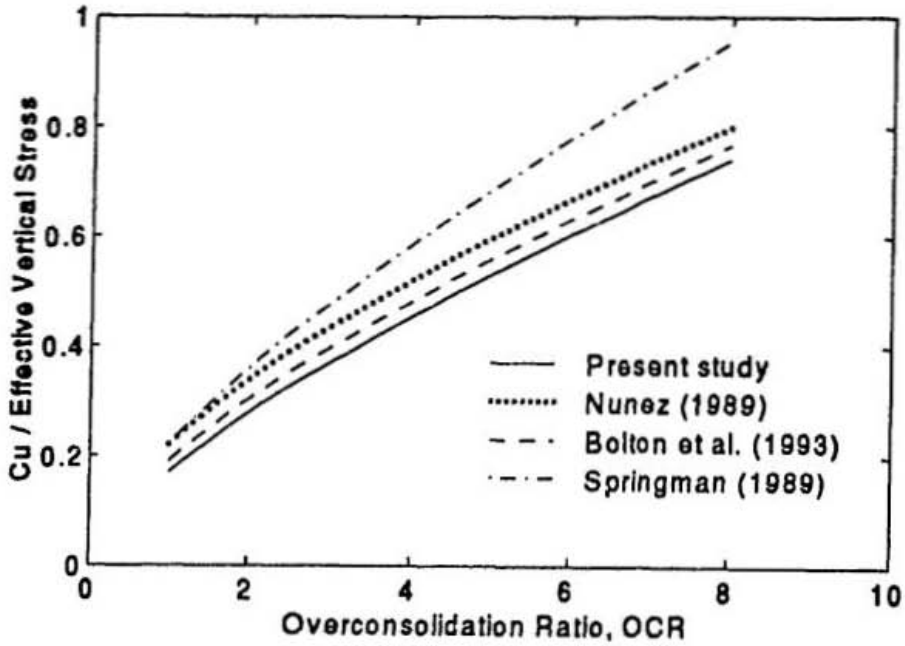

Figure 6.3: Comparison of Shear Strength of Kaolin from Vane Tests

6.2 Direct Shear and Vane Results

The test data shown in Table 4.1, Table 4.2, Table 4.4 and Table 4.5 indicate that the observed strength of both kaolin and K-S from direct shear testing differs from that obtained from shear vane testing. Figure 6.4 and Figure 6.5 show the strength comparisons of the two test methods using equation (4.2), equation (4.3), equation (4.8) and equation (4.9) respectively. It is obvious that at low OCR levels, the shear strength of the two soils obtained by the direct shear tests is greater than that from the shear vane tests; at high OCR values, the shear strength obtained from the vane tests becomes greater than the strength from the direct shear tests. Direct shear testing produces a greater value of the strength parameter α and a smaller value of β than those from shear vane testing.

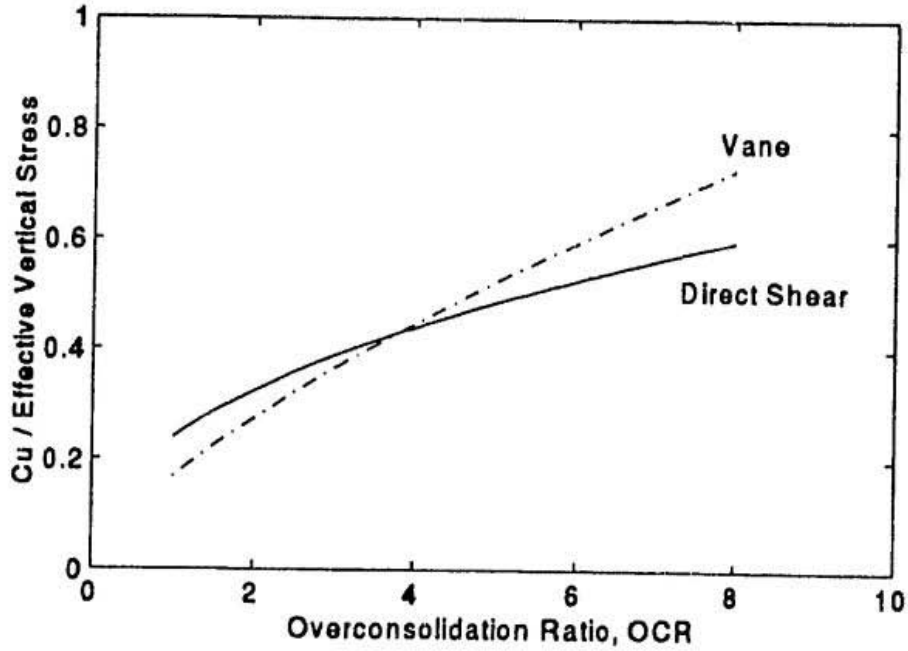

Figure 6.4: Shear Strength of Kaolin from Direct Shear and Vane Tests

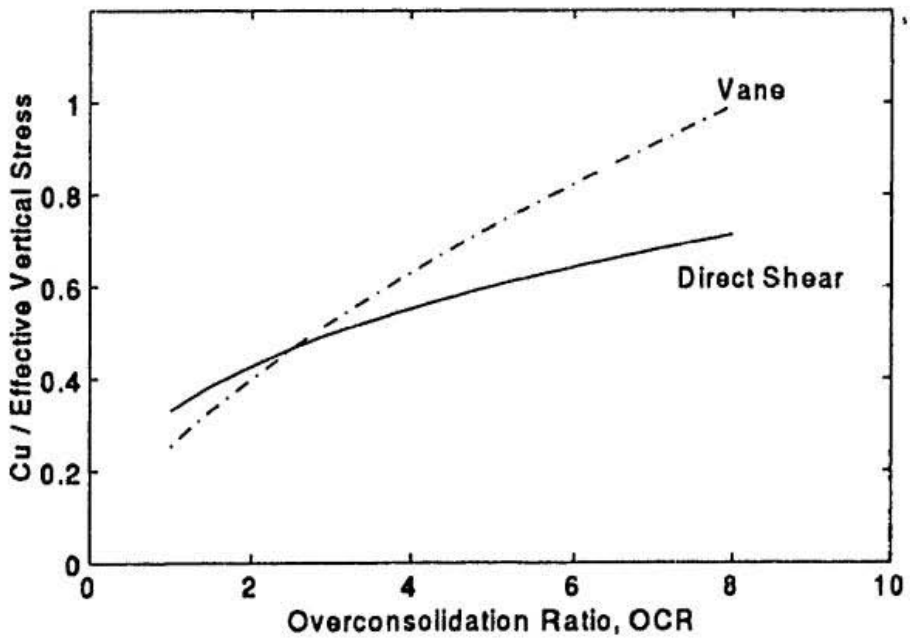

Figure 6.5: Shear Strength of K-S from Direct Shear and Vane Tests

The difference in strengths from direct shear and vane tests may be mainly due to stress anisotropy of the soils. As mentioned in chapter 4, the vane testing assumes that the soils are consolidated under isotropic stress conditions (vertical stress is equal to lateral stress). It is known, however, that when a soil is consolidated under K_o conditions, the effective lateral stress (σ_h') is smaller than the effective vertical stress (σ_v') in normally consolidated or lightly overconsolidated soils, while for heavily overconsolidated soils, σ_h' is greater than σ_v' (Wroth, 1975). In other words, for normally consolidated or lightly overconsolidated soils, K_o is smaller than 1, while for heavily overconsolidated soils, K_o is greater than 1.

Equation (4.5) indicates that in an isotropically consolidated soil, when the vane height is greater than one third of the diameter, M_s, the resisting moment of shear force of the side of the soil cylinder in Equation (4.4) is greater than $2M_e$ of the two ends of the soil cylinder. That is, in vane testing, the lateral stress is a more important factor influencing the test results than the vertical stress.

Therefore, for soils consolidated under K_o conditions, compared with direct shear testing, vane testing produces a smaller undrained shear strength of normally consolidated or lightly overconsolidated soils and a greater undrained shear strength of heavily overconsolidated soils. Mayne and Kulhawy (1982) relates K_o of soil to OCR using

$$K_o = (1 - sin\phi')(OCR)^{sin\phi'} \tag{6.1}$$

where ϕ' the effective internal friction angle of the soil.

The value of ϕ' of the kaolin is 23° (Al-Tabbaa, 1987). For K_o=1, Equation (6.1)

yields OCR=3.6, which means that when OCR is greater than 3.6, the kaolin in this study is heavily overconsolidated. This result is surprisingly in accordance with the data shown in Figure 6.4, in which the two curves of (c_u/σ'_v) - OCR relations of the kaolin from direct shear testing and vane testing also intersect at an OCR value of approximately 3.6.

The two curves of the K-S mixture in Figure 6.5 intersect at a lower OCR value of approximately 2.5 They would be expected to intersect at an OCR value higher than 3.6 according to Equation (6.1) because the ϕ' value of the K-S mixture should be greater than 23° (the ϕ' value of the kaolin). However the data shown in Figure 6.5 also indicates that compared with direct shear testing, vane testing produces a smaller shear strength of the K-S mixture at low OCR levels but yields a greater strength at higher OCR levels.

6.3 Comparison of CPT Results with Direct Shear and Vane Results

Chapter 5 has presented the data of the tip resistances of 4 typical cone penetration tests in centrifuge (L214, L230, L240, and L243) and the corresponding undrained shear strengths obtained from the tip resistances (q_c) using Equation (5.1). It is known that to obtain a reliable c_u value, N_c in Equation (5.1) must be properly selected. According to the results of Almeida and Parry (1983) and Francescon (1983), the values of N_c are calculated using Equation (5.2) in this study for obtaining c_u from measured q_c results.

In order to check the reliability of Equation (5.2) for the calculation of N_c,

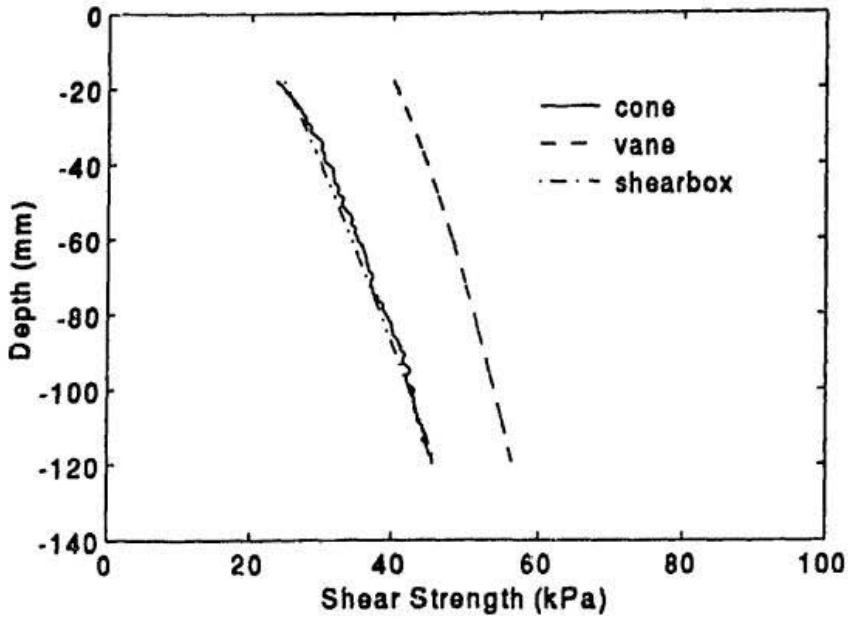

Figure 6.6: Comparison of Strengths from CPT, Direct Shear and Vane Tests

the average tip resistance, as shown in Figure 5.14, of the 4 typical cone tests mentioned above are used to make comparison with the direct shear and vane results. The effective vertical stress obtained from Equation (5.3) is shown in Figure 5.19 and the average OCR value from Equation (5.4) is shown in Figure 5.20. The shear strength from cone tests shown in Figure 6.6 are calculated from CPT data in Figure 5.14 using Equation (5.1) and Equation(5.2); the c_u values from direct shear tests and vane tests were predicted using Equation (4.3) and Equation (4.9) respectively. From Figure 6.6, it can be seen that the shear strength determined from cone penetration tests falls between the other two tests but it is closer to the strength from direct shear tests. The results indicate that N_c values from Equation (5.2) are acceptable.

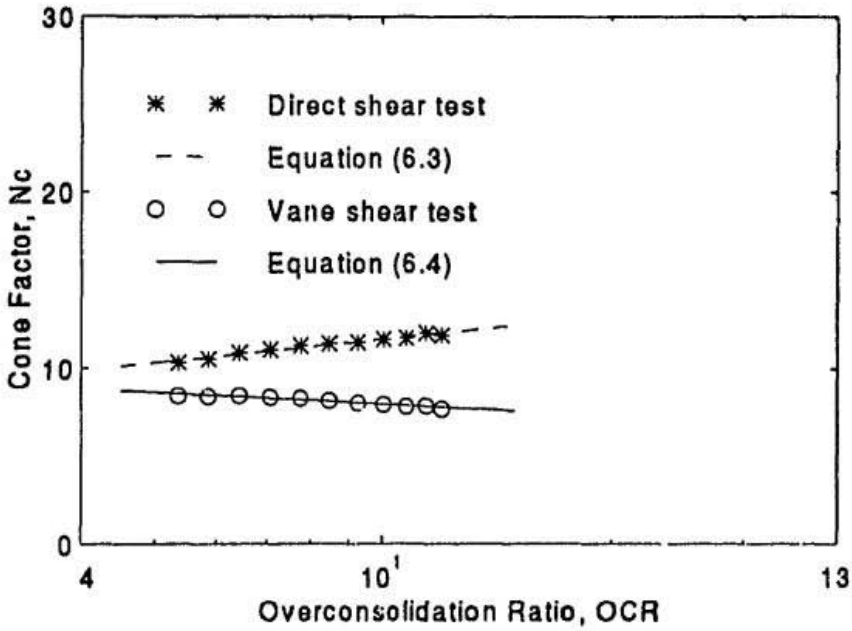

Figure 6.7: N_c Values from Direct Shear and Vane Tests

6.4 Correlation of N_c from Direct Shear and Vane Tests

Equation (5.2) has been used for the calculation of cone factor N_c in order to convert cone tip resistance to undrained shear strength using Equation (5.1). To calculate an N_c value corresponding to the direct shear and vane results, Equation (5.1) can be expressed as

$$N_c = \frac{q_c - \sigma_{vo}}{c_u} \tag{6.2}$$

where σ_{vo} is the total vertical stress.

For the q_c data shown in Figure 5.14, the values of σ'_v, σ_{vo} and OCR can be calculated (Figure 5.19) and the value of c_u can be predicted using Equation (4.3) from direct shear tests or Equation (4.9) from vane shear tests, hence the values of

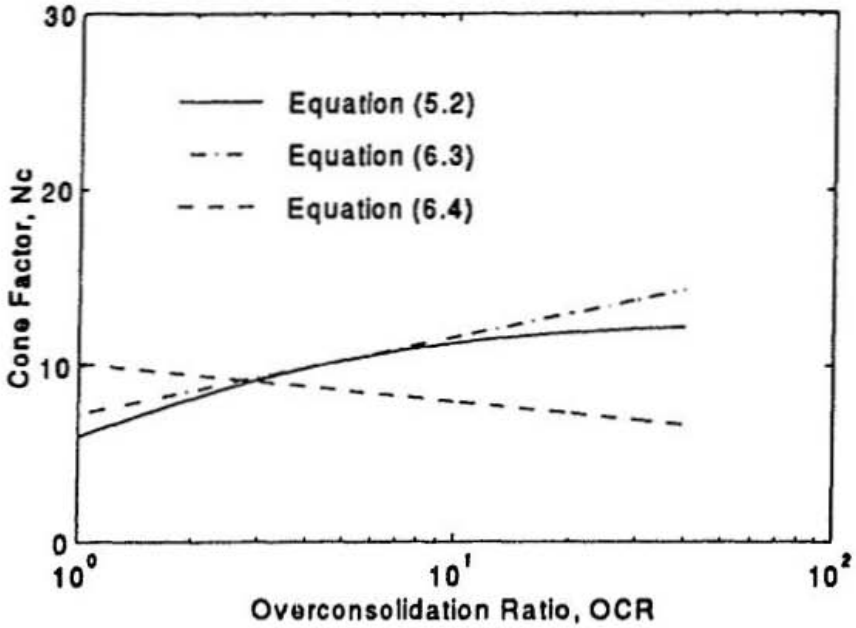

Figure 6.8: Comparison of N_c Values for K-S

N_c can be obtained, as shown in Figure 6.7. It can be seen from Figure 6.7 that the N_c values from direct shear tests may be expressed as

$$N_c = 7.2 + 1.9ln(OCR) \tag{6.3}$$

The N_c values from vane shear tests may be approximately expressed as

$$N_c = 10.1 - 0.94ln(OCR) \tag{6.4}$$

while the above two equations are less reliable when the OCR is smaller than 4 due to the lack of test data from the centrifuge CPT. The N_c values in Figure 6.7 obtained from vane shear tests appear not to increase with OCR, which is not in agreement with the results shown in Figure 5.11. This discrepancy may be because Equation (4.9) used to calculate the shear strength was obtained from vane tests when OCR$\leq$8 while the q_c values are from cone tests when OCR$\geq$5. Meanwhile,

as discussed above in this chapter, Equation (4.9) may overestimate the undrained shear strength of soils.

The comparison of Equation (5.2), Equation (6.3) and Equation (6.4) is shown in Figure 6.8. It can be seen that Equation (5.2) is close to Equation (6.3) obtained from direct shear tests; the difference between Equation (6.4) and Equation (5.2) is greater. However, the N_c values from these three equations are quite close.

Chapter 7

Summary and Conclusions

In order to determine the strength behaviour of a kaolin and a K-S mixture, a series of direct shear tests, shear vane tests and centrifuge cone penetration tests were conducted. The direct shear tests on both the kaolin and the K-S mixture were carried out under vertical stresses of 50 to 250 kPa with OCR levels ranging from 1 to 8. For the shear vane tests, the two soils were preconsolidated under a vertical stress of 400 kPa and were sheared at OCR levels ranging from 1 to 8. Centrifuge cone penetration tests were conducted only on the K-S mixture. After being consolidated under a vertical stress of 400 kPa and being unloaded to zero total vertical stress, the soil specimens were tested in a centrifuge at 50 gravities. Based on the test results and discussions in this thesis, the following conclusions can be drawn:

1. The undrained shear strength of clays can be determined by direct shear tests, shear vane tests or cone penetration tests. The measured shear strengths of the two soils in this study are related to many factors including soil type, stress and OCR levels, stress history and test method.

2. In both direct shear and shear vane testing, the undrained shear strength of the kaolin and the K-S mixture can be expressed as

$$\frac{C_u}{\sigma_v'} = \alpha(OCR)^{\beta}$$

. Compared with the K-S mixture, kaolin has a smaller value of the parameter α and a greater value of the parameter β in both direct shear tests and shear tests. At the same stress and OCR levels, the undrained shear strength of the K-S mixture is greater than that of pure kaolin. This indicates that silt mixed with kaolin will provide a stronger material than kaolin alone.

3. The difference in the test results from direct shear tests and vane tests may be mainly caused by the stress anisotropy of the soils. Theoretical analyses as well as test results from the kaolin and the K-S mixture indicate that for clays consolidated under K_o conditions, the undrained shear strength determined from direct shear tests is in agreement with the strength from shear vane tests only when the soil vertical stress is approximately equal to the lateral stress (K_o=1).

4. For normally consolidated or lightly overconsolidated soils, the strength from direct shear tests is greater than that from shear vane tests; the lower the OCR value, the greater the difference of the strengths from the two test methods. For heavily overconsolidated clays, the strength determined from direct shear tests is less than that from shear vane tests; the higher the OCR value, the greater the difference of the strengths from the two test methods. Compared with direct shear testing, shear vane testing may yield a smaller undrained shear strength of normally consolidated or lightly overconsolidated clays and may yield a greater strength of

heavily overconsolidated clays.

5. The shear vane results of the kaolin under repeated consolidation loading indicate that the repeated loading yields a greater parameter α and a smaller β. The undrained shear strength of the kaolin under repeated loading is higher than the strength under first consolidation loading. The ratio of the strength of the soil under repeated loading to the strength at first loading decreases with overconsolidation ratio (OCR); it is 1.46 when OCR=1 and is only 1.04 when OCR=8.

6. In centrifuge cone penetration tests on the K-S mixture, the cone tip resistance is related to soil depth, water table level, desiccation of soil during centrifuge flight and water migration from the backfilled clay. The phenomenon of desiccation in centrifuge flight is significant; it results in an increase in shear strength of the soil near the surface of the specimens.

7. The selection of the cone factor N_c is very important for determining the shear strength of soils using CPT data. The value of N_c, which is expressed by equation (5.2), increases with OCR. The cone tip resistance (q_c) of the tested soil can be converted to undrained shear strength using equation (5.1) and equation (5.2). The undrained shear strength of a K-S mixture specimen interpreted from CPT data falls between the strengths predicted by the relationships from the data of direct shear tests and shear vane tests.

8. The N_c value expressed by Equation (5.2) has been compared with Equation (6.3) correlated from direct shear tests and Equation (6.4) from vane shear tests and the results are quite close.

9. It should be mentioned that repeated loading in centrifuge testing may be a factor which could affect test results. The specimens prepared for the centrifuge cone tests were preconsolidated under vertical stress of 400 kPa and then were unloaded to zero total vertical stress. During centrifuge testing, the specimens were consolidated again under stresses due to self-weight of the soil at 50 gravities. Although the depth of each specimen was not greater than 205 mm and the consolidation stress during centrifuge flight was much lower than 400 kPa, the effect of repeated loading is still worthy to be studied.

References

Almeida, M. S. S., and Parry, R. H. G. (1983). "Tests with Centrifuge Vane and Penetrometer in a Normal Gravity Field." *Final Technical Report*, Engineering Department, University of Cambridge.

Al-Tabbaa, A. (1987) "Permeability and Stress-Strain Response of Speswhite Kaolin", Ph.D Thesis, Cambridge University.

Amar, S., Baguelin, F., Jezequel, J.F., and Le Mehaute, A. (1975). "In-situ Shear Resistance of Clays." ASCE-IMSP, Vol. 1, pp. 22-45.

Arman, A., Poplin, J. K., and Ahmad, N. (1975). "Studies of the Vane Shear." *Proc. In-Situ Measurement of Soil Properties*, ASCE, Vol. 1, pp. 93-120.

ASTM Committee (1993). "ASTM D2435-90: Test Method for One-Dimensional Consolidation Properties of Soils. " *1993 Annual Book of ASTM Standards*, Section 4, Vol. 04.08.

ASTM Committee (1993). "ASTM D2487-92: Test Method for Classification of Soils for Engineering Purposes." *1993 Annual Book of ASTM Standards*, Section 4, Vol. 04.08.

ASTM Committee (1993). "ASTM D4318-84: Test Method for Liquid Limit, Plastic Limit, and Plasticity Index of Soils." *1993 Annual Book of ASTM Standards*, Section 4, Vol. 04.08.

ASTM Committee (1993). "ASTM D4648-87: Test Method for Laboratory Miniature Vane Shear Test for Saturated Fine-Grained Clayey Soil." *1993 Annual Book of ASTM Standards*, Section 4, Vol. 04.08.

Atkinson, J. H., Richardson, D., and Robinson, P. J. (1987). "Compression and Extension of K_0 Normally Consolidated Kaolin Clay." *Journal of Geotechnical Engineering*, Vol. 113, No. 12, pp. 1468-1482.

Bolton M. D., Gui, M. W. and Phillips, R. (1993). "Review of Miniature Soil Probes for Model Tests.", *Proc. 11th SEAGC*, Singapore.

Bowles, J. E. (1977). "Foundation Analysis and Design", Second edition, McGraw-Hill Book Company.

Bowles, J. E. (1986). " Engineering Properties of Soils and Their Measurement." Third edition, McGraw-Hill Book Company.

Bransby, M. F. (1993). "Centrifuge Test Investigation of the Buttonhole Foundation Technique." Data Report, Cambridge University, England.

Cadling, L., and Odenstad, S. (1950). "The Vane Borer: An Apparatus for Determining the Shear Strength of Clay Soils Directory in the Ground." *Royal Swedish Geotechnical Institute Proc. 2.*

Craig, W. H. (1989) "Édouard Phillips (1821-89) and the Idea of Centrifuge Modelling." *Géotechnique*, Vol. 39, No. 4, pp. 679-700.

Cunard, C. G. (1993). "Design of an In-flight Cone Penetrometer for the Acutronic 680-2 geotechnical Centrifuge." C-CORE Internal Report, Memorial University.

Das, B. M. (1985). "Principles of Geotechnical Engineering." PWS Engineering, Boston.

Davies, M. C. R., Almeida, M. S. S., and Parry, R. H. G. (1989). "Studies with Centrifuge Vane and Penetrometer Apparatus in a Normal Gravity Field." *Geotechnical Testing Journal*, Vol. 12, No. 3, pp. 195-203.

De Ruiter, J. (1982). "The Static Cone Penetration Test: State-of the-Art-Report." *Proc. of the Second European Symposium on Penetration Testing*, Amsterdam, pp. 389-405.

Duncan, J. M., and Seed, H. B. (1966) "Anisotropy and Stress Reorientation in Clay," JSMFD, ASCE, Vol. 92, No. SM5, pp. 21-50.

Durgunoglu, H.T., and Mitchell, J.K. (1975). "Static Penetration Resistance of Soils." *Proc. of ASCE Conference on In-situ Measurement of Soil Properties*, Raleigh, pp. 151-188.

Eide, O. (1974). "Marine Soil Mechanics", presented at *Offshore North Sea Technology Conference and Exhibition*, Stavabger.

Ellis, E. A. (1993). "Lateral Loading of Bridge Abutment Piles due to Soil Movement." Cambridge University First Year Report, England.

Feng, G., and Hu, Y. (1988). "Centrifuge Model Test of a Highway Embankment on Soft Clay ", in *Centrifuge 88*, edt. by Corte, pp. 153-162.

Ferguson, K. A., and Ko, H. Y. (1981). "Centrifuge Model of the Cone Penetrometer." *Cone Penetrometer Testing and Exzperiences*, edt. by Norris, G. M. and Holtz, R. D., pp. 108-127.

Flaate, K. (1966). "Factors Influencing the Results of Vane Test." *Canadian Geotechnical Journal*, Vol. 3, No. 1, pp. 18-31.

Francescon, M. (1983) "Model Pile Tests in Clay", Ph. D Thesis, Cambridge University.

Head, K. H. (1982). *Manual of Soil Laboratory Testing*. Printed by Robert Hartnoll Limited, Bodmin, Cornwall.

Holtz, R.D., and Kovacs, W. D. (1981). *An Introduction to Geotechnical Engineering*. Prentice-Hall, Inc., Englewood Cliffs, New Jersey.

Hushmand, B., Scott, R. F., and Crouse, C. B. (1988). "Centrifuge Liquefaction Tests in a Laminar Box," *Geotechnique*, Vol. 38, No. 2, pp. 253-262.

Jamiolkowski, M. (1985). "New Developments in Field and Laboratory Testing of Soils." *Theme lecture, 11th International Conference on Soil Mechanics and Foundation Engineering*, San Francisco.

Juilie, Y., and Sherwood, D. E. (1983). "Improvement of Sabkha Soil of the Arabian Gulf Coast." *Proc of the 8th European Conference on Soil Mechanics and Foundation*, Helsinki, pp. 781-788.

Kavazanjian, Jr. E., and Mitchell, J. K. (1984). "Time Dependence of Lateral Earth Pressure." *Journal of Geotechnical Engineering*, Vol. 110, No. 4, pp. 530-533.

Kimura, T., Kusakabe, O., and Saitoh, K. (1984) "Undrained Deformation of Clay of Which Strength Increases Linearly with Depth," *Application of Centrifuge Modelling to Geotechnical Design*, edt. by Craig, W.H, pp. 315-335.

King, A. D. (1993). "Determination of Soil Parameter by Self-weight Consolidation in a Chemical Centrifuge." *Technical Report Series, 93003*, Faculty of Engineering and Applied Sciences, Memorial University of Newfoundland.

Konrad, J., and Law, J. (1987). "Undrained Shear Strength from Piezocone Tests." *Canadian Geotechnical Journal*, Vol. 24, No. 3, pp. 392-405.

Kutter, B. L., Abghari, A., and Shindae, S. B. (1988). "Modelling of Circular Foundations on Relatively Thin Clay Layers ", *Centrifuge 88*, edt. by Corte, pp. 337-344.

Ladd, C. C., Foott, R., Ishihara, K., Schlosser, F., and Poulos, H.J. (1977). "Stress-Deformation and Strength Characteristics. *Proc. of 9th International Conference on Soil Mechanics and Foundation Engineering*, Tokyo, Vol. 2, pp. 421-494.

Ladd, C. C., and Edgers. (1972) "Consolidated-undrained Direct-simple Shear Tests on Saturated Clays", Research Report R72-82, Dept. of Civil Eng., Massachusetts Institute of Technology, Cambridge.

Lawrence, D. M. (1980) "Some Properties Associated with Kaolinite Soils", M.Sc Thesis, Cambridge University.

Lee, F. H., and Schofield, A. N. (1988) "Centrifuge Modeling of Sand Embankments and Islands in Earthquake," *Géotechnique*, Vol. 38, No. 1, pp. 45-58.

Lunne, T., Eide, O., and De Ruiter, J. (1976). "Correlation between Cone Resistance and Vane Shear Strength in Some Scandinavian Soft to Medium Stiff Clays." *Canadian Geotechnical Journal*, Vol. 13, No. 4, pp. 76-107.

Lunne, T., and Kleven, A. (1981). "Role of CPT in North Sea Foundation Engineering." *Cone Penetration Testing and Experience*, edt. by G. M. Norris and R. D. Holtz, pp. 209-227.

Marsland, A., and Quarterman, R. S. (1982). "Factors Affecting the Measurements and Interpretation of Quasi-static Penetration Tests in Clays." *Proc. of 2nd European Symposium on Penetration Testing.* Amsterdam, pp. 697-702.

Mayne, P. W. and Holtz, R. D. (1988). "Profiling Stress History from Piezocone Soundings." *Soils and Foundations*, Vol. 28, No. 1, pp. 16-28.

Mayne, P. W. and Kulhawy, F. H. (1982). "K_o - OCR Relationship in Soil." *Journal of Geotechnical Engineering Division*, Vol. 108, No. GT6, pp. 851-872.

Meigh, A. C. (1987). *Cone Penetration Testing: Methods and Interpretation*, Butterworths, United Kingdom.

Mikasa, M., and Takada, N. (1973). "Significance of Centrifuge Model Test in Soil Mechanics," *Proc. 8th International Conf. on Soil Mechanics and Foundation Engineering*, Moscow. Vol. 1, pp. 273-278.

Mitchell, R. J. (1991). "Centrifuge Modelling as a Consulting Tool." *Canadian Geotechnical Journal*, Vol. 28, No. 1, pp. 162-167.

Mitchell, J. K. (1976). "Fundamentals of Soil Behaviour", John Wiley & Sons, New York.

Monney, N. T. (1969). "An Analysis of the Vane Test at Varying Rates of Shear." *Deep Sea Sediments: Physical and Mechanical Properties*, Inderbitzen, A. L. ed., Plenum Press, New York, N.Y. pp. 151-167.

Nunez, I. (1989). "Tension Piles in Clay." Ph. D Thesis, Cambridge University, England.

Parry, R. H. G., and Nadarajah, V. (1973). "Observations on Laboratory Prepared, Lightly Overconsolidated Specimens of Kaolin." *Géotechnique*, Vol. 24, No. 3, pp. 345-358.

Perlow, M., and Richards, A. F. (1977). "Influence of Shear Velocity on Vane Shear Strength." *Journal of Soil Mechanics and Foundation Engineering*, ASCE, Vol. 103, No. 1, pp. 19-32.

Poorooshasb, F. (1990). "On centrifuge Use for Ocean Research," *Marine Geotechnology*, Vol. 9, pp. 141-158.

Poorooshasb, F. (1991). "Centrifuge Modelling of Laterally Loaded Pipelines", Contract Report, 91-C14, Centre for Cold Ocean Resources Engineering.

Rossato, G., Ninis, N. L. and Jardine, R. J. (1992). "Properties of Some Kaolin-Based Model Clay Soils." *Geotechnical Testing Journal*, Vol. 15, No. 2, pp. 166-179.

Rowe, P. W. (1975). "Displacement and Failure Modes of Model Offshore Gravity Platforms Founded on Clay." in *Conference of Offshore Europe*, 1975, Spearhead Publications, Aberdeen.

Schcherbina, V. I. (1988). "Earth Pressure Studies on Retaining Walls by Centrifuge Modelling ", *Centrifuge 88*, edt. by Corte, pp. 421-428.

Schmertmann J.H. (1975). "Measurement of In-situ Shear Strength." *Proc. of ASCE Conference on In-situ Measurement of Soil Properties*, Raleigh, pp. 57-138.

Schofield, A. N. (1980). "Cambridge Geotechnical Centrifuge Operation." *Geotechnique*, Vol. 30, No. 3, pp. 227-268.

Sharma, J. S. (1993). "Construction of Reinforced Embankments on Soft Clay." Forthcoming Ph. D Thesis, Cambridge University, England.

Silvestri, V., Aubertin, M. and Chapuis, R. P. (1993). "A Study of Undrained Shear Strength Using Various Vanes." *Geotechnical Testing Journal*, Vol. 16, No. 2, pp. 228-237.

Springman, S. M. (1993). "Centrifuge Modelling in Clay: Marine Applications." *Proc. of the 4th Canadian Conference on Marine Geotechnical Engineering*, Vol. 3, pp. 853-896.

Springman (1989). "Lateral Loading on Piles due to Simulated Embankment Construction." Cambridge University Ph.D. Thesis.

Sully, J. P., and Campanella, R. G. (1991). "Effect of Lateral Stress on CPT Penetration Pore Pressures." *Journal of Geotechnical Engineering*, Vol. 117, No. 7, pp. 1082-1088.

Vey, E., (1955). "Discussion: Field Vane Shear Tests of Sensitive Cohesive Soils." *Proc. ASCE 81*, pp. 17-20.

Vickers, B. (1983). "Laboratory Work in Soil Mechanics", Granada Publishing.

Wood, D. M., (1990). "Soil Behaviour and Critical State Soil Mechanics", Cambridge University Press.

Wroth, C. P. (1975). "In Situ Measurement of Initial Stresses and Deformatiton Characteristics." Reprinted from the Proc. of the Special Conference on In Situ Measurement of Soil Properties.

Zhou, S. G. (1981). "Evaluation of the Liquefaction of Sand by Static Cone Penetration Test." *Proc. of 7th World Conference on Earthquake Engineering*, Istanbul, Vol. 1, pp. 156-162.

Appendix A

Factors for Area Correction in Direct Shear Tests

The area of the shear surface in direct shear test changes during the process of sample shearing. The initial area of the surface is a perfect circle with a diameter of D. The final shear surface, however, becomes smaller with its shear displacement of S. Figure B.1 shows the area of the shear surface before and after the specimen is sheared. From this figure, the final area of the shear surface (area $abcd$) can be calculated using the following equation:

$$\begin{aligned} A_{abcd} &= 2(A_{abco_2} - A_{aco_2}) \\ &= 2(\frac{1}{2}\frac{D}{2}\frac{D}{2}\theta - (\frac{S}{2})^2 tan(\frac{\theta}{2})) \\ &= \frac{1}{4}(D^2\theta - 2S^2 tan(\frac{\theta}{2})) \end{aligned}$$

where, $cos(\frac{\theta}{2}) = \frac{S}{D}$.

The area correction factor k is defined as

$$k = \frac{\pi D^2/4}{A_{abcd}}. \tag{A.1}$$

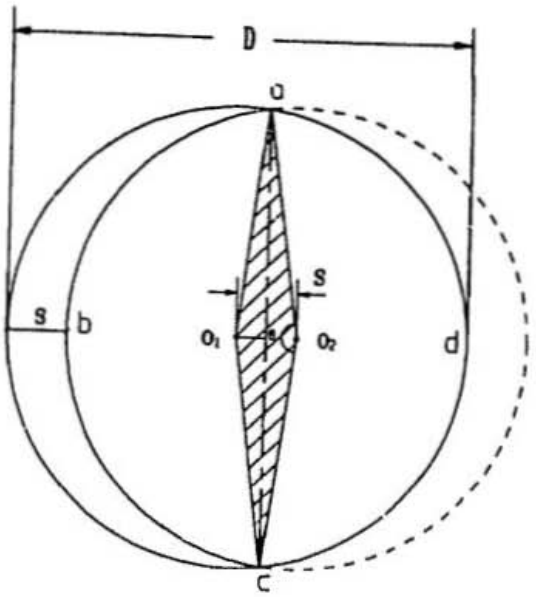

Figure A.1: Area Change of Specimen during Shearing

In the direct shear tests introduced in Chapter 4, the diameter of the direct shear, D, was 61.8mm, the shear displacement S was dominated by the time elapsed from the beginning of the shearing, which was

$$S = \frac{1.26t}{60} \tag{A.2}$$

where t is the elapsed shearing time and 1.26 refers to the shear rate of 1.26 mm/min. The shear displacement and the area correction factor k corresponding to different elapsed shear times are given in Table B.1.

Table A.1: Factors for Area Correction

t	S	k
20	0.42	1.0087
40	0.84	1.0176
60	1.26	1.0267
80	1.68	1.0359
100	2.10	1.0452
120	2.52	1.0548
140	2.94	1.0645
160	3.36	1.0744
180	3.78	1.0845
200	4.20	1.0948

Appendix B

Records of Cone Tip Resistance during CPT

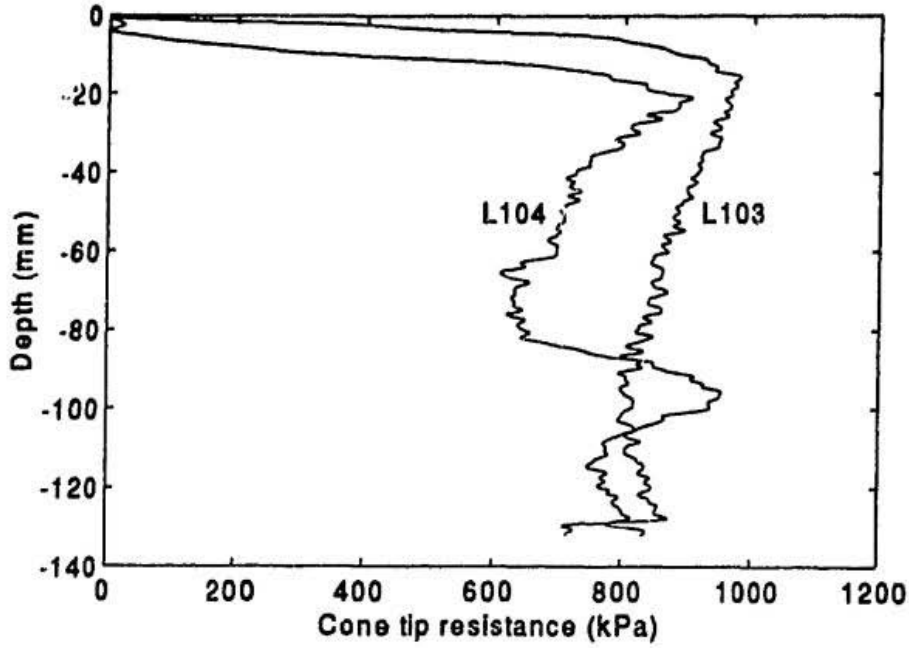

Figure B.1: Cone Tip Resistance of L103 and L104

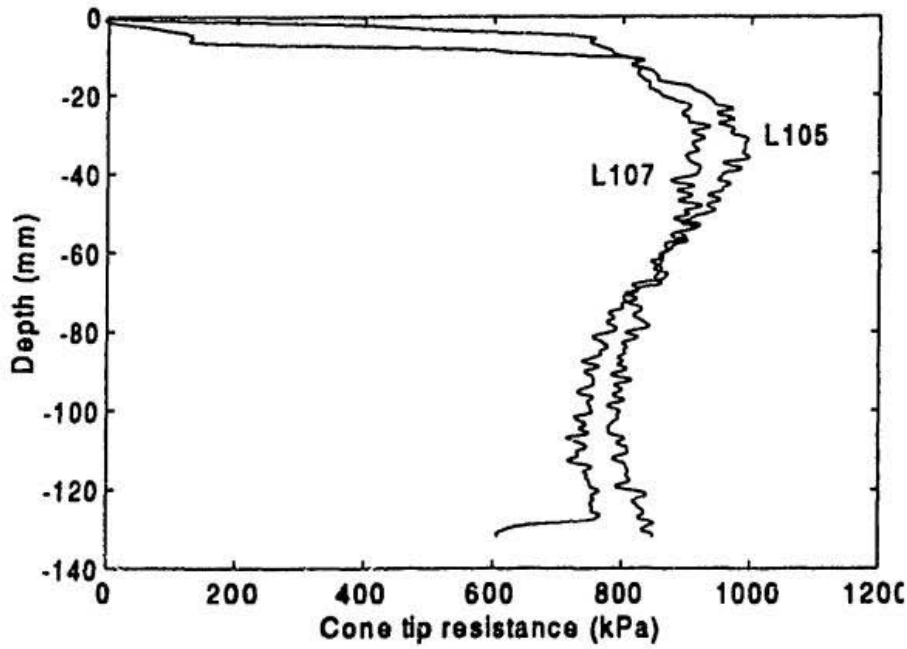

Figure B.2: Cone Tip Resistance of L105 and L107

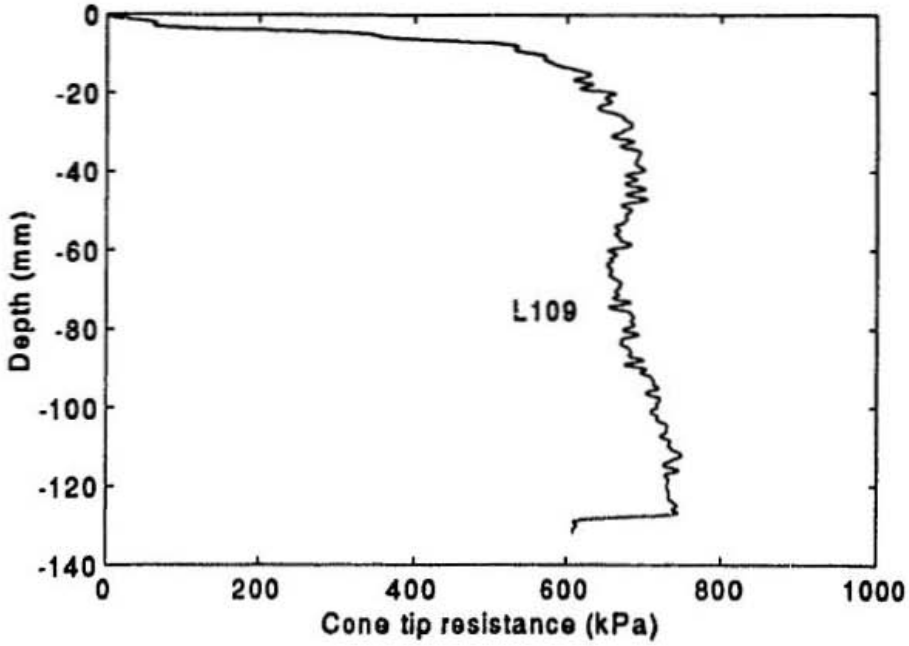

Figure B.3: Cone Tip Resistance of L109

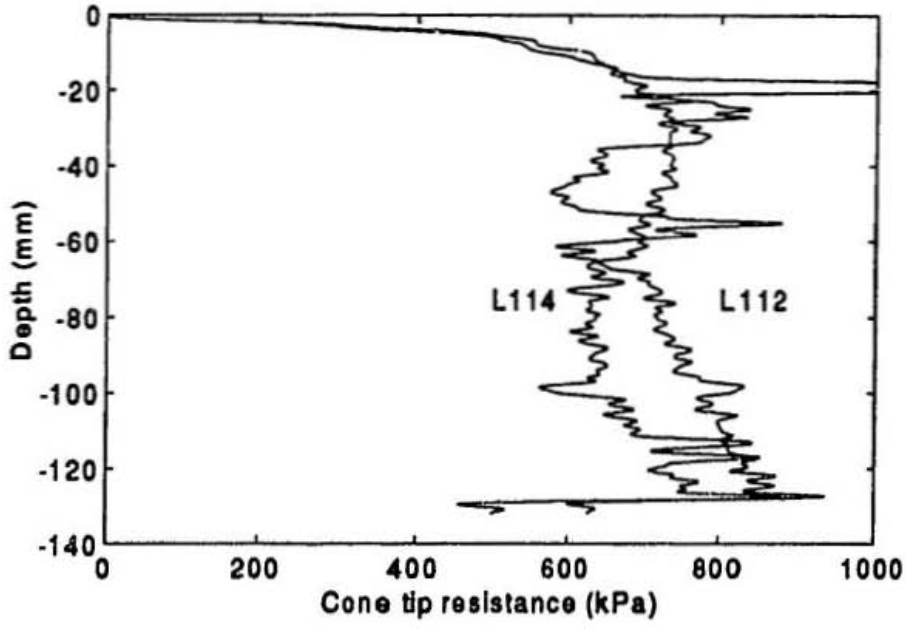

Figure B.4: Cone Tip Resistance of L112 and L114

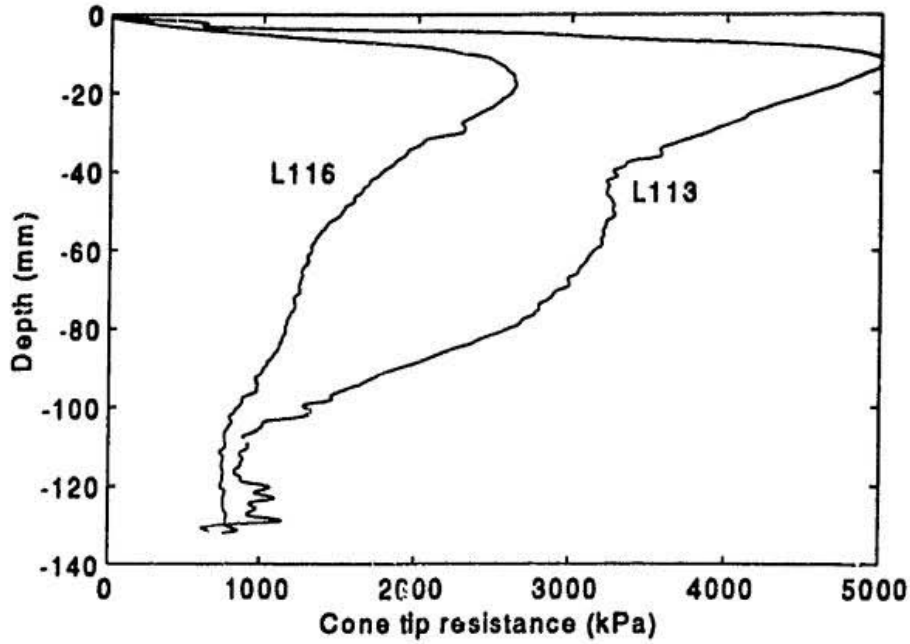

Figure B.5: Cone Tip Resistance of L113 and L116

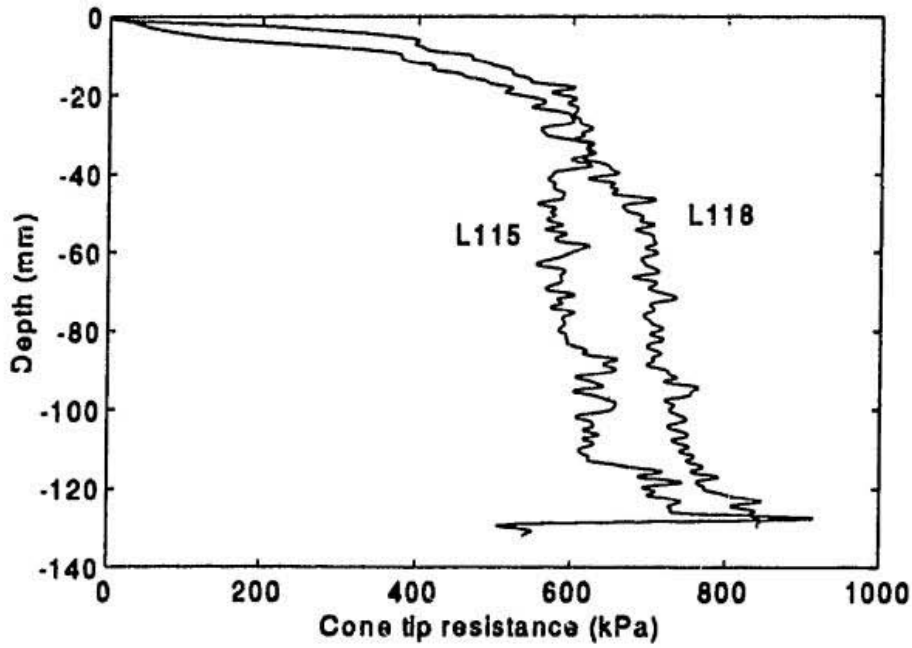

Figure B.6: Cone Tip Resistance of L115 and L118

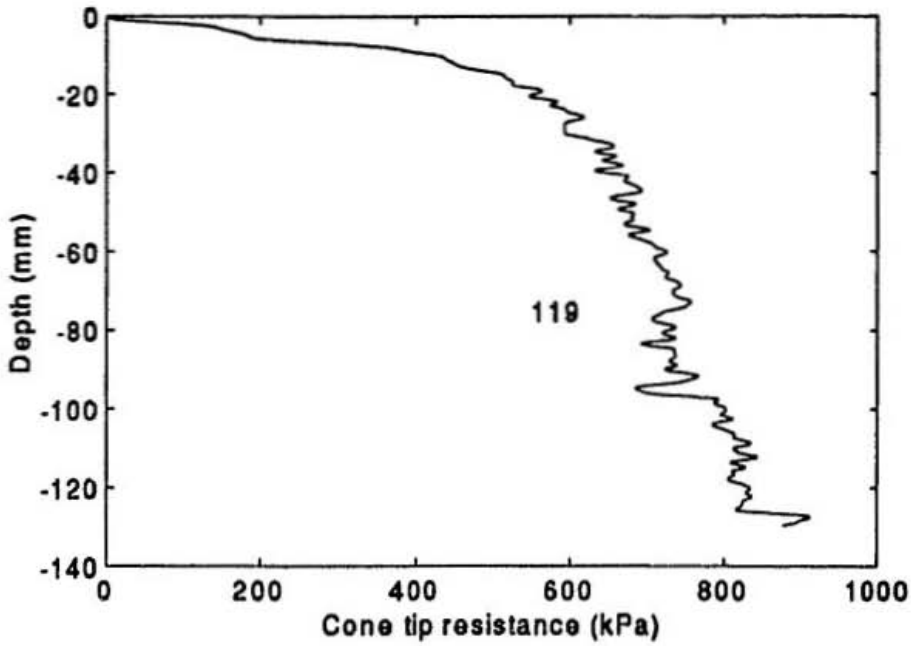

Figure B.7: Cone Tip Resistance of L119

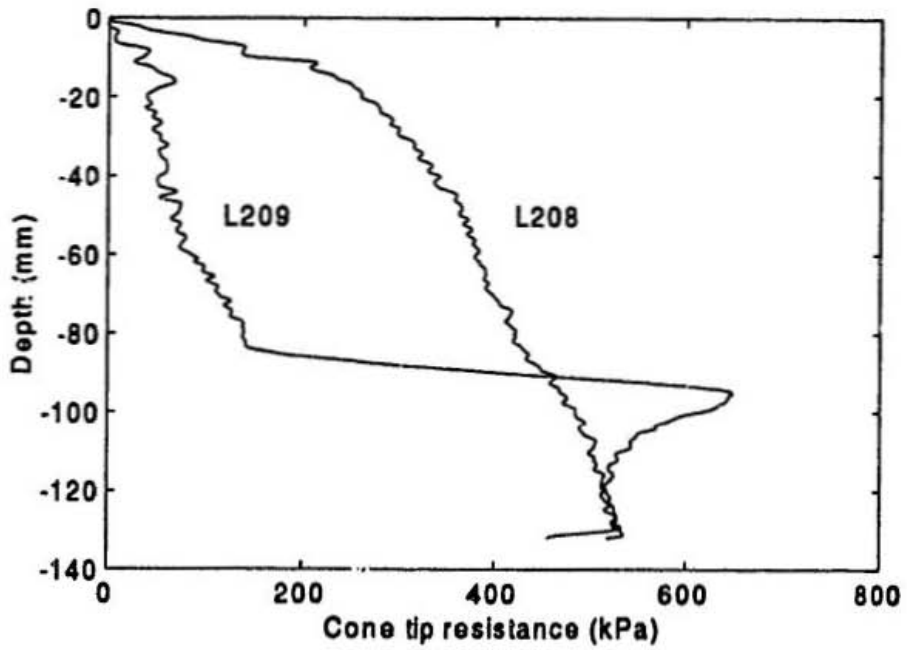

Figure B.8: Cone Tip Resistance of L208 and L209

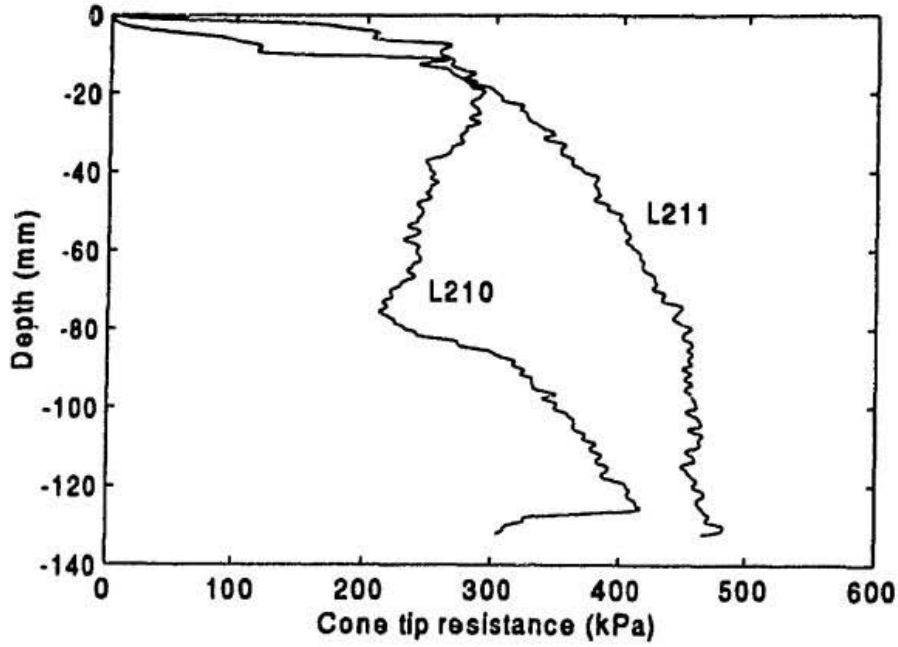

Figure B.9: Cone Tip Resistance of L210 and L211

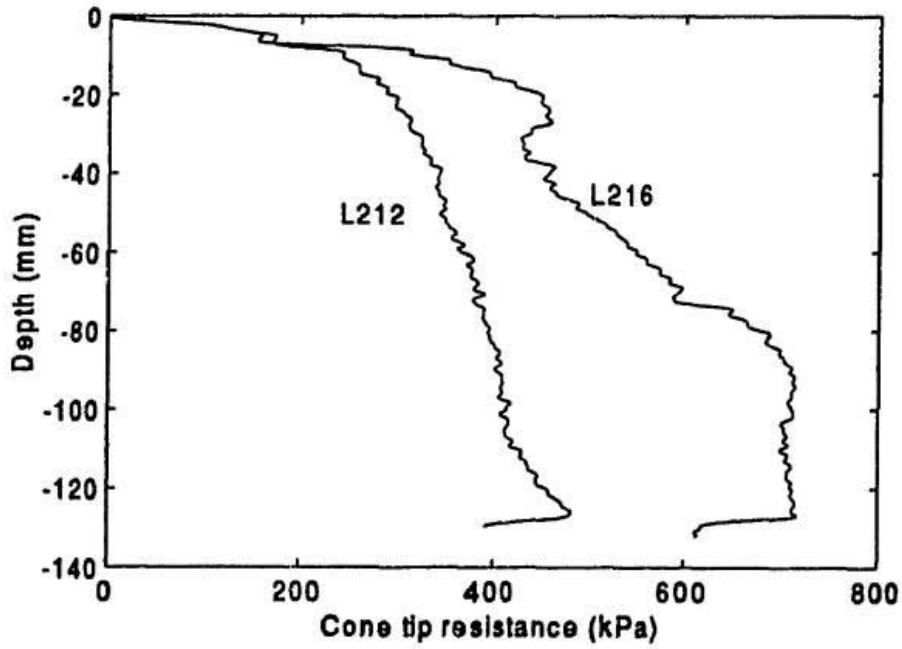

Figure B.10: Cone Tip Resistance of L212 and L216

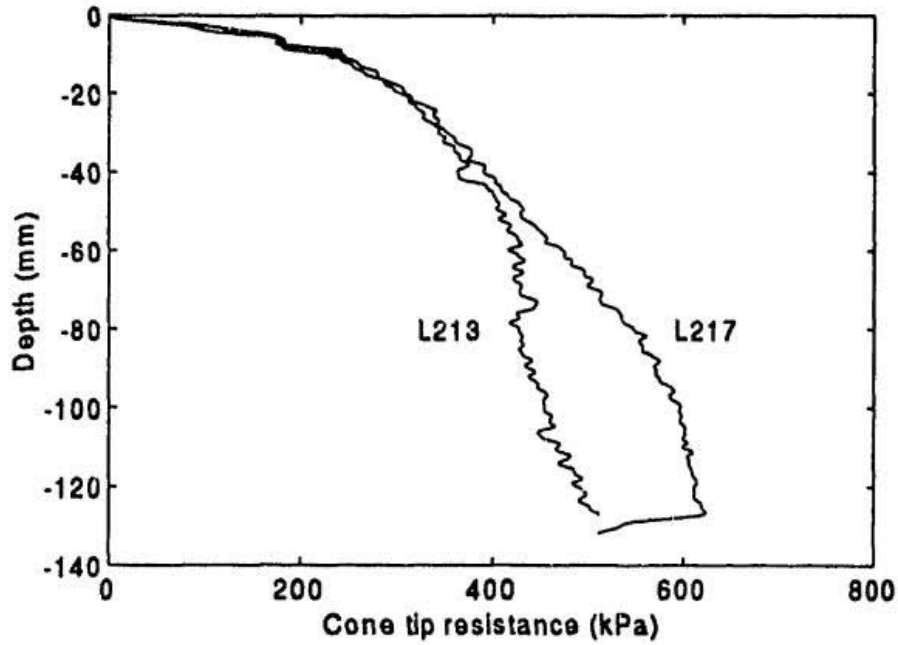

Figure B.11: Cone Tip Resistance of L213 and L217

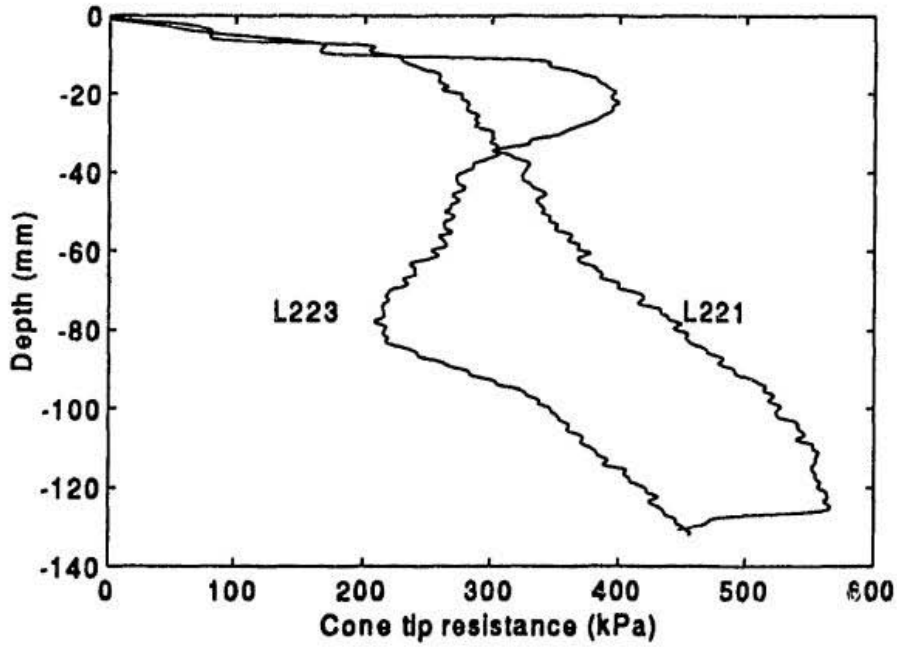

Figure B.12: Cone Tip Resistance of L221 and L223

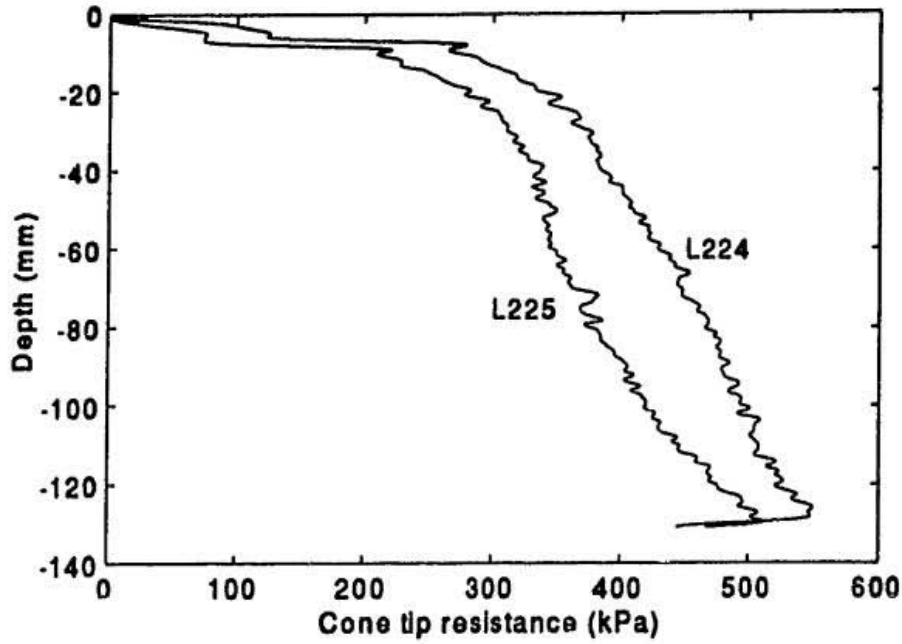

Figure B.13: Cone Tip Resistance of L224 and L225

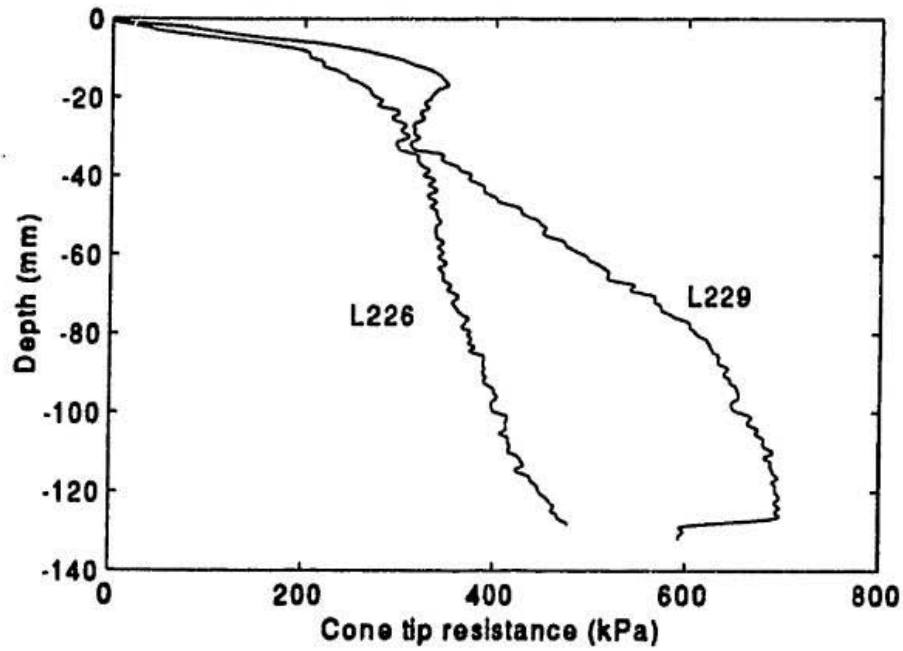

Figure B.14: Cone Tip Resistance of L226 and L229

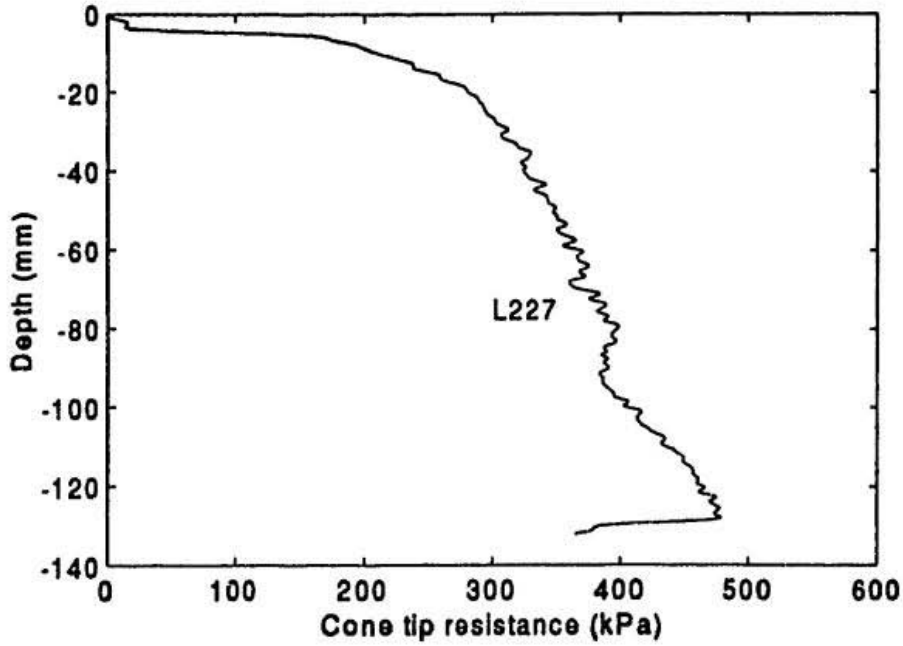

Figure B.15: Cone Tip Resistance of L227

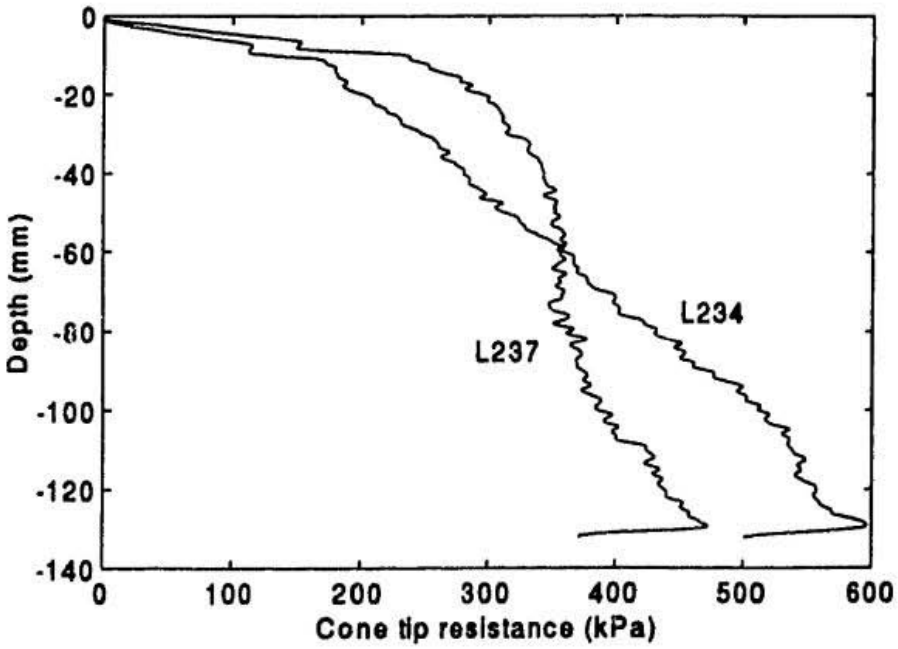

Figure B.16: Cone Tip Resistance of L234 and L237

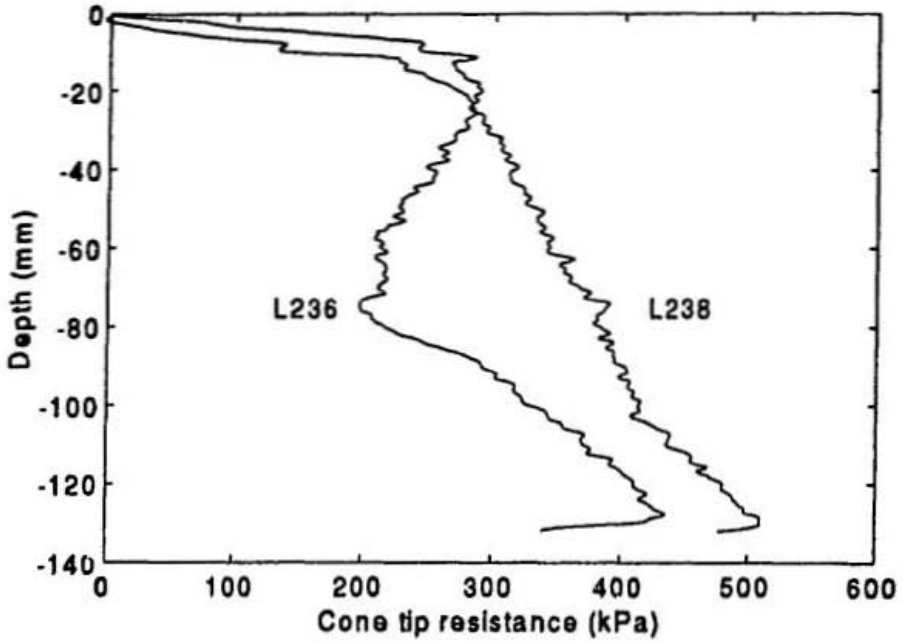

Figure B.17: Cone Tip Resistance of L236 and L238

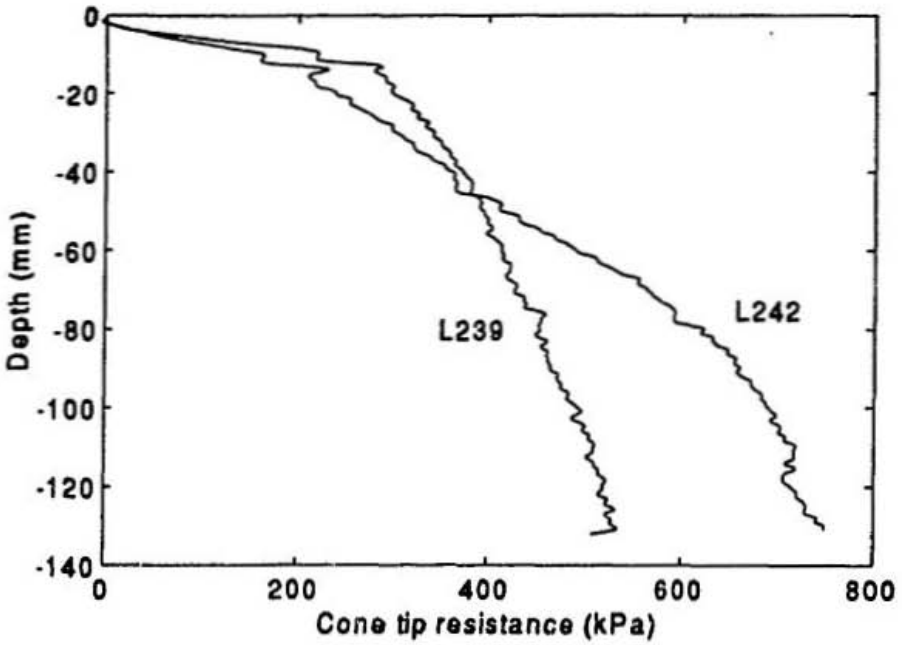

Figure B.18: Cone Tip Resistance of L239 and L242

Appendix C

LDT Results during Consolidation of Large Tub II

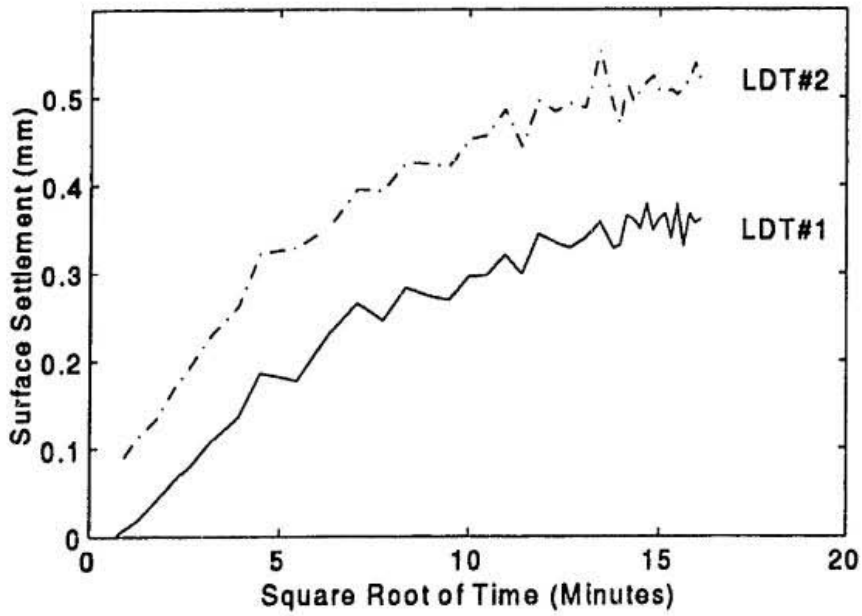

Figure C.1: Surface Settlement of Transect B-B

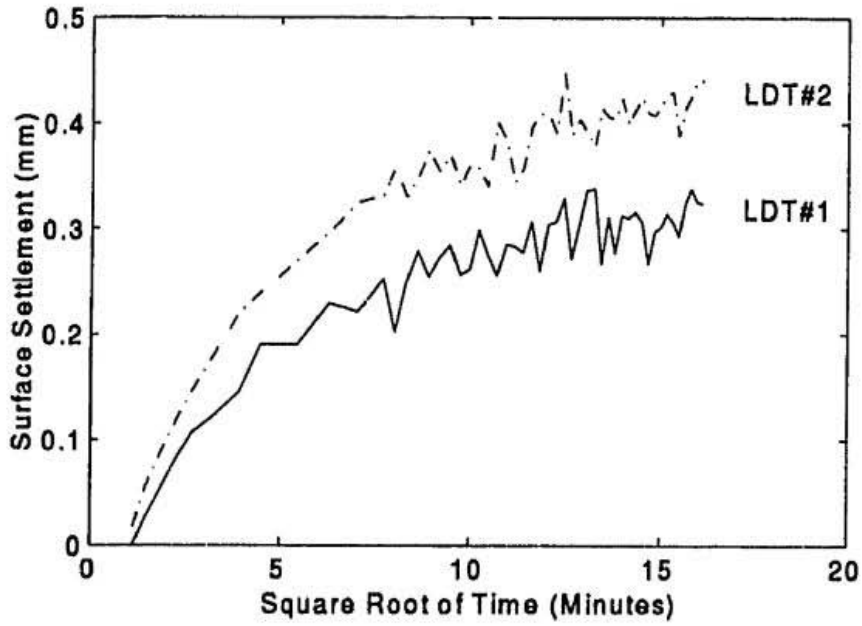

Figure C.2: Surface Settlement of Transect C-C